THE PHYSICAL REVIEW

VOLUME 47 *Second Series* NUMBER 7

APRIL 1, 1935

Published for the

AMERICAN PHYSICAL SOCIETY

by the

AMERICAN INSTITUTE OF PHYSICS
Incorporated

LANCASTER, PA., AND NEW YORK, N. Y.

THE AMERICAN PHYSICAL SOCIETY

OFFICERS OF THE SOCIETY

L. W. WOOD, *President*
The Johns Hopkins University
Baltimore, Maryland

W. L. SEVERINGHAUS, *Secretary*
Columbia University
New York, New York

JOHN T. TATE, *Editor*
University of Minnesota
Minneapolis, Minnesota

F. K. RICHTMYER, *Vice President*
Cornell University
Ithaca, New York

G. B. PEGRAM, *Treasurer*
Columbia University
New York, New York

L. B. LOEB, *Local Secretary for the Pacific Coast*
University of California
Berkeley, California

THE PHYSICAL REVIEW

BOARD OF EDITORS

JOHN T. TATE, *Editor* J. W. BUCHTA, *Assistant Editor*

Associate Editors

K. K. DARROW
J. C. HUBBARD
A. E. RUARK
A. ELLETT
L. A. TURNER
G. E. UHLENBECK
W. V. HOUSTON
R. S. MULLIKEN
I. I. RABI

THE PHYSICAL REVIEW, which was established [illegible] 1893, is a journal of experimental and theoretical physics. It is published for the American Physical Society by the American Institute of Physics Incorporated. There are two volumes annually with twelve issues in each volume.

Manuscripts for publication should be submitted to [illegible] Tate, University of Minnesota, Minneapolis, Minnesota.

Exchanges and all correspondence concerning papers in the process of publication, should be addressed to the Editorial Secretary, American Institute of Physics, 11 East 38th Street, New York, New York.

Subscription price: United States and Possessions and Canada, $15.00; Foreign, $16.50. Subscriptions and orders for back numbers should be addressed to Prince and Lemon Streets, Lancaster, Pennsylvania, or to the American Institute of Physics, 11 East 38th Street, New York, New York.

Advertising is not accepted for the *Physical Review* but attention is called to the *Review of Scientific Instruments* with *Physics News and Views*, a companion publication of the Institute, and a medium through which the field of physics can be reached most effectively. Rates and other information will be furnished on request to the Editorial Secretary.

Changes of address and complaints of failure to receive the *Physical Review*, in the case of members of the American Physical Society, should be addressed to the Treasurer; in the case of other subscribers, to the Editorial Secretary. New copies can be sent free in response to complaints of non-delivery only if notice of non-delivery is received within three months of date of issue.

The Physical Review is published semi-monthly at Prince and Lemon Streets, Lancaster, Pennsylvania.

Entered at the Post Office at Lancaster, Pennsylvania, as second class matter.

Acceptance for mailing at special rate of postage provided for in section 1103, Act of October 3, 1917, authorized September 6, 1926.

THE
PHYSICAL REVIEW
A Journal of Experimental and Theoretical Physics
VOL. 47, NO. 7 APRIL 1, 1935 SECOND SERIES

The Secondary and Tertiary Particles Produced by Cosmic Rays

J. H. SAWYER, JR., *The Rice Institute, Houston, Texas*
(Received December 17, 1934)

Cosmic-ray secondaries and tertiaries have been studied in a series of experiments. It has been shown that the secondaries from lead have little power to produce detectable tertiaries or showers from lead or aluminum. The secondaries from aluminum have been found to produce more showers in lead than the secondaries from air. The absorption coefficient of the secondaries from aluminum has been found to be 0.7 cm^{-1} Pb and the absorption coefficient of their lead tertiaries 2.0 cm^{-1} Pb. The values for secondaries from air and a heavy roof, and their lead tertiaries were previously found to be 0.5 cm^{-1} Pb and 2.58 cm^{-1} Pb. The values obtained from Rossi's and Funfer's data are 0.32 cm^{-1} Pb for the air secondaries and 1.18 cm^{-1} Pb for their lead tertiaries. It follows that the air secondaries and their lead tertiaries have greater energies than the aluminum secondaries and their lead tertiaries. It has been found that a component of the cosmic rays even softer than the corpuscular component is probably the chief source of the secondaries producing the showers. There is some evidence that non-ionizing particles produce a portion of the showers and that possibly non-ionizing secondaries are produced in lead and that these particles can produce ionizing particles in aluminum.

THIS paper contains an account of experiments on the production and absorption of cosmic-ray secondary and tertiary particles. It follows the work of a previous paper.[1] The results of these new experiments and those of other workers, B. Rossi,[2] Funfer,[3] Ackemann[4] and Hummel,[5] help to confirm the assumptions made and the theory proposed in the previous paper.

If we place an absorbing layer of lead in the path of the cosmic-ray primaries and secondaries, we obtain tertiary rays produced by the absorption of the secondaries. At the same time the primary cosmic rays produce secondary particles in the lead. These lead secondary particles are strongly absorbed. After a certain thickness their number reaches a constant ratio with the number of primaries.

In the previous paper the number of tertiary particles ejected by cosmic-ray secondaries from an absorbing layer was shown to be given by the equation

$$\bar{n}_t = K\mu_s e^{-\mu_s l}\left[\frac{1-e^{-l(\mu_t-\mu_s)}}{\mu_t-\mu_s}\right]. \qquad (1)$$

Here n_t is the number of tertiaries emerging from the bottom of a layer of thickness, l, K is a constant, μ_s is the absorption coefficient of the secondaries, and μ_t is the absorption coefficient of the tertiaries. A similar result was obtained at the same time by Bhabha.[6]

The violent bursts of ejected particles, Hoffmann Stösse, produce triple coincidences in the usual arrangement shown in Fig. 1. The Stösse, however, are rare events in comparison with the frequent production of tertiary particles. Messerschmidt[7] has shown that the number of Stösse per

[1] J. H. Sawyer, Jr., Phys. Rev. **44**, 241 (1933).
[2] B. Rossi, Zeits. f. Physik **82**, 151 (1933).
[3] E. Funfer, Zeits. f. Physik **83**, 92 (1933).
[4] F. Ackemann, Naturwiss. **22**, 169 (1934).
[5] R. M. Hummel, Naturwiss. **22**, 170 (1934).
[6] H. J. Bhabha, Zeits. f. Physik **86**, 190 (1933).
[7] W. Messerschmidt, Physik. Zeits. **34**, 897 (1933).

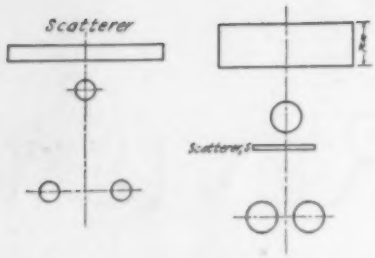

FIG. 1. FIG. 2.

FIG. 1. Diagram of usual cosmic-ray apparatus for investigating showers.

FIG. 2. Arrangement for investigating lead secondaries.

hour from a large mass of material is only about 0.5 to 1.0. This is certainly small in comparison with the production of tertiaries at a rate usually as high as 10 or more per hour. Also the number of Stösse is roughly proportional to the amount of material present, hence in the present experiments, where usually small amounts of absorbers are used, the number of Stösse is much smaller than 0.5 to 1 per hour and so the Stösse can be neglected.

The lead secondaries are assumed to be projected in an almost straight-ahead direction so that they could not produce triple coincidences in a counter arrangement similar to Fig. 1. This assumption was experimentally verified in (1). A beam was defined by two counters and a search with a third counter was made for secondaries produced in a large lead block. No secondaries were found at any angle hence they must have been projected in a straight-ahead beam. We neglected in (1) the possibility that these secondaries of the absorbing material might produce a portion of the tertiary particles by their absorption in the same material. In most experiments the absorbing material is lead so we have made an experimental test for lead tertiaries produced by lead secondaries.

The apparatus used in these experiments is essentially the same as that used in (1). The three Geiger counters are 4.8 cm in diameter and 20 cm effective length. They contain argon at 3 cm pressure and operate at about 2000 volts. They are connected to the usual selecting amplifier with a thyratron counting circuit.

The arrangement of Fig. 2 was used for this test for lead tertiaries produced by lead secondaries. A large block of lead 7 cm thick, 14 cm wide and 40 cm long above the counters cut out the air secondaries in the solid angle defined by the counters and replaced them with lead secondaries. These pass through the top counter and fall on the scattering layer S where they are absorbed with the production of tertiaries.

With this arrangement, counts were made with the lead block in and with or without the scattering layer S. A count was also made with S in and the block removed so that the air secondaries produced tertiaries in S. From the results shown in Table I, we see that the tertiaries

TABLE I.

S	0.63 cm Pb	0.16 cm Pb	0.63 cm Al	0.32 cm Al
COUNTING RATE WITH Pb BLOCK AND S	4.10±0.17	3.5 ±0.25	4.3 ±0.20	4.4±0.21
COUNTING RATE WITH Pb BLOCK ALONE	4.02±0.19	3.3 ±0.20	4.2 ±0.18	4.5±0.22
COUNTING RATE WITH S ALONE	6.94±0.24	4.76±0.18	4.33±0.20	4.7±0.17

produced in S by the lead secondaries do not affect the count.

The lead secondaries have lower energy than light element secondaries and their lead tertiaries have still lower energies. This is evident from a consideration of the absorption coefficients: For air secondaries, 0.32 cm^{-1} Pb (calculated later); for aluminum secondaries, 0.7 cm^{-1} Pb (also obtained later). Hence, the absorption coefficient of the lead secondaries is much greater and the corresponding energy is much smaller than the energy of light element secondaries. Hence only a very small number of these tertiaries get out of the lead. These are probably absorbed in the counter walls or in the steel cylinder which shields the counters from electrical disturbances. Hence they do not affect the count.

An experiment was performed to test the assumption that tertiary particles are produced by light element secondaries. For this purpose a block of aluminum 15.5 cm thick, 13 cm wide and 36 cm long was substituted for the lead block in Fig. 2. This thickness of aluminum is sufficient to absorb all the air secondaries. Also it replaces them with the equilibrium amount of aluminum secondaries.

Runs were made with lead scatterers of various thicknesses, with and without the heavy aluminum block. Sample results are shown in Table II. The increase with the aluminum block over the

TABLE II. *Counting rate with and without aluminum block with various thicknesses.*

LEAD THICKNESS	COUNTING RATE WITH Al BLOCK	COUNTING RATE WITHOUT Al BLOCK
0.32 cm	10.7 ±0.3	7.5 ±0.6
0.47 cm	14.9 ±0.8	9.2 ±0.7
0.63 cm	13.6 ±0.7	11.5 ±0.7
1.9 cm	10.4 ±0.4	8.1 ±0.6

counters indicates a higher equilibrium value of secondaries from aluminum than from the materials of the roof and the air ordinarily above the counters. It is also possible that aluminum secondaries are more efficient in producing lead tertiaries than air secondaries are, or a combination of the two processes may be the correct explanation.

It will be noted that the counting rate has increased in Table II. This change is due to a change in the counters themselves. From time to time during the course of these experiments, it was found necessary to change the gas in the counters and hence to change their counting rate.

The sources of error, other than that due to statistical fluctuations, are those generally found with Geiger counters and coincidence circuits. One source of error is variation in the counting rate of the counters. The causes of any such variation are usually voltage fluctuations in the high tension and leakage at the condenser-high resistance coupling to the first tube. This latter was minimized even for adverse weather conditions by coating with cerosin, a wax with high resistance to surface leakage. The high tension is taken from a rectifier whose a.c. input is regulated with a voltage regulator. The output voltage was constant to ±15 volts as checked by a 3 megohm leak and a milliammeter over a long period. This voltage fluctuation is not sufficient to alter appreciably the counting rate.

The next source of error is due to the fact that the triple coincidence selector does not function perfectly. Changes in the efficiency of the circuit due to plate voltage fluctuations were reduced by floating the B battery with a rectifier so that no current was drawn out of the battery. Filament battery voltages were also kept within restricted ranges. However, there might have been some variation in the screen voltage since the current to the screens was not balanced out.

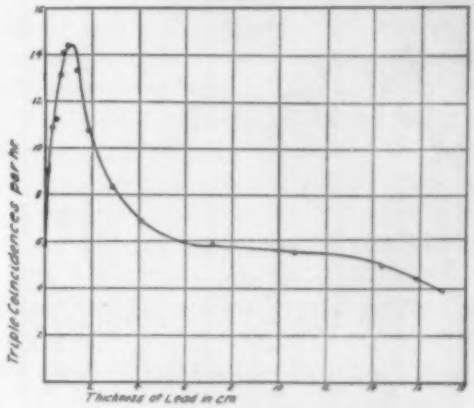

FIG. 3. Absorption-in-lead curve for aluminum secondaries.

Finally, the apparatus was checked from time to time for long period fluctuations by observing the chance count. This chance count over such periods was found to be constant within the statistical error of the rates obtained in the experiment. Hence, we conclude that long period fluctuations are negligible compared to the statistical error. However, there are probably short period fluctuations which are at least as great as the statistical fluctuation due to a finite count.

The thickness of the lead scatterer was varied with the aluminum block over the top counter. The results are plotted in the curve of Fig. 3. It is interesting to note that the curve shows some evidence of a small second maximum. This second rise in the curve occurs at large thicknesses of lead. This doubtful maximum is in accord with the results of Ackemann[4] and of Hummel[5] with two horizontal counters arranged side by side. However, their maxima are much more pronounced. This difference indicates that the particles causing this second increase are in the main uncharged. For if the particles are uncharged, the top counter of the apparatus would not be set off unless a charged particle was ejected from the counter walls. However, in the arrangement of Ackemann and Hummel both charged and uncharged particles can eject charged lead tertiaries into their two counters to produce coincidences.

There has been some indication of the presence of uncharged secondaries in other work. This point we discuss later. The character of the particles producing this second maximum is being investigated.

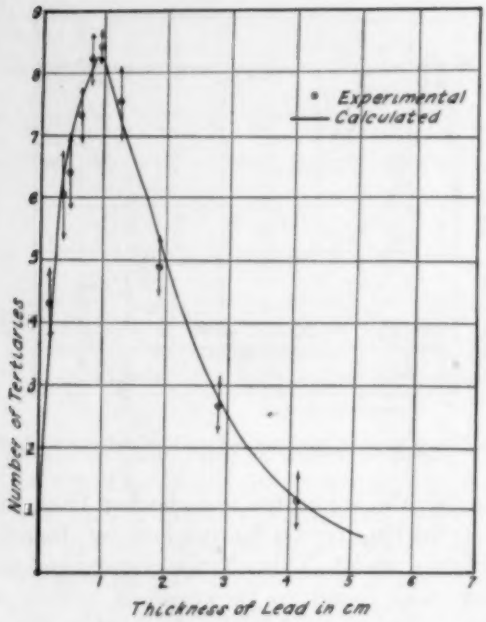

FIG. 4. Calculated absorption curve for aluminum secondaries with experimental points plotted.

From the data of Fig. 3 by means of Eq. (1) we can calculate the absorption coefficients. The absorption coefficient of the lead tertiaries produced by the aluminum secondaries is found to be 2.0 cm^{-1} Pb. The absorption coefficient of the aluminum secondaries in the lead is 0.7 cm^{-1} Pb. The curve obtained from these two calculated absorption coefficients is shown in Fig. 4. The experimental values are plotted on this curve as circles and the statistical errors as the length of the vertical lines through the circles.

Funfer[2] and Rossi[3] have done the most extensive work with Geiger counters on absorption of cosmic-ray particles. Funfer's arrangement is that of Fig. 1 and Rossi's is shown in schematic diagram in Fig. 5. Rossi's curve for the variation of the triple coincidence count with the thickness of S does not agree with Funfer's curve. However, in Rossi's arrangement it is evident that pairs of particles at small angles may produce triple coincidences. This difference is partly due to the bottom counter being twice the size of the other two counters. An example of this is shown in the two ray paths drawn dotted in the figure.

In Fig. 6 Rossi's and Funfer's curves are given and the difference is plotted as the dotted curve.

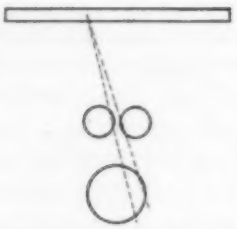

FIG. 5. Rossi's arrangement for investigating air secondaries.

These two curves are reduced to a common basis by considering their respective chance counts, which are a criterion for the sensitivity of the apparatus. Rossi's chance count is approximately twice Funfer's so the ordinate scale of Rossi is made twice that of Funfer. This amounts to plotting the two curves as fractions of the chance counts and the difference curve is obtained in the same way. This difference is due partly to the above property of Rossi's apparatus and partly to the fact that he had heavy blocks of lead protecting the counters at the sides and bottom. These blocks of lead should produce an increase similar to the dotted curve. In fact, Funfer has placed heavy lead blocks at the sides of and beneath his counters and found a very similar increase of the counting rate over that with no protecting blocks. The difference between Rossi's and Funfer's curves is no doubt due to the presence of the heavy lead blocks in Rossi's experiments. Therefore, we have computed the absorption coefficients from Funfer's curve. The

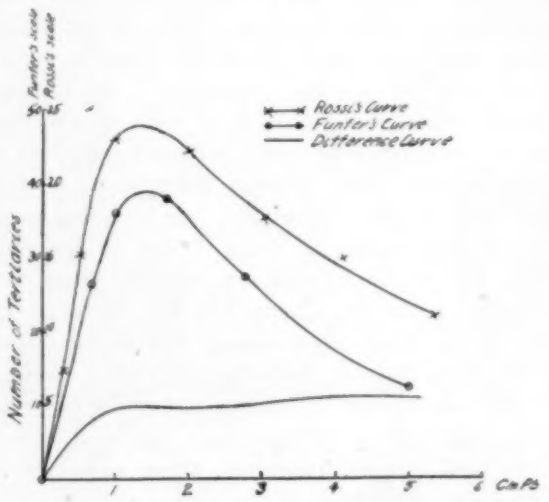

FIG. 6. Rossi's and Funfer's experimental results.

absorption coefficient of air secondaries is found to be 0.32 cm^{-1} Pb, and the absorption coefficient of the lead tertiaries produced by these secondaries is found to be 1.18 cm^{-1} Pb. The values of these coefficients found in our previous paper were 0.5 cm^{-1} Pb for the secondaries and 2.58 cm^{-1} Pb for their tertiaries. This difference is probably due to the fact that there was a heavy roof over our apparatus composed of an inch of tile, 4 inches of concrete and a ceiling. Hence, most of the secondaries probably came from the materials of the roof instead of the air.

The comparison between the absorption coefficients obtained from the data presented here and those obtained from Rossi's and Funfer's data is interesting. The secondaries produced in the aluminum evidently have a lower energy than the air secondaries in Rossi's and Funfer's experiments. This follows from the fact that μ_s for aluminum, 0.7, is greater than for air, 0.32. The comparison is made with Rossi's and Funfer's results for air instead of our previous results on account of the error due to the heavy roof over our apparatus. We see also that the absorption coefficient of the tertiaries from aluminum secondaries, 2.0 cm^{-1} Pb, is greater than that for tertiaries produced by air secondaries, 1.18 cm^{-1} Pb.

The particles which produce this effect are charged particles according to Johnson.[8] He draws this conclusion from a study of the counting rates with the lead scatterer just below and just above the top counter. If there are any uncharged particles ejecting showers of particles from the lead they would not produce triple coincidences with the lead in the first position since the uncharged particle could not actuate the top counter. If any uncharged particles are present the count with the lead above the top counter should therefore be greater than the count with the lead below it.

Johnson found such an increase. However, he maintains that a correction must be applied to the count with lead above the top counter. With no lead present he assumes all the triple coincidences to be caused by showers created in the material of the top counter. These particles would be absorbed with the lead below the top counter and unaffected with the lead above the top counter. Therefore, he subtracts the number of coincidences with no lead present from the number with the lead above the top counter. Then he finds the counting rate with lead above the top counter slightly greater than the rate with the lead below the top counter.

It seems probable that some of the coincidences with no lead present are due to showers from the air and any other materials above the counter. Such shower particles would be absorbed equally with the lead in either position.

Johnson's work has been repeated using also a third position of the lead, just above the bottom counter. This position gives another value of the scattering angle and effective area of the lead plate. The three positions of the lead are shown in Fig. 7 and the results in Table III.

TABLE III. *Counting rate for different positions of S.*

POSITION OF *S*	TOTAL COUNT	TOTAL TIME	RATE
1. JUST ABOVE BOTTOM COUNTERS	330	37.2 hr.	8.87 ±0.32
2. JUST BELOW TOP COUNTER	479	49.6 hr.	9.66 ±0.30
3. JUST ABOVE TOP COUNTER	262	18.0 hr.	14.5 ±0.58

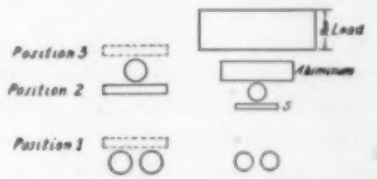

FIG. 7. FIG. 8.

FIG. 7. Arrangement for investigating non-ionizing primaries which cause showers.

FIG. 8. Arrangement for investigating hardness of primaries which produce tertiaries.

There is a substantial increase in the counting rate with the lead just above the top counter as Johnson found. This increase might be ascribed to the fact that the scattering angle is decreased when the lead is moved from beneath to above the top counter. However, the scattering angle was increased even more by moving the lead from position 1 to position 2 and the count was not affected. Hence this was probably not the cause of the increase.

Also there might be an increase due to the edges of the lead plate being effective in position 3 and not in position 2. However, the edges are effective also in position 1 and there is no increase; so this is probably not the cause of the

[8] T. H. Johnson, Phys. Rev. **45**, 581 (1934).

increase. Hence, it seems probable that there are non-ionizing particles causing some of the showers. This causes the large increases in counting when the lead is moved from position 2 to position 3.

Recent work by Gilbert[9] and Johnson[8] has shown that the production of tertiary particles increases greatly at high altitudes. Johnson compares the intensity of tertiaries (denoted showers by Johnson and Gilbert) at two high altitudes. He finds the ratio of these two intensities the same as the ratio of the intensities of the soft corpuscular component of the primary radiation at the same altitudes. He concludes therefore that the soft corpuscular component is the principal source of showers.

In order to test this conclusion the arrangement of Fig. 8 was employed. Here, the heavy lead block cuts down the intensity of the soft, corpuscular component and does not appreciably affect the intensity of the penetrating cosmic particles. If the primary rays causing the effect were the penetrating component, then they would knock secondaries from the aluminum block as before. These secondaries should have almost the same intensity as when the heavy lead block was not there. This follows since the intensity of the primary penetrating rays is only slightly reduced by 7 cm of lead. Then, these aluminum secondaries should pass through the top counter and eject tertiaries from S into the bottom counters.

On the other hand, if the primary particles causing this effect are the soft corpuscular ones, the 7 cm of lead should cut out about $\frac{1}{3}$ of the primary shower-producing rays. These rays should build up aluminum secondaries to an equilibrium value as the thickness of the aluminum is increased. These aluminum secondaries will produce tertiaries in the scatterer S.

However, in this experiment it was found that the triple coincidence count increased with the thickness of the aluminum to a maximum and then decreased with greater thicknesses to the chance count.

Table IV gives the results obtained in several different cases.

It is easily seen from these results that the increase is due both to the presence of the aluminum and the scatterer. Hence we conclude that the secondary particles from the aluminum are producing showers in the lead scatterer. It will also be noted that the increased count is considerably less than the count without the lead block present.

[9] C. W. Gilbert, Proc. Roy. Soc. **A144**, 559 (1934).

TABLE IV. *Counting rates for different thicknesses of blocks.*

Thickness of top Pb block	Thickness of Al block	Thickness of Pb scatterer	Rate
7	3.8	0.0	16.8±0.6
7	3.8	0.63	18.3±0.6
7	0.0	0.63	16.8±0.6
0	3.8	0.63	27.0±0.8

Next, the variation of this triple coincidence count with the thickness of aluminum was obtained. The results are shown in Table V.

It follows from these results and the results of Table IV that the primary particles causing the showers are probably even softer than the soft corpuscular component of Johnson. We see this from a comparison of Table V with Fig. 3. In Fig. 3 the increase over the chance count for the 0.63 cm Pb scatterer and the 15.5 cm aluminum block is about 7 or a little over 100 percent of the chance count. In Table V, placing the 7 cm of Pb over the 15.5 cm aluminum block completely absorbs the effect so that we merely obtain the chance count. Thus the particles which excited secondaries in the aluminum in the first case being completely absorbed in 7 cm Pb, must be softer than Johnson's corpuscular component which would only be about 33 percent absorbed.

The manner in which the number of coincidences in Table V increases with the thickness of Al and then decreases is difficult to explain. We might explain this decrease of the effect with increased thickness of aluminum in the following way. The aluminum first builds up secondaries to produce showers in the lead and then with increased thicknesses begins to absorb out the primary particles which excite the

TABLE V. *Increase of counting rate due to aluminum block.*

Thickness of top Pb block	Thickness of Al block	Thickness of Pb scatterer	Rate	Increase due to Al
7	0.0	0.63	16.8±0.6	—
7	1.27	0.63	19.9±0.7	3.1
7	2.54	0.63	20.9±0.9	4.1
7	3.8	0.63	18.3±0.6	1.5
7	7.6	0.63	16.4±0.6	−0.4
7	15.5	0.63	16.6±0.7	−0.2

aluminum secondaries. But the primary particles would have to be exceptionally soft to be absorbed by 8 cm of aluminum, and so this explanation contradicts the fact that they were penetrating enough to go through 7 cm of Pb.

Another explanation is that these particles are some kind of radiation excited in the lead block. It has been shown that lead secondaries are not effective in the usual experiments. However, these particles from the lead might be of a non-ionizing nature. Then, they would not be effective in the previous experiment. In this case the non-ionizing particles would have an opportunity to excite ionizing particles in the aluminum. Then, these particles could produce the usual showers in the lead scatterer. This explanation seems rather complex; but it is the only one evident at present.

The non-ionizing character of the rays from the lead block was investigated in the usual way. An aluminum block 2.54 cm thick, was first placed above the top counter and then below it. The same scatterer, a 0.63 cm Pb sheet, was used in both cases. The two counts were: 18.1 ± 0.4 with the aluminum above the top counter and 14.5 ± 0.4 with the aluminum below the top counter which is equal to the chance count. Thus the rays from the lead do not affect the top counter, but they produce rays in the aluminum which do effect it. The rays from the lead must therefore be non-ionizing rays, possibly neutrons.

I wish to express my sincere gratitude to Professor H. A. Wilson for his kindly interest in this work and for the many helpful interviews with him during its progress.

APRIL 1, 1935 PHYSICAL REVIEW VOLUME 47

The Deep Configurations of Cobalt

H. H. MARVIN, *Brace Laboratory of Physics, University of Nebraska*

(Received January 7, 1935)

The energy matrix of electrostatic and magnetic spin-orbit interaction is set up for d^7s^2, d^8s and d^9, taking into account the mutual interactions of these configurations. The secular equations are fitted to the deep configurations of Co I, separately, by selecting suitable values for the interaction parameters. The uncertainty existing concerning the assignments of a^2D, a^2G and b^2D is removed. The g-factors for the Zeeman effect in intermediate coupling are calculated for comparison with experimental values presented in the following paper. The mutual interactions of $3d^84s$ with $3d^74s^2$ and $3d^9$ are found to be relatively insignificant. The secular equations are fitted to $3d^74s^2$ and $3d^9$ together, tentatively, in order to observe the effect of mutual interaction upon the values of certain terms which have not yet been discovered, and upon the g-factors. The interaction parameters are compared with those of the deep configurations of Ni I.

THE deep electron configurations of the cobalt atom are $3d^74s^2$, $3d^84s$ and $3d^9$, according to Hund's theory. The most extensive classification of the Co I spectrum has been given by Catalán,[1] who has assigned the deep terms to $3d^74s^2$ and $3d^84s$. The assignments of the quartet and doublet F and P terms, based upon the intensities of their numerous combinations with terms which belong to the intermediate configurations $3d^74s4p$ and $3d^84p$, are certain. The combinations of the other deep terms are both few in number and weak. The assignments of a^2D to $3d^74s^2$, and a^2G and b^2D to $3d^84s$ are tentative. This appears to have been overlooked by Kayser and Konen,[2] who have taken these assignments as assured. Bacher and Goudsmit[3] have assigned a^2G definitely and a^2D tentatively to $3d^74s^2$, and b^2D definitely to $3d^9$.

Such uncertainty concerning the assignment of multiplets is by no means uncommon where two or more configurations overlap. The theoretical study of the configurations d^7s^2, d^8s and d^9, which is presented in this paper, shows that it is possible to remove the uncertainty when the departure from LS coupling is not extreme.

[1] Catalán, An. soc. espan. fis. y quim. **27**, 832 (1929).

[2] Kayser and Konen, *Handbuch der Spektroscopie*, VIII, p. 501.

[3] Bacher and Goudsmit, *Atomic Energy States*, p. 150.

The Energy Matrix

The energy matrix in LS coupling of a configuration which contains an almost complete electron shell can be computed rather simply[4] with the aid of the eigenfunctions of the corresponding configuration which contains an almost empty shell. The matrices of d^7s^2, d^8s and d^9 are identical in form with those of d^3, d^2s and ds^2, except for the constant parts of their diagonal elements. The elements of electrostatic interaction of the latter group are known.[5] The elements of mutual electrostatic interaction between the configurations have been given by Ufford.[6]

[4] Shortley, Phys. Rev. **40**, 185 (1932); Johnson, Phys. Rev. **43**, 632 (1933).
[5] Condon and Shortley, Phys. Rev. **37**, 1025 (1931); Ufford and Shortley, Phys. Rev. **42**, 167 (1932).
[6] Ufford, Phys. Rev. **44**, 732 (1933).

The deep configurations of cobalt deviate sufficiently from LS coupling so that the complete matrices are needed. Consequently, the first order eigenfunctions of d^3, d^2s and ds^2 were set up in exact accord, as to the phases of their components, with those employed by Ufford, and the spin-orbit matrices were computed. The elements of electrostatic interaction were taken from the references. The matrices are valid for d^7s^2, d^8s and d^9.

The diagonal elements of electrostatic interaction of the first-order eigenfunctions of d^7s^2, referred to ^4F as zero, are

^2H: $9F_2+60F_4$,	^2F: $24F_2-15F_4$,	^4P: $15F_2-75F_4$,
^2G: $4F_2+85F_4$,	$^2D^a$: $22F_2+135F_4$,	^2P: $9F_2+60F_4$,
^4F: 0,	$^2D^b$: $18F_2+15F_4$,	

and the non-diagonal element between the two ^2D multiplets is

$$(^2D^a|e^2/r_{ij}|^2D^b)=(189)^{\frac{1}{2}}(F_2-5F_4).$$

The matrix of spin-orbit interaction for d^7s^2, factored according to values of J, is

$J=11/2$

	^2H
^3H	$\frac{1}{2}a$

$J=9/2$

	^2H	^2G	^4F
^2H	$-(3/5)a$	$(66/25)^{\frac{1}{2}}a$	0
^2G	$(66/25)^{\frac{1}{2}}a$	$(3/5)a$	$(5/2)^{\frac{1}{2}}a$
^4F	0	$(5/2)^{\frac{1}{2}}a$	$(3/2)a$

$J=7/2$

	^2G	^4F	^2F
^2G	$-(3/4)a$	$(5/8)^{\frac{1}{2}}a$	$(15/16)^{\frac{1}{2}}a$
^4F	$(5/8)^{\frac{1}{2}}a$	0	$-(3/8)^{\frac{1}{2}}a$
^2F	$(15/16)^{\frac{1}{2}}a$	$-(3/8)^{\frac{1}{2}}a$	$-(1/4)a$

$J=5/2$

	^4F	^2F	$^2D^a$	$^2D^b$	^4P
^4F	$-(7/6)a$	$-(5/18)^{\frac{1}{2}}a$	$-(14/15)^{\frac{1}{2}}a$	$(10/9)^{\frac{1}{2}}a$	0
^2F	$-(5/18)^{\frac{1}{2}}a$	$(1/3)a$	$(7/3)^{\frac{1}{2}}a$	$(1/3)a$	0
$^2D^a$	$-(14/15)^{\frac{1}{2}}a$	$(7/3)^{\frac{1}{2}}a$	$(1/2)a$	$-(7/12)^{\frac{1}{2}}a$	$-(12/5)^{\frac{1}{2}}a$
$^2D^b$	$(10/9)^{\frac{1}{2}}a$	$(1/3)a$	$-(7/12)^{\frac{1}{2}}a$	$-(1/6)a$	0
^4P	0	0	$-(12/5)^{\frac{1}{2}}a$	0	$(1/2)a$

$J=3/2$

	^4F	$^2D^a$	$^2D^b$	^4P	^2P
^4F	$-2a$	$-(21/10)^{\frac{1}{2}}a$	$(5/2)^{\frac{1}{2}}a$	0	0
$^2D^a$	$-(21/10)^{\frac{1}{2}}a$	$-(3/4)a$	$(21/16)^{\frac{1}{2}}a$	$-(2/5)^{\frac{1}{2}}a$	$-(7/8)^{\frac{1}{2}}a$
$^2D^b$	$(5/2)^{\frac{1}{2}}a$	$(21/16)^{\frac{1}{2}}a$	$(1/4)a$	0	$(27/8)^{\frac{1}{2}}a$
^4P	0	$-(2/5)^{\frac{1}{2}}a$	0	$-(1/3)a$	$-(35/9)^{\frac{1}{2}}a$
^2P	0	$-(7/8)^{\frac{1}{2}}a$	$(27/8)^{\frac{1}{2}}a$	$-(35/9)^{\frac{1}{2}}a$	$(1/3)a$

$J=1/2$

	^4P	^2P
^4P	$-(5/6)a$	$-(14/9)^{\frac{1}{2}}a$
^2P	$-(14/9)^{\frac{1}{2}}a$	$-(2/3)a$

The diagonal elements of electrostatic interaction of d^8s, referred to ^4F as zero, are:

^2G: $12F_2'+10F_4'+G_2'$, ^2D: $5F_2'+45F_4'+G_2'$, ^2P: $15F_2'-75F_4'+3G_2'$,
^4F: 0, ^4P: $15F_2'-75F_4'$, ^2S: $22F_2'+135F_4'+G_2'$.
^2F: $3G_2'$,

The matrix of spin-orbit interaction for d^8s, factored according to values of J, is

$J=9/2$

	^2G	^4F
^2G	0	$-a'$
^4F	$-a'$	$(3/2)a'$

$J=7/2$

	^2G	^4F	^2F
^2G	0	$-(1/2)a'$	$-(3/4)^{\frac{1}{2}}a'$
^4F	$-(1/2)a'$	0	$(3/4)^{\frac{1}{2}}a'$
^2F	$-(3/4)^{\frac{1}{2}}a'$	$(3/4)^{\frac{1}{2}}a'$	a'

$J=5/2$

	^4F	^2F	^2D	^4P
^4F	$-(7/6)a'$	$(5/9)^{\frac{1}{2}}a'$	$(16/15)^{\frac{1}{2}}a'$	0
^2F	$(5/9)^{\frac{1}{2}}a'$	$-(4/3)a'$	$-(4/3)^{\frac{1}{2}}a'$	0
^2D	$(16/15)^{\frac{1}{2}}a'$	$-(4/3)^{\frac{1}{2}}a'$	0	$(21/10)^{\frac{1}{2}}a'$
^4P	0	0	$(21/10)^{\frac{1}{2}}a'$	$(1/2)a'$

$J=3/2$

	^4F	^2D	^4P	^2P
^4F	$-2a'$	$(12/5)^{\frac{1}{2}}a'$	0	0
^2D	$(12/5)^{\frac{1}{2}}a'$	0	$(7/20)^{\frac{1}{2}}a'$	$(7/4)^{\frac{1}{2}}a'$
^4P	0	$(7/20)^{\frac{1}{2}}a'$	$-(1/3)a'$	$(5/36)^{\frac{1}{2}}a'$
^2P	0	$(7/4)^{\frac{1}{2}}a'$	$(5/36)^{\frac{1}{2}}a'$	$(1/3)a'$

$J=1/2$

	^4P	^2P	^2S
^4P	$-(5/6)a'$	$(1/18)^{\frac{1}{2}}a'$	$-2a'$
^2P	$(1/18)^{\frac{1}{2}}a'$	$-(2/3)a'$	$(2)^{\frac{1}{2}}a'$
^2S	$-2a'$	$(2)^{\frac{1}{2}}a'$	0

In d^9, the diagonal element of spin-orbit interaction for $^2D_{5/2}$ is a'' and that for $^2D_{3/2}$ is $-3/2a''$. The parameters a, a' and a'' are the negatives of the spin-orbit interaction integrals for a d electron of d^7s^2, d^8s and d^9, respectively.

The electrostatic interaction elements between the first order eigenfunctions of multiplets in different configurations are

$$(d^7s^2\ ^2G\ |e^2/r_{ij}|\ d^8s\ ^2G) = (50)^{\frac{1}{2}}{}'R_2,$$
$$(d^7s^2\ ^4F\ |e^2/r_{ij}|\ d^8s\ ^4F) = 0,$$
$$(d^7s^2\ ^2F\ |e^2/r_{ij}|\ d^8s\ ^2F) = (90)^{\frac{1}{2}}{}'R_2,$$
$$(d^7s^2\ ^2D^a|e^2/r_{ij}|\ d^8s\ ^2D) = -(35/2)^{\frac{1}{2}}{}'R_2,$$
$$(d^7s^2\ ^2D^b|e^2/r_{ij}|\ d^8s\ ^2D) = (135/2)^{\frac{1}{2}}{}'R_2,$$
$$(d^7s^2\ ^4P\ |e^2/r_{ij}|\ d^8s\ ^4P) = 0,$$
$$(d^7s^2\ ^2P\ |e^2/r_{ij}|\ d^8s\ ^2P) = (315)^{\frac{1}{2}}{}'R_2,$$
$$(d^7s^2\ ^2D^a|e^2/r_{ij}|\ d^9\ \ ^2D) = 2''G_2,$$
$$(d^7s^2\ ^2D^b|e^2/r_{ij}|\ d^9\ \ ^2D) = 0,$$
$$(d^8s\ \ ^2D\ |e^2/r_{ij}|\ d^9\ \ ^2D) = (70)^{\frac{1}{2}}{}''R_2,$$

where $'R_2 = (d^7s^2,\ d^8s)(1/35)R^2(nd,\ nd;\ nd,\ n's)$,
$''R_2 = (d^8s,\ d^9)(1/35)R^2(nd,\ nd;\ nd,\ n's)$

in terms of Ufford's integrals,[6] and

$$''G_2 = (d^7s^2,\ d^9)(1/5)G^2(nd,\ n's).$$

The interaction elements are zero between multiplets which have unequal S or L quantum numbers. There are no spin-orbit interactions between these configurations.

The Cobalt Configurations

The complete energy matrices were set up for the configurations separately, as the first step, by adding the electrostatic elements to the corresponding elements of spin-orbit interaction. The secular equations, formed by subtracting the term value symbol W from each diagonal element and equating the resulting determinant

to zero, factor according to values of J. The degree of each equation is determined by the number of rows in the corresponding matrix.

The roots of these equations were fitted to the empirical term values by selecting appropriate values for the interaction parameters. Since the departure of these configurations from LS coupling is moderate, approximate values of the parameters were found by ignoring the non-diagonal matrix elements. The complete secular equations were then employed, and the values of the parameters were adjusted so that the deviations of the computed term values from the empirical values were fairly well balanced. The values of the parameters are $F_2=1522$, $F_4=112.3$, $a=-520$ for $3d^74s^2$; $F_2'=1225$, $F_4'=110.9$, $G_2'=1290$, $a'=-465$ for $3d^84s$; and $a''=-493$ for $3d^9$.

The calculated term values are compared with the empirical values given by Catalán, in Table I. In the last two columns the g-factors in intermediate coupling, computed by the method previously described by the author,[7] are compared with their values in LS coupling.

The values of the parameters F_2 and F_4 are determined by the intervals b^4P-a^4F and b^2P-a^4F. When calculated from these values, a^2G fits into $3d^74s^2$ nicely, but $^2D^-$ and $^2D^+$ fall so high that a^2D and b^2D cannot belong to this configuration. The multiplet a^2D is assigned to $3d^84s$ because, like ^2D of that configuration, it is not inverted. The assignment is confirmed by the reasonable values obtained for F_2' and F_4'. This leaves b^2D to be assigned to $3d^9$. The assignments to configurations, except that of a^2D, agree with those of Bacher and Goudsmit.

The deep cobalt configurations appear to be rather strongly perturbed, the calculated term values differing from the empirical values by several hundred units in a few instances. Since their mutual interactions do not affect their quartets directly, the distortions of a^4P and b^4P and their displacements relative to a^4F and b^4F

[7] Marvin, Phys. Rev. **44**, 818 (1933).

TABLE I. *Term values and g-factors for cobalt, without configuration interaction.*

Configuration	Term	W(cm^{-1}) obs.	W(cm^{-1}) calc.	g LS	g calc.
$3d^74s^2$	$a^4F_{9/2}$	0	0	1.333	1.330
	$a^4F_{7/2}$	816	808	1.238	1.238
	$a^4F_{5/2}$	1407	1402 (1402)*	1.029	1.030 (1.030)*
	$a^4F_{3/2}$	1809	1808 (1808)	0.400	0.401 (0.401)
	$b^4P_{5/2}$	15134	14955 (14936)	1.600	1.597 (1.597)
	$b^4P_{3/2}$	15774	15205 (15204)	1.733	1.720 (1.720)
	$b^4P_{1/2}$	16196	15590	2.667	2.645
	$a^2G_{9/2}$	16468	16051	1.111	1.112
	$a^2G_{7/2}$	17234	16838	0.889	0.889
	$b^2P_{3/2}$	20501	20878 (20850)	1.333	1.282 (1.272)
	$b^2P_{1/2}$	21216	21665	0.667	0.689
	$^2H_{11/2}$		20992	1.091	1.091
	$^2H_{9/2}$		21695	0.909	0.913
	$^2D^-_{5/2}$		22962 (23843)	1.200	1.202 (1.202)
	$^2D^-_{3/2}$		24130 (24882)	0.800	0.863 (0.824)
	$^2F_{7/2}$		35798	1.143	1.143
	$^2F_{5/2}$		35478 (35471)	0.857	0.857 (0.856)
	$^2D^+_{5/2}$		56272 (56371)	1.200	1.200 (1.200)
	$^2D^+_{3/2}$		55920 (56021)	0.800	0.800 (0.800)
$3d^84s$	$b^4F_{9/2}$	3483	3483	1.333	1.333
	$b^4F_{7/2}$	4143	4145	1.238	1.237
	$b^4F_{5/2}$	4690	4683	1.029	1.028
	$b^4F_{3/2}$	5076	5079	0.400	0.402
	$a^2F_{7/2}$	7442	7629	1.143	1.142
	$a^2F_{5/2}$	8461	8679	0.857	0.859
	$a^4P_{5/2}$	13795	13857	1.600	1.579
	$a^4P_{3/2}$	14036	14355	1.733	1.719
	$a^4P_{1/2}$	14399	14598	2.667	2.664
	$a^2D_{5/2}$	16778	16799	1.200	1.219
	$a^2D_{3/2}$	16471	16440	0.800	0.879
	$a^2P_{3/2}$	18390	18194	1.333	1.268
	$a^2P_{1/2}$	18775	18415	0.667	0.671
	$^2G_{9/2}$		21294	1.111	1.111
	$^2G_{7/2}$		21298	0.889	0.890
	$^2S_{1/2}$		47421	2.000	2.000
$3d^9$	$b^3D_{3/2}$	21920	21920 (21918)	1.200	1.200 (1.200)
	$b^2D_{3/2}$	23153	23153 (23165)	0.800	0.800 (0.850)

* Term values and g-factors calculated with configuration interaction between $3d^74s^2$ and $3d^9$ are in parentheses.

may perhaps be ascribed to the influence of intermediate or high configurations which, having sextets, are capable of interacting with the quartets of other configurations. These interactions cannot be studied until the eigenfunctions of certain five-electron systems are developed.

The mutual interaction between $3d^74s^2$ and $3d^84s$ is so small that it is masked by other effects. The calculated values of a^2P and b^2P, which would be pushed apart most vigorously by this interaction, are already farther apart than the empirical values in Table I. The interaction parameter $'R_2$ must be small. This is in accord with the results of Ufford[6] for Ti II and Zr II. The parameter $''R_2$ of interaction between $3d^84s$ and $3d^9$ is probably of the same order of magnitude. The effect of this interaction is probably insignificant, since the D doublets which are directly affected are far apart.

The interaction between $3d^74s^2$ and $3d^9$ should be considerable, since $''G_2$ should be not much smaller than G_2'. Unfortunately, the number of secular equations is insufficient to evaluate the unknown parameters. A calculation was deemed worth while, nevertheless, in order to study the effect of the interaction on the d doublets and the g-factors. The matrices, each six elements square, were set up for the terms with $J=5/2$ and $J=3/2$ with the elements of configuration interaction included. A parameter, denoted by B, was added to the diagonal elements for $^2D_{5/2}$ and $^2D_{3/2}$ of $3d^9$ in order to place this multiplet relative to a^4F of $3d^74s^2$. A reasonable value was *assumed* for $''G_2$, the parameters of $3d^74s^2$ were retained unchanged, and the secular equations were fitted to the empirical term values by adjusting the parameters B and a''. The values of the parameters are $''G_2=1000$, $B=22{,}510$ and $a''=-440$.

The term values and g-factors for the terms affected by configuration interaction are given in parentheses in Table I. The multiplets b^2D and $^2D^-$ are pushed apart about 1000 units by the interaction which has been assumed, and the other terms involved are displaced by lesser amounts. The values given for the $^2D^-$ terms must be considered uncertain to the extent of several hundred units, owing to the fact that $''G_2$ may actually be considerably larger or smaller than the value assumed. These terms should be sought in the region 23,500–25,500 cm^{-1}. The assignment of b^2D to $3d^9$ was confirmed by solving the secular equations by approximations, considering that configuration interaction adds an increment to each term value. The ^2D terms of $3d^9$ are displaced downward and those of $3d^74s^2$ are raised.

The g-factors in intermediate coupling, without configuration interaction, are near to their values for LS coupling, except for a few terms with low values of J which exhibit moderate deviations. Configuration interaction between $3d^74s^2$ and $3d^9$ tends to reduce these deviations. The calculated g-factors for the F and G terms agree very well with the experimental values presented in the following paper. The considerable discrepancies which are found for the P and D terms are further evidence of unidentified perturbations.

The interaction parameters are collected in Table II, together with the parameters of the deep configurations of nickel.[8] The parameters calculated with configuration interaction are in parentheses. The parameters of cobalt are smaller than those of nickel, as the smaller atomic number leads one to expect. Corresponding parameters diminish in magnitude as the number of $3d$ electrons is increased. The fact that $''G_2$ and a'' are smaller than G_2' and a', respectively, when calculated with configuration interaction,

TABLE II. *Interaction parameters of the deep configurations of cobalt and nickel.*

Cobalt		Nickel	
$3d^74s^2$	$F_2=1522$ $F_4=112.3$ $a=-520$	$3d^84s^2$	$F_2=1653$ $F_4=124.0$ $a=-655.8$
$3d^84s$	$F_2'=1225$ $F_4'=110.9$ $G_2'=1290$ $a'=-465$	$3d^94s$	$G_2'=1334$ $a'=-603.6$
$3d^9$	$a''=-493$ (-440)*		
$3d^74s^2-3d^9$	$''G_2=(1000)$ $B=(22510)$		

* With configuration interaction.

[8] Marvin and Baragar, Phys. Rev. **43**, 973 (1933). F_2 and F_4 of Ni $3d^84s^2$ are calculated from the constants, which should be labelled δ, γ, β, α, in the order in which they appear, to agree with Johnson's notation. G_2' of Ni $3d^84s$ is equal to one-half of the a^1D-a^3D interval, and $a'=2\gamma$.

indicates that the interaction assumed is of the right order of magnitude.

Merrill[9] has considered Co I $3d^8(^3F)4s$ as a three-vector problem, assuming Russell-Saunders coupling in the parent ion. His $2A=-456.34$ compares favorably with $a'=-465$ for the interaction integral for the $3d$ electrons. His $-B/2=1210.9$, calculated from the interval a^2F-b^4F, is considerably less than $G_2'=1290$, which is influenced by a^2D and a^2P as well as by a^2F. While the approximations made in the three vector problem have some effect, the difference between the values of these parameters is ascribed mainly to the influence of second order interactions which have not yet been identified.

[9] Merrill, Phys. Rev. **46**, 487 (1934).

APRIL 1, 1935 PHYSICAL REVIEW VOLUME 47

Zeeman Effect in the Arc Spectrum of Cobalt

FRANK L. ROTH AND PAUL F. BARTUNEK,* *Brace Laboratory of Physics, University of Nebraska*

(Received January 7, 1935)

Zeeman patterns for 151 lines in the range λ3200 to λ6500 are measured and g-factors for 100 terms are determined. All the experimental g-factors are compared with their theoretical values for LS coupling and those for the deep even terms are compared with theoretical values for intermediate coupling. The experimental values for the multiplets, b^4P, a^2D, m^2D°, y^4F° and m^2P° deviate rather widely from the theoretical values. The Zeeman patterns indicate changes in classifications for λ4549.67 and λ6450.24 and decide the quantum numbers for two incompletely analyzed terms.

ANALYSIS of the cobalt arc spectrum[1, 2] has been extended to include more than twelve hundred lines and many of the terms have been assigned to electron configurations. This analysis makes possible a study of the Zeeman effect in electron coupling intermediate between the LS and (jj) types for even multiplicity. No extensive work has been done on the Zeeman effect in the cobalt arc spectrum. Unresolved Zeeman separations have been measured for a number of lines by several observers,[3, 4] but the data are neither sufficiently accurate nor complete to permit the determination of g-factors.

This article presents an investigation of the Zeeman effect for 151 lines in the range λ3200 to λ6500 from which the g-factors for 100 terms are calculated. The experimental values for the deep, even terms are compared with the theoretical g-factors given by Marvin in the preceding article. Zeeman patterns calculated from the g-factors are compared with the resolved patterns observed by Rybár.[4]

The spectrograph, an Anderson 21-foot concave grating on a Paschen mounting, as well as the magnet, and Gaertner comparator were those used by Marvin and Baragar[5] in their investigation on nickel. The quartz lens and calcite plate were also used to form separate images of the components of vibration parallel and perpendicular to the magnetic field, in order that they might be photographed separately. Strips of carbon and electrolytic cobalt, crossing each other at right angles between the magnetic poles, were used for arc electrodes. The cobalt electrode was fixed in position and insulated from the magnet pole by a fused quartz disk. The carbon electrode was vibrated by means of a cam arrangement to produce an intermittent arc. To prevent excessive heating and melting of the cobalt due to continuous arcing the cam was arranged to keep the electrodes separated during

* Mr. Bartunek is now at The University of Michigan.
[1] M. A. Catalán, Zeits. f. Physik **47**, 89 (1928).
[2] An. soc. espán. fis y quim. **27**, 832 (1929).
[3] N. A. Kent, Astrophys. J. **13**, 289 (1901); I. M. Graftdijk, Arch. neérlandaises, Series 3a, **2**, 192 (1912).
[4] Rybár, Physik. Zeits. **12**, 889 (1911).
[5] H. H. Marvin and A. E. Baragar, Phys. Rev. **43**, 973 (1933).

about one-eighth of each revolution. The current from a 220-volt d.c. source was controlled by a variable series resistance. Since the carbon electrode had to be replaced every few minutes and magnetic debris had to be removed from the arc even more often, the arc was operated in open air. A slight broadening of the lines has no serious detrimental effect on unresolved patterns. The spectrum was photographed several times in the range λ3200 to λ5000. The time of exposure was about six hours. The three best perpendicular component spectrograms and the two best parallel component spectrograms were measured in the second and third orders. Only one measurable spectrogram of each component was made in the range λ5000 to λ6500. The time of exposure for each of these spectrograms was about forty hours. They were measured in the first and second orders.

The field strength, about 25,000 gauss, was calculated for the range λ3200 to λ5000 from the Zeeman patterns of the Ca II lines λ3934 and λ3968 and the Ca I line λ4227. The sodium *D* lines were used for the longer wavelength range. Measurements made on the Zeeman pattern for the cobalt line λ4867.68 in both ranges were consistent.

Several sets of nine measurements each were made on each pattern at intervals of a few weeks or more in order to reduce personal bias to the status of indeterminate error. The total number of measurements made on each line ranged from about 60 on the stronger patterns to about 150 on some of the weaker patterns. Lines having terms with nearly equal *g*-factors give unresolved Zeeman patterns which are easily measured. In the case of more widely differing *g*-factors the patterns are nebulous, and the center of intensity is not well defined. In most cases it appears to have a position nearer the strongest component than that given by the formulae of Shenstone and Blair,[6] which were used in calculating the *g*-factors. In a number of cases where the patterns were extremely broad an attempt was made to measure the magnetic shift of the strongest component in the pattern. The *g*-factors calculated from these measurements are generally consistent with those calculated from other patterns, but they were given minor weight in fixing average values. In the case of resolved patterns the *g*-factors were calculated by the method of Landé.

Lines for which Zeeman shifts were present in both parallel and perpendicular component patterns were considered first, since from these measurements the *g*-factors could be calculated directly. Combinations of intermediate terms with the terms of the deep multiplets a^4F, b^4F, and a^2F were considered next. From four to twelve combinations were found with each of these terms. The values of the *g*-factors were weighted according to the apparent quality of the patterns and the precision of the measurements. The balance of the quartet and doublet terms were then approached through combinations with terms for which the *g*-factors were already determined. The intermediate sextet terms were approached through combinations with deep quartet terms. In a few instances values calculated from *LS* coupling were assigned to *g*-factors and were later adjusted to produce the best self-consistency among all the terms affected. The *g*-factors for the high even terms were calculated from combinations with the intermediate terms. Finally, the *g*-factors for a few intermediate sextet terms had to be calculated from combinations with high terms. The *g*-factors were all adjusted and readjusted throughout the work to obtain what seemed to be the best possible self-consistency of the results as a whole.

Most of the lines in the range λ3400 to λ3600 and a few lines of longer wavelengths showed strong self-reversals in the no-field spectrograms and a decided tendency toward reversal in the Zeeman patterns. For the lines λ3405.12 and λ3453.51 the reversals of the Zeeman patterns were clean cut and complete. The reversals had little detrimental effect on the measurements of unresolved patterns for which the magnetic shifts were relatively large, but small shifts which were reversed could not be measured.

Table I shows the wavelengths, the classification of the lines, the observed Zeeman patterns, and the weighted average *g*-factors. Zeeman patterns are calculated from these *g*-factors for comparison with the observed patterns. Most of the wavelengths are taken from the tables of

[6] Shenstone and Blair, Phil. Mag. **8**, 765 (1929).

TABLE I. *Zeeman patterns and g-factors for lines of the Co I spectrum.*

λ	Combination $x-y$	Zeeman Effect Patterns Observed		Calculated	g-Factors g_x	g_y
3247.18	$b^4P_{5/2} - [F^o_{7/2}D^o_{7/2}]$	(0), 1.330		(0), 1.329	1.534	1.443
3254.20	$b^4P_{3/2} - (^4P^o_{3/2})$	(0), 1.377		(0), 1.377	1.534	1.743
3283.45		(0), 1.096				
3334.15	$b^4F_{9/2} - y^4F^o_{7/2}$	(0), 1.675		(0), 1.663	1.334	1.146
3354.39	$b^4F_{7/2} - y^4F^o_{5/2}$	(0), 2.200	(a)	(0), 2.195	1.245	0.865
3367.11	$b^4F_{9/2} - y^4G^o_{7/2}$	(0), 2.310	(a)	(0), 2.325	1.334	1.051
3385.23	$b^4F_{7/2} - y^4G^o_{5/2}$	(1.303), 2.548	(b)	(1.310), 2.560	1.245	0.719
3388.18	$b^4F_{5/2} - y^4F^o_{3/2}$	(0.893), 1.930	(b)	(0.892), 1.932	1.040	0.445
3395.38	$b^4F_{5/2} - y^4G^o_{7/2}$	(0), 0.787		(0), 0.781	1.040	0.925
3405.12	$b^4F_{9/2} - y^4F^o_{9/2}$	(0), 1.324		(0.074), 1.324	1.334	1.314
3409.18	$b^4F_{7/2} - y^4F^o_{7/2}$	(−), 1.195		(0.292), 1.195	1.245	1.146
3414.74	$b^4F_{5/2} - z^2D^o_{3/2}$	(0.611), −	(c)	(0.612), 0.604	0.400	0.808
3417.16	$b^4F_{5/2} - y^4F^o_{5/2}$	(−), 0.952		(0.383), 0.952	1.040	0.865
3431.58	$a^4F_{7/2} - z^4D^o_{5/2}$	(0), 1.110		(0), 1.103	1.237	1.344
3433.04	$b^4F_{3/2} - y^4F^o_{3/2}$	(−), 0.423		(0.063), 0.423	0.400	0.445
3442.92	$a^4F_{5/2} - z^4D^o_{3/2}$	(0), 0.952		(0), 0.951	1.042	1.163
3443.65	$b^4F_{7/2} - y^4G^o_{7/2}$	(−), 1.148		(0.573), 1.148	1.245	1.051
3453.51	$b^4F_{9/2} - y^4G^o_{11/2}$	(0), 1.100		(0), 1.100	1.334	1.262
3455.24	$a^4F_{3/2} - z^4D^o_{1/2}$	(−), 0.596	(a)	(0.196), 0.597	0.401	0.009
3461.17	$z^6D^o_{9/2} - [F_{9/2}G_{11/2}]$	(0), 1.278			1.525	
3462.81	$b^4F_{3/2} - y^4F^o_{3/2}$	(0), 1.593	(a)	(0), 1.563	0.400	0.865
3465.80	$a^4F_{9/2} - z^4G^o_{11/2}$	(0), 1.153		(0), 1.148	1.333	1.276
3474.02	$b^4F_{5/2} - y^4F^o_{7/2}$	(0), 1.280		(0), 1.279	1.040	1.146
3483.42	$b^4F_{7/2} - y^4F^o_{9/2}$	(0), 1.435		(0), 1.435	1.245	1.314
3485.35		(0), 1.170				
3489.41	$a^4F_{7/2} - y^4D^o_{5/2}$	(0), 1.113		(0), 1.113	1.148	1.176
3491.32	$a^4F_{3/2} - z^4D^o_{3/2}$	(1.140), −	(c)	(1.143), 0.782	0.401	1.163
3495.69	$b^4F_{3/2} - y^4G^o_{5/2}$	(0), 0.950		(0), 0.958	0.400	0.719
3496.68	$b^4F_{1/2} - z^4G^o_{1/2}$	(1.178), −	(c)	(1.183), 1.076	1.245	0.907
3502.28	$b^4F_{9/2} - y^4D^o_{7/2}$	(0), 1.213		(0), 1.212	1.334	1.404
3506.32	$b^4F_{7/2} - y^4D^o_{5/2}$	(0), 1.133		(0), 1.131	1.245	1.336
3509.84	$b^4F_{5/2} - y^4G^o_{7/2}$	(0), 1.063		(0), 1.065	1.040	1.051
3510.42	$a^4F_{7/2} - z^4D^o_{7/2}$	(0.569), 1.316	(c)	(0.581), 1.320	1.237	1.403
3512.64	$b^4F_{5/2} - y^4D^o_{3/2}$	(0), 0.926		(0), 0.922	1.040	1.197
3513.48	$a^4F_{7/2} - z^4G^o_{9/2}$	(0), 1.102		(0), 1.094	1.237	1.185
3518.35	$a^2F_{5/2} - y^2D^o_{3/2}$	(0), 0.896		(0), 0.896	0.870	0.835
3520.09	$a^4F_{7/2} - z^4F^o_{9/2}$	(0), 1.746	(a)	(0), 1.745	1.237	1.034
3521.37	$b^4F_{9/2} - z^4F^o_{7/2}$	(0), 1.625		(0), 1.597	1.334	1.184
3523.44	$b^4F_{3/2} - y^4D^o_{1/2}$	(−), 0.570	(a)	(0.170), 0.570	0.400	0.060
3526.86	$a^4F_{9/2} - z^4F^o_{9/2}$	(0), 1.338		(0.026), 1.337	1.333	1.340
3529.04	$a^4F_{5/2} - z^4G^o_{7/2}$	(0), 0.974		(0), 0.977	1.042	1.013
3529.82	$b^4F_{7/2} - y^4G^o_{9/2}$	(0), 1.003		(0), 0.984	1.245	1.150
3533.36	$a^4F_{3/2} - z^4G^o_{5/2}$	(0), 0.697		(0), 0.697	0.401	0.570
3543.27	$b^4P_{3/2} - (m^4F^o_{7/2})$	(0), 1.058		(0), 1.073	1.534	1.329
3550.60	$a^4F_{5/2} - z^4F^o_{3/2}$	(0.317), (0.948), 1.980	(a)(d)	(0.321), (0.963), 2.005	1.042	0.400
3552.99	$b^4P_{3/2} - (m^2D^o_{3/2})$	(−), 1.322		(0.560), 1.321	1.513	1.128
3560.90	$b^4F_{3/2} - y^4D^o_{3/2}$	(1.192), 0, 0.803, 1.584	(c)(e)	(1.196), 0.002, 0.799, 1.596	0.400	1.197
3564.96	$b^4F_{5/2} - z^4G^o_{7/2}$	(0), 0.742		(0), 0.741	1.040	0.907
3569.38	$a^2F_{7/2} - y^2F^o_{7/2}$	(0), 1.144		(0.009), 1.147	1.148	1.145
3574.96	$b^4F_{5/2} - y^4D^o_{5/2}$	(0.743), 1.188	(c)	(0.740), 1.188	1.040	1.336
3585.16	$b^4F_{7/2} - y^4D^o_{7/2}$	(0.464), 1.328		(0.469), 1.325	1.245	1.404
3587.19	$a^2F_{5/2} - y^2F^o_{5/2}$	(0), 0.870		(0), 0.870	0.870	0.870
3594.87	$a^4F_{5/2} - z^4F^o_{5/2}$	(0), 1.038		(0.018), 1.038	1.042	1.034
3602.08	$a^4F_{3/2} - z^4F^o_{3/2}$	(0), 0.400		(0.001), 0.401	0.401	0.400
3605.37	$b^4F_{1/2} - z^4F^o_{1/2}$	(−), 1.214		(0.180), 1.215	1.245	1.184
3611.70		(0), 0.907				
3627.81	$b^4F_{7/2} - z^4G^o_{9/2}$	(0), 0.884		(0), 0.890	1.245	1.116
3631.34	$a^4F_{7/2} - z^4F^o_{9/2}$	(0), 1.516		(0), 1.520	1.237	1.340
3632.84		(0), 1.152				
3634.72		(0), 0.871				
3641.79	$a^2D_{3/2} - (m^4D^o_{3/2})$	(0), 1.296	(a)	(0), 1.300	1.100	1.180
3643.19	$a^2D_{3/2} - (m^2D^o_{3/2})$	(0), 1.115		(0.039), 1.114	1.100	1.128
3647.66	$a^4F_{3/2} - z^4F^o_{3/2}$	(0), 1.996)	(a)	(0), 1.984	0.401	1.034
3652.54	$a^4F_{1/2} - z^4F^o_{1/2}$	(0), 1.526		(0), 1.526	1.042	1.257
3662.16		(0), 1.152				
3676.56		(0), 1.062				
3683.05	$a^2D_{5/2} - (m^2D^o_{5/2})$	(−), 1.220		(0.170), 1.219	1.258	1.180
3684.48	$a^2D_{5/2} - (m^2D^o_{3/2})$	(0), 1.466	(a)	(0), 1.453	1.258	1.128
3693.12	$a^2D_{5/2} - [a^2F^o_{7/2}]$	(0), 1.039	(f)	(0), 1.040	1.258	1.161
3693.48	$a^2D_{3/2} - (m^4P^o_{3/2})$	(0), 1.118		(0.067), 1.124	1.100	1.148
3702.25		(0), 0.962				
3704.06	$a^2F_{5/2} - y^4F^o_{7/2}$	(0), 1.867	(a)	(0), 1.833	0.870	1.145
3708.83	$a^2D_{3/2} - (n^2F^o_{5/2})$	(0), 1.127		(0), 1.126	1.100	1.115
3730.48	$b^4P_{3/2} - z^4P^o_{3/2}$	(0), 1.369		(0), 1.369	1.534	1.754
3732.40	$b^4P_{5/2} - z^4P^o_{3/2}$	(0), 1.548		(0.061), 1.548	1.534	1.562
3733.50	$a^2D_{5/2} - (n^2F^o_{7/2})$	(0), 1.163		(0), 1.163	1.258	1.216
3734.15	$a^2D_{3/2} - (m^2F^o_{5/2})$	(0), 1.074		(0), 1.074	1.100	1.085
3735.93	$a^2D_{3/2} - (m^2P^o_{3/2})$	(0), 1.425	(a)	(0), 1.423	1.258	1,148
3745.50	$a^2F_{7/2} - y^2D^o_{7/2}$	(0.673), 1.038		(0.658), 1.037	1.148	0.925

TABLE I—(*Continued*).

λ	Combination $x-y$	Zeeman Effect Patterns Observed		Zeeman Effect Patterns Calculated	g-Factors g_x	g-Factors g_y
3749.93	$a^3D_{3/2} - (z^3P^\circ_{1/2})$	(−), 1.200		(0.200), 1.200	1.100	0.700
3755.45	$a^3D_{3/2} - (m^3F^\circ_{7/2})$	(0), 1.431		(0), 1.418	1.258	1.329
3842.06	$a^3F_{7/2} - z^3D^\circ_{5/2}$	(0), 1.086		(0), 1.086	1.148	1.198
3845.47	$a^3F_{7/2} - y^3G^\circ_{9/2}$	(0), 1.201		(0), 1.201	1.148	1.167
3861.17	$a^3F_{5/2} - z^3D^\circ_{3/2}$	(0), 0.916		(0), 0.917	0.870	0.808
3873.12	$b^4F_{9/2} - z^4D^\circ_{7/2}$	(0), 1.212		(0), 1.213	1.334	1.403
3873.96	$b^4F_{7/2} - z^4D^\circ_{5/2}$	(0), 1.115		(0), 1.121	1.245	1.344
3876.84	$b^4F_{9/2} - z^4G^\circ_{9/2}$	(0.669), 1.255	(c)	(0.670), 1.260	1.334	1.185
3881.88	$b^4F_{3/2} - z^4D^\circ_{3/2}$	(0), 0.947		(0), 0.948	1.040	1.163
3894.09	$a^3F_{5/2} - y^3G^\circ_{7/2}$	(0), 0.991		(0), 0.994	0.870	0.925
3894.48	$b^4F_{3/2} - z^4D^\circ_{1/2}$	(0.195), 0.592	(a)	(0.196), 0.598	0.400	0.009
3906.30	$b^4F_{7/2} - z^4G^\circ_{7/2}$	(0.771), −	(c)	(0.812), 1.129	1.245	1.013
3909.94	$a^4F_{9/2} - z^6G^\circ_{11/2}$	(0), 1.356		(0), 1.356	1.333	1.340
3917.13	$a^3P_{2/2} - (m^3D_{3/2})$	(0.250), 1.210	(c)	(0.249), 1.211	1.294	1.128
3935.97	$a^3F_{7/2} - y^4F^\circ_{9/2}$	(0), 1.674		(0), 1.605	1.148	1.314
3940.90	$b^4F_{3/2} - z^4D^\circ_{3/2}$	(1.145), −	(c)	(1.145), 0.782	0.400	1.163
3941.74	$b^4F_{9/2} - z^4G^\circ_{11/2}$	(0), 1.138		(0), 1.146	1.334	1.276
3945.32	$a^3F_{7/2} - z^3F^\circ_{5/2}$	(0), 1.809	(a)	(0), 1.828	1.148	0.876
3952.92	$a^3F_{7/2} - z^3G^\circ_{7/2}$	(0.727), 1.031		(0.712), 1.028	1.148	0.907
3957.94	$b^4F_{5/2} - z^4D^\circ_{5/2}$	(0.769), 1.190	(c)	(0.770), 1.192	1.040	1.344
3969.13		(0), 1.162				
3973.15	$b^4P_{5/2} - z^4D^\circ_{5/2}$	(0.322), 1.454		(0.331), 1.459	1.534	1.383
3974.73	$b^4F_{7/2} - z^4D^\circ_{7/2}$	(0.564), 1.319	(c)	(0.553), 1.324	1.245	1.403
3978.66	$b^4F_{7/2} - z^4G^\circ_{9/2}$	(0), 1.060		(0), 1.080	1.245	1.185
3979.53	$a^4F_{7/2} - z^6G^\circ_{9/2}$	(0), 1.340		(0), 1.331	1.237	1.271
3990.31	$b^4P_{3/2} - z^4D^\circ_{3/2}$	(0.383), 1.391	(c)	(0.365), 1.392	1.513	1.270
3991.69	$b^4F_{5/2} - z^4G^\circ_{7/2}$	(0), 0.977		(0), 0.979	1.040	1.013
3995.31	$a^3F_{7/2} - y^4G^\circ_{9/2}$	(0), 1.145		(0), 1.154	1.148	1.150
3997.91	$a^3F_{5/2} - y^4F^\circ_{7/2}$	(0), 1.846	(a)	(0), 1.836	0.870	1.146
4013.95	$b^4P_{1/2} - z^4D^\circ_{1/2}$	(1.311), 1.324		(1.315), 1.328	2.642	0.013
4020.90	$b^4F_{9/2} - z^4F^\circ_{9/2}$	(0), 1.136		(0.022), 1.337	1.334	1.340
4035.56	$z^4G^\circ_{11/2} - f^4H_{13/2}$	(0), 1.176		(0), 1.176	1.276	1.249
4045.40	$a^3F_{4/2} - y^4G^\circ_{7/2}$	(0), 1.294		(0), 1.277	0.870	1.051
4058.60	$b^4P_{1/2} - z^4D^\circ_{3/2}$	(0.687), 0.592	(a)	(0.686), 0.584	2.642	1.270
4066.38	$a^3F_{7/2} - y^4D^\circ_{7/2}$	(0.770), 1.265		(0.756), 1.276	1.148	1.404
4068.55	$b^4P_{3/2} - z^4D^\circ_{5/2}$	(0), 1.290		(0), 1.286	1.513	1.383
4086.31	$b^4P_{5/2} - z^4D^\circ_{7/2}$	(0), 1.328		(0), 1.327	1.534	1.442
4092.40	$a^3F_{7/2} - z^3F^\circ_{7/2}$	(0), 1.168		(0.106), 1.166	1.148	1.184
4110.54	$a^3F_{4/2} - z^3F^\circ_{5/2}$	(0), 0.873		(0.013), 0.873	0.870	0.876
4118.78	$a^3F_{4/2} - z^3G^\circ_{5/2}$	(0), 0.953		(0), 0.953	0.870	0.907
4121.33	$a^3F_{7/2} - z^3G^\circ_{9/2}$	(0), 1.063		(0), 1.060	1.148	1.116
4339.64	$b^3P_{2/2} - (m^3P^\circ_{3/2})$	(0.233), 1.241	(c)	(0.257), 1.234	1.319	1.148
4466.89	$z^6F^\circ_{7/2} - e^6F_{7/2}$	(0.144), 1.412		(0.139), 1.416	1.439	1.392
4469.57	$z^6F^\circ_{9/2} - e^6F_{9/2}$	(−), 1.452		(0.104), 1.454	1.468	1.440
4471.58	$z^6F^\circ_{5/2} - e^6F_{5/2}$	(0), 1.342		(0.018), 1.342	1.338	1.346
4530.99	$z^6F^\circ_{11/2} - e^6F_{11/2}$	(0), 1.463		(0.018), 1.463	1.465	1.461
4534.00	$z^6F^\circ_{3/2} - e^6F_{3/2}$	(0), 1.509		(0), 1.509	1.129	1.346
4543.81	$b^3D_{3/2} - (m^3D^\circ_{1/2})$	(0.142), 1.214		(0.146), 1.214	1.247	1.180
4549.67	$z^6F^\circ_{5/2} - e^6F_{7/2}$	(0), 1.459		(0), 1.459	1.338	1.392
4565.60	$z^6F^\circ_{7/2} - e^6F_{9/2}$	(0), 1.444		(0), 1.436	1.439	1.438
4581.62	$z^6F^\circ_{9/2} - e^6F_{11/2}$	(0), 1.435		(0), 1.445	1.468	1.461
4629.38	$z^6D^\circ_{9/2} - e^6F_{9/2}$	(0.320), 1.487		(0.323), 1.482	1.525	1.438
4663.41	$z^6D^\circ_{7/2} - e^6F_{7/2}$	(0.458), 1.469		(0.458), 1.470	1.547	1.392
4682.36	$z^6D^\circ_{5/2} - e^6F_{5/2}$	(0.753), −	(c)	(0.753), 1.497	1.648	1.346
4749.68	$z^6D^\circ_{9/2} - e^6F_{11/2}$	(0), 1.330		(0), 1.317	1.525	1.461
4776.33	$z^6G^\circ_{3/2} - e^6F_{1/2}$	(0.343), 0.404		(0.343), 0.404	0.162	−0.484
4780.00	$z^6G^\circ_{5/2} - e^6F_{3/2}$	(0), 0.702		(0), 0.702	0.865	1.082
4792.87	$z^6G^\circ_{7/2} - e^6F_{5/2}$	(0), 0.909		(0), 0.909	1.152	1.346
4813.48	$z^6G^\circ_{9/2} - e^6F_{7/2}$	(0), 1.054		(0), 1.059	1.271	1.392
4840.27	$z^6G^\circ_{11/2} - e^6F_{9/2}$	(0), 1.130		(0), 1.123	1.341	1.438
4867.68	$z^6G^\circ_{13/2} - e^6F_{11/2}$	(0), 1.176		(0), 1.176	1.385	1.461
5212.70	$z^4F^\circ_{9/2} - f^4F_{9/2}$	(−), 1.356		(0.110), 1.354	1.340	1.368
5266.48	$a^2G_{9/2} - y^2F^\circ_{7/2}$	(0), 1.075		(0), 1.075	1.120	1.145
5280.63	$z^4G^\circ_{9/2} - f^4F_{7/2}$	(0), 1.024	(a)	(0), 1.024	1.185	1.231
5352.05	$z^4G^\circ_{11/2} - f^4F_{9/2}$	(0), 1.075		(0), 1.069	1.276	1.368
5369.58	$a^4P_{3/2} - y^4D^\circ_{5/2}$	(0), 1.026		(0), 1.023	1.754	1.336
5483.34	$a^4P_{5/2} - y^4D^\circ_{7/2}$	(0), 1.013	(a)	(0), 0.957	1.585	1.404
6082.49	$z^4F^\circ_{9/2} - e^4F_{9/2}$	(−), 1.332		(0.074), 1.330	1.340	1.320
6116.98	$a^4P_{1/2} - z^4D^\circ_{1/2}$	(1.348), −		(1.348), 1.357	2.705	0.009
6282.64	$a^4P_{3/2} - z^4D^\circ_{3/2}$	(0), 1.033		(0), 1.037	1.754	1.344
6450.24	$a^4P_{5/2} - z^4D^\circ_{7/2}$	(0), 1.160		(0), 1.176	1.585	1.403
6455.03	$z^4D^\circ_{7/2} - e^4F_{9/2}$	(0), 1.168		(0), 1.175	1.403	1.320

(a) Strongest components in the σ-pattern.
(b) Strongest components in both patterns.
(c) Strongest components in the π-pattern.
(d) π-pattern completely resolved.
(e) σ-pattern completely resolved.
(f) Components of adjacent lines overlap.

TABLE II. *Comparison of observed g-factors with their theoretical values for LS and intermediate couplings.*

CONFIGURATION	TERM	g-FACTORS LS	Obs.	Int.	CONFIGURATION	TERM	g-FACTORS LS	Obs.
$3d^74s^3$	$a^4F_{9/2}$	1.333	1.333	1.330	$3d^74s4p$ (^5F)	$z^6G^\circ_{13/2}$	1.385	1.38
	$a^4F_{7/2}$	1.238	1.237	1.238		$z^6G^\circ_{11/2}$	1.343	1.34
	$a^4F_{5/2}$	1.029	1.042	1.030		$z^6G^\circ_{9/2}$	1.272	1.27
	$a^4F_{3/2}$	0.400	0.401	0.401		$z^6G^\circ_{7/2}$	1.143	1.15
	$b^4P_{3/2}$	1.600	1.53	1.597		$z^6G^\circ_{5/2}$	0.857	0.87
	$b^4P_{5/2}$	1.733	1.51	1.720		$z^6G^\circ_{3/2}$	0.000	0.16
	$b^4P_{1/2}$	2.667	2.64	2.645		$z^6F^\circ_{11/2}$	1.455	1.46
	$a^2G_{9/2}$	1.111	1.12	1.112		$z^6F^\circ_{9/2}$	1.434	1.47
	$b^2P_{3/2}$	1.333	1.32	1.272		$z^6F^\circ_{7/2}$	1.397	1.44
						$z^6F^\circ_{5/2}$	1.314	1.34
$3d^64s$	$b^6F_{9/2}$	1.333	1.334	1.333		$z^6F^\circ_{3/2}$	1.067	1.13
	$b^6F_{7/2}$	1.238	1.245	1.237		$z^6D^\circ_{9/2}$	1.556	1.53
	$b^6F_{5/2}$	1.029	1.040	1.028		$z^6D^\circ_{7/2}$	1.587	1.55
	$b^6F_{3/2}$	0.400	0.400	0.402		$z^6D^\circ_{5/2}$	1.657	1.65
	$a^4P_{5/2}$	1.600	1.58	1.579		$z^6G^\circ_{11/2}$	1.273	1.28
	$a^4P_{3/2}$	1.733	1.75	1.719		$z^6G^\circ_{9/2}$	1.172	1.19
	$a^4P_{1/2}$	2.667	2.71	2.664		$z^6G^\circ_{7/2}$	0.984	1.01
	$a^2F_{7/2}$	1.143	1.148	1.142		$z^6G^\circ_{5/2}$	0.571	0.57
	$a^2F_{5/2}$	0.857	0.870	0.859		$z^6F^\circ_{9/2}$	1.333	1.34
	$a^2D_{5/2}$	1.200	1.26	1.219		$z^6F^\circ_{7/2}$	1.238	1.26
	$a^2D_{3/2}$	0.800	1.10	0.879		$z^6F^\circ_{5/2}$	1.029	1.03
	$a^2P_{3/2}$	1.333	1.29	1.268		$z^6F^\circ_{3/2}$	0.400	0.40
						$z^6D^\circ_{7/2}$	1.429	1.40
$3d^5$	$b^3D_{3/2}$	1.200	1.25	1.200		$z^6D^\circ_{5/2}$	1.371	1.34
						$z^6D^\circ_{3/2}$	1.200	1.16
						$z^6D^\circ_{1/2}$	0.000	0.01
$3d^74s4p$ (^5F)	$x^4D^\circ_{7/2}$	1.429	1.44		$y^4F^\circ_{7/2}$	1.238	1.15
	$x^4D^\circ_{5/2}$	1.371	1.38		$y^4F^\circ_{5/2}$	1.029	0.87
	$x^4D^\circ_{3/2}$	1.200	1.27		$y^4F^\circ_{3/2}$	0.400	0.45
	$x^4D^\circ_{1/2}$	0.000	0.01		$y^4D^\circ_{7/2}$	1.429	1.40
	$z^6G^\circ_{9/2}$	1.111	1.12		$y^4D^\circ_{5/2}$	1.371	1.34
	$z^6G^\circ_{7/2}$	0.889	0.91		$y^4D^\circ_{3/2}$	1.200	1.20
	$z^6F^\circ_{11/2}$	1.143	1.18		$y^4D^\circ_{1/2}$	0.000	0.06
	$z^6F^\circ_{9/2}$	0.857	0.88		$y^6G^\circ_{9/2}$	1.111	1.17
	$z^6D^\circ_{9/2}$	1.200	1.20		$y^6G^\circ_{7/2}$	0.889	0.92
	$z^6D^\circ_{3/2}$	0.800	0.81		$y^6F^\circ_{7/2}$	1.143	1.14
					$y^6F^\circ_{5/2}$	0.857	0.87
$3d^74s4p$ $(-)$	$z^4P^\circ_{5/2}$	1.600	1.56		$y^6D^\circ_{5/2}$	1.200	1.18
	$z^4P^\circ_{3/2}$	1.733	1.75		$y^6D^\circ_{3/2}$	0.800	0.83
	$(m^2F^\circ_{7/2})$	1.143	1.33				
	$(m^2F^\circ_{5/2})$	0.857	1.09	$3d^74s5s$ (^5F)	$e^6F_{11/2}$	1.455	1.46
	$(n^2F^\circ_{7/2})$	1.143	1.22		$e^6F_{9/2}$	1.434	1.44
	$(n^2F^\circ_{5/2})$	0.857	1.12		$e^6F_{7/2}$	1.397	1.39
	$(m^2D^\circ_{5/2})$	1.200	1.18		$e^6F_{5/2}$	1.314	1.35
	$(m^2D^\circ_{3/2})$	0.800	1.13		$e^6F_{3/2}$	1.067	1.08
					$e^6F_{1/2}$	−0.667	−0.48
$3d^64p$ (^7F)	$y^4G^\circ_{11/2}$	1.273	1.26		$f^6F_{9/2}$	1.333	1.37
	$y^4G^\circ_{9/2}$	1.172	1.15		$f^6F_{7/2}$	1.238	1.23
	$y^4G^\circ_{7/2}$	0.984	1.05				
	$y^4G^\circ_{5/2}$	0.571	0.72	$3d^65s$ (^7F)	$e^4F_{9/2}$	1.333	1.32
	$y^4F^\circ_{9/2}$	1.333	1.31				

Kayser and Konen,[7] volume VIII, though a few wavelengths for unclassified lines are found in volume VII. The term notation for the completely analyzed terms is that suggested by Russell, Shenstone and Turner.[8] In Catalán's tables[1] λ4549.67 is assigned to the transition $Z^4D^\circ_{7/2}-[^4G_{9/2}\ ^4F_{7/2}]$ and the transition $Z^6F^\circ_{5/2}-e^6F_{7/2}$ is given for λ4543.84 in the earlier tables.[9] It is evident from the term values that the latter transition corresponds to λ4549.67 giving alternative classifications for this line. Judging from the Zeeman pattern, $Z^6F^\circ_{5/2}-e^6F_{7/2}$ seems to be the more probable classification. λ6450.24 is assigned to $a^2G_{7/2}-Z^2G^\circ_{7/2}$ by Catalán in 1928,[1] but considering the Zeeman pattern as well as the very great relative intensity of the line, the classification[9] $a^4P_{5/2}-Z^4D^\circ_{7/2}$ was chosen instead. The difference of the term values for this classification is also more consistent with the assigned wavelength of the line.

In Table II the weighted, average g-factors are compared with their theoretical values for *LS* coupling. For the deep terms the theoretical g-values given in the preceding article on intermediate coupling are also listed for comparison. The observed values are fairly consistent with those calculated by Marvin except for the multiplets b^4P, a^2D and b^2D, where $j=5/2$ or $3/2$. Most of the g-factors are estimated to be reliable to about 0.01, but the reliability varies greatly with the number of combinations of the terms and the type of Zeeman patterns. Because of their many combinations the multiplets a^4F, b^4F and a^2F are probably reliable to 0.005. The g-factors for terms which appear in only one combination or those which appear in lines of wavelengths longer than λ5000 may be uncertain by 0.03 or even more.[10]

A number of the observed g-values differ rather widely from the values given by *LS*

TABLE III. *Incompletely analyzed terms with suggested classifications and the corresponding LS and observed g-factors.*

TERM VALUE	SUGGESTED CLASSIFICATIONS Catalán	Authors	g-factors LS	Obs.
43130.13	$(z^2P^\circ_{1/2})$	$(z^2P^\circ_{1/2})$	0.667	0.700
43537.62	$(m^2P^\circ_{3/2})$	$(m^2P^\circ_{3/2})$	1.333	1.148
43847.86	$[o^2F^\circ_{7/2}]$	$[o^2F^\circ_{7/2}]$	1.143	1.161
45904.66	$(^4P^\circ_{3/2})$	$(^4P^\circ_{3/2})$	1.733	1.743
45971.09	$[F^\circ_{7/2},D^\circ_{7/2}]$	$^4D^\circ_{7/2}$	1.429	1.443
53511.70	$F_{9/2},G_{11/2}$	$^6F_{11/2}$	1.455	1.449
53617.94	$f^4H_{13/2}$	$f^4H_{13/2}$	1.231	1.249

[7] Kayser and Konen, *Handbuch der Spectroscopie*.
[8] Russell, Shenstone and Turner, Phys. Rev. **33**, 900 (1929).
[9] Catalán and Beckert, Zeits. f. Physik **32**, 336 (1925).
[10] Because of systematic errors due to personal judgment and other causes which cannot be completely eliminated, the probable errors of the measurements give a false impression of the accuracy of the results and are therefore omitted from this discussion.

TABLE IV. *Comparison of resolved Zeeman patterns observed by Rybár[4] with those calculated from our experimental g-factors.*

λ		Zeeman Patterns								
3385.23	Rybár	(0.26),	(0.82),	(1.37),	—,	—,	—,	—,	2.01,	2.51
	Cal.	(0.26),	(0.79),	(1.32),	−0.07,	0.46,	0.98,	1.51,	2.03,	2.56
3388.18	Rybár	(0.32),	(0.83),	—,	0.76,	1.34,	1.93			
	Cal.	(0.30),	(0.89),	0.15,	0.74,	1.34,	1.93			
3462.81	Rybár	(0.24),	(0.73),	—,	0.67,	1.16,	1.63			
	Cal.	(0.23),	(0.70),	0.17,	0.63,	1.10,	1.56			
3491.32	Rybár	(—),	(1.18),	0.02,	0.80,	1.59				
	Cal.	(0.38),	(1.14),	0.02,	0.78,	1.54				
3495.69	Rybár	(0.17),	(0.48),	—,	—,	0.91,	1.18			
	Cal.	(0.16),	(0.48),	0.24,	0.56,	0.88,	1.20			
3550.60	Rybár	(0.30),	(0.91),	—,	—,	1.28,	1.90			
	Cal.	(0.32),	(0.96),	0.08,	0.72,	1.36,	2.01			
3560.90	Rybár	(—),	(1.22),	0.00,	0.82,	1.60				
	Cal.	(0.40),	(1.20),	0.00,	0.80,	1.60				
3704.06	Rybár	(0.20),	(0.53),	(—),	—,	—,	—,	—,	1.44,	1.74
	Cal.	(0.14),	(0.41),	(0.69),	0.46,	0.73,	1.01,	1.28,	1.56,	1.83
3940.90	Rybár	(—),	(1.17),	0.00,	0.80,	1.59				
	Cal.	(0.38),	(1.14),	0.02,	0.78,	1.54				

coupling. These differences may be substantiated in part by unmistakable peculiarities in certain observed patterns. In the case of λ3543.27, which is due to the transition $b^4P_{5/2}-(m^2F^\circ_{7/2})$, the magnetic shifts of the σ components are given for *LS* coupling by 0, 0.46, 0.92, 1.37, 1.83, 2.29, the two strongest components having no magnetic displacement. A relatively large split, sharp on the inner edge and shaded off on the outer edge, is observed. In case of *LS* coupling for λ3552.99, $b^4P_{3/2}-(m^2D^\circ_{3/2})$, the stronger component in the π pattern has a magnetic shift of 1.40 while the observed shift was not large enough to permit measuring. The magnetic shift of the stronger component in the π pattern of λ3693.48, $a^2D_{3/2}-(m^2P^\circ_{3/2})$, is 0.800 for *LS* coupling, but the observed pattern shows no shift. For λ4339.64, $b^2P_{3/2}-(m^2P^\circ_{3/2})$, *LS* coupling predicts no shift, but a shift of 0.233 was observed. Assuming *LS* coupling for λ3643.19, $a^2D_{3/2}-(m^2D^\circ_{3/2})$, the σ pattern is a sharp doublet with a shift of 0.800, while the observed pattern shades off on either side showing the presence of other components, and the measured shift of the center of intensity is 1.115. Although the type of pattern observed for each of these lines is consistent with its classification, the *g*-factors for one or both terms in each case must differ rather widely from those given for *LS* coupling.

Table III is a list of seven incompletely analyzed terms and their probable *g*-factors. The term values and the classifications suggested by Catalán[1, 2] are given in the first two columns. The last three columns show respectively the classifications indicated by the Zeeman effect, the *LS* *g*-factors, and the observed *g*-factors.

Of the previous investigations on the Zeeman effect in the cobalt arc spectrum,[3, 4] Rybár's work seems to be the most accurate. The sixteen unresolved patterns which are listed in his article show fair agreement with our observed patterns. Table IV is a comparison of Rybár's nine resolved patterns with the corresponding patterns calculated from our experimental *g*-factors. His magnetic shifts on either side of the central position are averaged and reduced to the normal field of about 21,400 gauss for convenience in comparison.

The *M* Series of Element 91-Protactinium

W. C. PIERCE AND A. V. GROSSE, *Department of Chemistry, University of Chicago*

(Received February 9, 1935)

Fourteen lines of the *M* series have been identified and their wavelength determined. The corresponding *M* lines for uranium were measured and Lindberg's values confirmed.

THE *L* series of protactinium was measured in 1930,[1] but no measurements have been reported for the *M* series. The recent isolation of larger quantities of protactinium[2] and the availability of a vacuum spectrograph now make possible the determination of the *M* series. As a check on the experimental accuracy the *M* series of uranium has also been measured and the values of Lindberg[3] confirmed.

A high vacuum Bragg spectrograph was used with a gypsum crystal. Ordinary typist's carbon paper was used as a slit cover to exclude light. About four milligrams of pure protactinium pentoxide (Pa_2O_5), was used as a source. It was rubbed onto the target in the usual manner and adhered well.[4]

The spectrograph is designed for x-ray film which is held in a curved casette about the crystal axis. Its radius is *ca.* 15 cm. Wavelengths are determined by the distance of a line from a selected reference line, in this case Cu $K\alpha_1^{II}$. Distances are measured by a Gaertner comparator to 0.01 mm except for the weaker lines that are invisible under magnification. Measurement of several known lines gave the factor: 1 mm on film = 11.29_2 minutes (crystal rotation). $2d$ for the gypsum crystal is taken as 15.158_1A for first order and 15.166_6A for second order.

Weaker lines were registered in a series of three-hour exposures, each with crystal rocking of three degrees. Separate shorter exposures were taken for the stronger lines. Longer exposures were useless for at three hours the background, due to general radiation and to fluorescence from the crystal, was quite strong. The x-ray tube was operated at 10–15 ma with a peak voltage of about 9–10 kv. Full wave kenotron rectification was used without smoothing.

Results are summarized in Table I. The calculated values for element 91 are from the arithmetic mean of Lindberg's $(\nu/R)^{\frac{1}{2}}$ values for thorium and uranium. Relative intensity values are based on visual observation only (f = faint, s = strong).

The agreement is good for all strong lines, except $M_{II}N_{IV}$, where we could not check Lindberg's value for uranium. Among the weaker lines the agreement is as good as may be expected from the uncertainty in measuring their position on the film. The three short wave satellites could not be detected for either protactinium or

TABLE I. *Wavelengths (X.U.) of uranium and protactinium M series.*

Line	Uranium		Protactinium		
	Obs.	Lindberg	Obs.	Calc.	Int.
$M_{II}O_{IV}$	2436	2440	2522	2523	ff
$M_{I}N_{III}$	—	2745	—	2839	—
$M_{II}N_{IV}$	2810	2813	2904	2907	s
$M_{III}O_{V}$	2942	2941	3032	3031	s
$M_{III}O_{I}$	3106	3114	3238	—	ff
$M_{II}N_{I}$	3322.5	3322	3434	—	ff
γ'	—	3463	—	—	—
$M_{III}N_{V}(\gamma)$	3473	3473	3570	3571	s
$M_{III}N_{IV}$	3514	3514	3607	3609	s
$M_{IV}O_{II}$	3568	3570	3683	3683	f
β'	—	3698	—	—	—
$M_{IV}N_{VI}(\beta)$	3708	3708	3819	3818	ss
α'	—	3886	—	—	—
$M_{V}N_{VII}(\alpha_1)$	3902	3902	4014	4015	ss
$M_{V}N_{VI}(\alpha_2)$	3916.5	3916	4027	4026	f
$M_{III}N_{I}$	4319	4322	4441	4434	f
$M_{IV}N_{III}$	—	4615	—	4754	—
$M_{V}N_{III}$	4936	4937	5081 5066	5079	s s
$M_{IV}N_{II}$	5040	5040	5182	5179	s

[1] H. Beuthe and A. V. Grosse, Zeits. f. Physik **61**, 170 (1930).

[2] A. V. Grosse and M. S. Agruss, J. Am. Chem. Soc. **56**, 2200 (1934); Ind. Eng. Chem. April (1935).

[3] E. Lindberg, Nova Acta Reg. Soc. Scient. Upsaliensis [4] **7**, No. 7 (1931).

[4] Best results were obtained by pricking the surface of a copper target with a small sewing needle clamped to an electric massage vibrator. The sample was floated onto the target in suspension in alcohol and was finally pressed into the pits with a smooth agate pestle. Any grinding motion must be avoided as this covers the sample with copper. Some 95 percent of the sample was recovered after the determination.

uranium, because of intense "spark spectra" on the short wave side of the strong lines. In addition to these $M_{I}N_{III}$ and $M_{IV}N_{III}$ could not be detected for either element. $M_{II}N_{I}$ for Pa is very doubtful for the line does not have the typical diffuse appearance of other M lines. It is not reported for thorium by Lindberg. Pa $M_{V}N_{III}$ shows an anomalous doublet structure for in addition to the line at 5081 X.U. there is another equally strong line at 5066 X.U.

One of us (G.) has the pleasure to acknowledge the support of this investigation by a grant from the Penrose Fund of the American Philosophical Society.

APRIL 1, 1935 PHYSICAL REVIEW VOLUME 47

The Constancy of the Velocity of Light

ROY J. KENNEDY, *University of Washington, Seattle*

(Received February 4, 1935)

It is shown that hypotheses of variable velocity of light of the sort advanced by several recent writers are in conflict with experimental and astronomical data which greatly outweigh in probability the data correlated by these authors.

THE hypothesis that the velocity of light is a variable with time has appeared in several forms during the last few years, its basis being correlations of the results of direct measurements of the velocity. It is the purpose of this paper to demonstrate the great lack of plausibility of such a supposition.

De Bray's theory[1] that the velocity is a linear function of time has been shown by Wilson[2] and by the present writer[3] to be quite untenable; if it were correct the interference pattern in a fixed interferometer would shift with time at a rate about a thousand times as great as an observed (and presumably accidental) rate. However, by a curious coincidence, the more accurate of the interference data invoked against De Bray are quite useless as evidence for or against the recent theory of Edmondson.[4] This hypothesis is based on the measurements correlated by De Bray together with those of several other investigators. The data are surprisingly accurately represented by the relation

$$c = 299{,}885 + 115 \sin (2\pi/40)(t - 1901),$$

where c stands for the velocity of light and t is the date, A.D. This function evidently has a minimum sometime in 1931, and at that time would be approximately constant. The writer's interference data referred to above were mainly gathered during this time and so are irrelevant to this latter theory.

But in 1934, according to this equation, c should vary at rate of about 9 km per second per year, or about one part in 10^{13} per second, whereas some incidental observations of the writer during last summer indicated that no interference shift exists corresponding to a change in velocity of one part in about 4×10^{14} per second. It is practically certain that no effect 40 times as great (that required by the theory) could have escaped notice.

It is not surprising that the interferometer test is so far superior to the direct measurement in deciding as to the constancy of velocity. Small variations in any quantity are not customarily sought by taking differences between measurements of the whole, but rather by some such differential method as that provided by the interferometer.

The facts set forth above would be a complete refutation but for one possibility. It is to be emphasized that the velocity of light is an inferred rather than a directly measured quantity, and likewise its constancy is inferred from observation of other things. In the determination of the velocity we come finally to taking the

[1] De Bray, Nature **120**, 602 (1927); **133**, 464, 759, 948 (1934) and elsewhere.
[2] Wilson, Nature **130**, 25 (1932).
[3] Kennedy, Nature **130**, 277 (1932).
[4] Edmondson, Nature **133**, 759 (1934).

product of a length (that of the light-path) and a frequency which is measured in terms of the rotational frequency of the earth; and in inferring a variation of velocity the tacit assumption is made that lengths and the earth's angular velocity are not varying. Contrariwise, in inferring constancy of velocity from interference observations, it must be assumed that the product of length of light-path and frequency of source of light is constant. Now as to lengths, the situation is the same in both cases; if the light-path in a measurement varies with time, so will it presumably in a fixed interferometer. But the possible loophole is suggested by the fact that the frequencies involved are characteristic of such different structures, the earth and the atom. It is not altogether absurd to suppose that whatever caused the variation in velocity might leave the length of day unaffected, while modifying the frequency of a spectral line just enough to offset the effect of the variation in velocity on the positions of the interference bands. However, the supposition would seem far-fetched and without sufficient warrant at present. Furthermore, unless the whole supposed phenomena were to be attributed to something other than gravitation, we have excellent evidence against it in an argument advanced by Eddington. He showed[5] (before the effect had been definitely established) that if no red-shift were found in the solar lines it was not to be hoped that its absence could be attributed to a modification of the emitting atom by the gravitational field of the sun; the argument applies as well even for great cosmic gravitational potentials, particularly since in the present case only their time-variation is important.

More impressive perhaps than the experimental evidence against the variable-velocity hypotheses, is the comparison with observation of some of their astronomical consequences. It is a simple matter to show that the hypothesis of De Bray would require an absurdly large red-shift of nebular lines, while that of Edmondson would yield an alternately red- and violet-shift depending on time of emission and distance of source of stellar lines; in both cases, of course, the shifts would be superimposed on any real Doppler or other shifts.

For a star at distance l at time t_1 of emission of light observed at time t_2 we may write, on setting the variable velocity of light equal to $c(t)$,

$$l=\int_{t_1}^{t_2} c(t)dt.$$

Disregarding the motion of the star, since we are here interested only in one effect,

$$dl=\frac{\partial l}{\partial t_1}dt_1+\frac{\partial l}{\partial t_2}dt_2=0,$$

and so

$$\frac{dt_1}{dt_2}=-\frac{\partial l/\partial t_2}{\partial l/\partial t_1}=\frac{c(t_2)}{c(t_1)}.$$

If dt_1 is taken as the period of the light when emitted, dt_2 is evidently the period when received, and

$$\frac{dt_1}{dt_2}=\frac{\nu_2}{\nu_1}=\frac{\nu_1+\delta\nu_1}{\nu_1}=1+\frac{\delta\nu_1}{\nu_1}. \quad \therefore \frac{\delta\nu_1}{\nu_1}=\frac{c(t_2)}{c(t_1)}-1, \quad (1)$$

where ν_1 is the initial frequency.

Applying this equation first to De Bray's function $c(t)=c_0+kt$ we find

$$\frac{\delta\nu_1}{\nu_1}=\frac{c_0+kt_2}{c_0+kt_1}-1=\frac{k}{c_0}(t_2-t_1), \quad \text{approximately.}$$

Using De Bray's value of $k=-0.013$ cm/sec.^{2} in the last formula, it is found that for a star only 100 light-years distant (i.e., for $t_2-t_1=100$ years) there would be a negative fractional frequency shift $\delta\nu_1/\nu_1$ of more than one part in a thousand, while for stars outside the galactic system the shift would be enormous. Hence the hypothesis is definitely ruled out by observation.

Applying Eq. (1) to Edmondson's function,

$$c(t)=c_0+k\sin\omega(t-t_0)$$

we find

$$\frac{\delta\nu_1}{\nu_1}=\frac{c_0+k\sin\omega(t_2-t_0)}{c_0+k\sin\omega(t_1-t_0)}-1$$

$$=\frac{k}{c_0}[\sin\omega(t_2-t_0)-\sin\omega(t_1-t_0)]$$

$$=-\frac{2k}{c_0}\sin\frac{\omega}{2}(t_2-t_1)\cos\frac{\omega}{2}(t_2+t_1-2t_0),$$

approximately.

[5] Eddington, *The Mathematical Theory of Relativity*, 2nd Ed. p. 92.

Hence it is evident that for a given (fixed) distance of a star from the earth, since then t_2-t_1 is approximately constant, there would occur a relative frequency shift varying nearly sinusoidally with time and having amplitude $(2k/c_0)\sin(\omega/2)(t_2-t_1)$ and period $2\pi/\omega$. Likewise, for a given time of reception t_2 there would be a similar variation with the distances of stellar sources (t_1 being nearly proportional to the distance). Edmondson's values, $\omega=2n/40$ per year, $k=115$ km per second, give for the case of a star at a distance such that $(\omega/2)(t_2-t_1)=n/2$, i.e., 20 light-years, the maximum amplitude $2k/c_0=7.6\times10^{-4}$ and require for stars at various distances a sinusoidal variation with distance having the same amplitude. So large a systematic effect (several hundred times as great as the solar gravitational shift) could scarcely have escaped observation.

It is perhaps worth while to point out that although the velocity of light must be regarded, in one sense, as a variable if we adopt the hypothesis of an expanding universe, nevertheless its variability is not detectable by interference or other means carried out within a small region. This seems the more worthy of demonstration because it turns out that the coordinate velocity changes at a rate which would not be impossible to measure if there were not other compensating variations. In the paper mentioned above[5] it was shown that a probable error in the determination of the variation as small as 6.1×10^{-6} cm per sec.^{2} had been attained. If the coefficients in the line-element of Friedman, Lemaitre, Robertson and Tolman[6] are substituted in the expression for c derived below, its time derivative turns out to be 4.9×10^{-7} cm per sec.^{2}; this result suggests that by a reasonable refinement of technique and increase in the number of data the latter rate might be detected.

The obvious interference method[7] would be to use an arrangement of interfering beams with large path-difference; then the number n of waves by which one beam was retarded with respect to the other would be related to the path-difference l, the frequency ν and the velocity c by the equation, $n=\nu l/c$; the same relation applies to any method of measuring the velocity if the terms are given the corresponding meanings. The test would consist in determining whether n varied with the time.

In the small region of space with which we are concerned we can adopt rectangular coordinates x, y, z and time t. The most general quadratic line-element can then be given the form

$$ds^2=A(dx)^2+B(dy)^2+C(dz)^2+D(dt)^2$$

where the coefficients may be any functions of x, y, z and t. Indicating values of the various functions at time t_0 by use of a subscript, we have by the usual reasoning,

$$dx=(A_0/A)^{\frac{1}{2}}dx_0,\quad dy=(B_0/B)^{\frac{1}{2}}dy_0,\quad dz=(C_0/C)^{\frac{1}{2}}dz_0,\quad dt=(D_0/D)^{\frac{1}{2}}dt_0.$$

Hence $\nu=(D/D_0)^{\frac{1}{2}}\nu_0$ and $c^2=\dfrac{A_0D}{AD_0}\left(\dfrac{dx_0}{dt_0}\right)^2+\dfrac{B_0D}{BD_0}\left(\dfrac{dy_0}{dt_0}\right)^2+\dfrac{C_0D}{CD_0}\left(\dfrac{dz_0}{dt_0}\right)^2.$

$$\therefore\qquad n^2=\frac{\nu^2l^2}{c^2}=\frac{D}{D_0}\nu_0^2\left[\frac{\dfrac{A_0}{A}lx_0^2+\dfrac{B_0}{B}ly_0^2+\dfrac{C_0}{C}lz_0^2}{\dfrac{A_0D}{AD_0}\left(\dfrac{dx_0}{dt_0}\right)^2+\dfrac{B_0D}{BD_0}\left(\dfrac{dy_0}{dt_0}\right)^2+\dfrac{C_0D}{CD_0}\left(\dfrac{dz_0}{dt_0}\right)^2}\right]=\frac{\nu_0^2l_0^2}{c_0^2}$$

since $lx_0/dx_0=ly_0/dy_0=lz_0/dz_0$.

That is, there is no effect to be expected in such a test.

[6] Tolman, Proc. Nat. Acad. Sci. **16**, No. 9, 582–594 (1930).
[7] Kennedy and Thorndike, Phys. Rev. **42**, 400 (1932).

Hyperfine Structures in La III. Nuclear Magnetic Moment of Lanthanum

M. F. CRAWFORD AND NORMAN S. GRACE, *McLennan Laboratory, University of Toronto*

(Received February 8, 1935)

Hyperfine structures of the resonance lines of La III have been measured and the hfs separations of $6s\,^2S_{1/2}$, $6p\,^2P_{1/2,\,3/2}$ determined. A consistent value of 2.8 nuclear magnetons is obtained for the magnetic moment of the lanthanum nucleus from these separations. The $g(I)$ factors of several M odd Z odd nuclei with $I=7/2$ are compared.

HYPERFINE structures in La I and II have been studied by Meggers and Burns,[1] White and Anderson[2] and Anderson.[3] The latter investigators have shown from their measurements of La I structures that the nuclear mechanical moment of $_{57}La^{139}$ very probably is $7/2\cdot h/2\pi$. The value of the nuclear magnetic moment also is of interest. As it can be determined most unequivocally from the hyperfine structures of a one-electron spectrum we have measured the structures of the resonance lines of La III and from the observed separations evaluated the nuclear magnetic moment.

La III[4] was excited by an electrodeless discharge[5] in $LaCl_3$ vapor. The lines were photographed in the fourth, fifth and sixth orders of the department's new twenty-one foot concave grating[6] with exposures as short as ten minutes. The resonance lines 3517A and 3172A ($6s\,^2S - 6p\,^2P$) were clearly resolved into four and two components, respectively, with the separations and intensities (visual estimates) listed in Table I. The intervals recorded for each multiplet transition are the averages of measurements made in two orders on several sets of plates. The observed intensity is placed above and the theoretical intensity below each component.

TABLE I. *Hyperfine structure separations and intensities in the resonance lines of La III.*

WAVE-LENGTH	CLASSIFICATION	Hfs SEPARATIONS, cm^{-1}, INCREASING $\nu\rightarrow$			
3517A	$6s\,^2S_{1/2}-6p\,^2P^o_{1/2}$	10 0.000 10	6 0.240 7	3 1.093 3	9 1.327 10
3172A	$6s\,^2S_{1/2}-6p\,^2P^o_{3/2}$	10 0.000 10	8 1.02 8		

The structure of 3517A, which is completely resolved, can be interpreted uniquely when the theoretical intensity relations[7] are taken into consideration. The analysis gives the doublet splitting of $6s\,^2S_{1/2}$ as normal and equal to 1.09 cm^{-1}, and that of $6p\,^2P_{1/2}$ as normal and equal to 0.237 cm^{-1}. The interval factors calculated on the basis of $I=7/2$ from the above separations are $a_{6s}=0.272$ cm^{-1} and $a_{6p}(1/2)=0.059$ cm^{-1}.

The structure of 3172A is not completely resolved. Six components are predicted whereas two are observed with a separation of 1.02 cm^{-1}, slightly smaller than the splitting of $^2S_{1/2}$ determined from 3517A. This decrease is attributable to a small splitting in the $6p\,^2P_{3/2}$ term.

The magnitude of the $^2P_{3/2}$ splitting was determined by a graphical analysis.[8] A graph of the hyperfine pattern as a function of the ratio $a_{6p}(3/2)/a_{6s}$ was constructed using $I=7/2$ and $a_{6s}=0.272$ cm^{-1}. The components were assigned their theoretical intensities and the centroids (of intensity) of the two groups, each with three components, were then drawn. The position on the graph where the separation between the two centroids equalled 1.02 cm^{-1}, the measured interval, corresponded to $a_{6p}(3/2)=0.010$ cm^{-1}. The total hyperfine separation of $^2P_{3/2}$ derived from this value is 0.12 ± 0.02 cm^{-1}.

[1] W. F. Meggers and K. Burns, J. O. S. A. and R. S. I. **14**, 449 (1927).
[2] H. E. White and O. E. Anderson, Phys. Rev. **44**, 128 (1933).
[3] O. E. Anderson, Phys. Rev. **45**, 685; **46**, 473 (1934).
[4] H. N. Russell and W. F. Meggers, Bur. Standards J. Research **9**, 625 (1932).
[5] A. B. McLay and M. F. Crawford, Phys. Rev. **44**, 986 (1933).
[6] M. F. Crawford and S. Bateson, Canadian J. Research, **10**, 693 (1934).
[7] H. E. White and A. Y. Eliason, Phys. Rev. **44**, 753 (1933).
[8] R. A. Fisher and S. Goudsmit, Phys. Rev. **37**, 1057 (1931).

Independent calculations of the nuclear g-factor can be made from the three interval factors a_{6s}, $a_{6p}(1/2)$, $a_{6p}(3/2)$.

For the $6s$ electron of La III $g(I)$ is given by the formula[9]

$$g(I)=\frac{3\cdot a_{6s}\cdot n^3_{\text{eff}}\cdot 1838}{8Rc^2Z_iZ_0^3K(1/2,Z_i)}, \qquad (1)$$

where $Z_i=57$, $Z_0=3$, $n_{\text{eff}}=2.646$, $K(1/2,Z_i)=1.43$, and $a_{6s}=0.272$ cm^{-1}. These values substituted in Eq. (1) give $g(I)=0.814$. According to Fermi and Segrè[10] the right-hand side of Eq. (1) should be multiplied by a correction factor when the ^2S sequence is non-Rydbergian. Although only two members of the ^2S sequence of La III have been identified, extrapolation from the quantum defects of the corresponding sequences of Cs I and Ba II indicates that the correction factor is approximately equal to $1/1.05$.[4] The inclusion of this factor in Eq. (1) reduces the value of $g(I)$ to 0.78.

In the case of the p electron $g(I)$ is given by the formula[9]

$$g(I)=\frac{a_{6p}(j)\cdot Z_i}{\Delta\nu}\cdot\frac{j(j+1)(l+\frac{1}{2})}{l(l+1)}\cdot\frac{\lambda(l,Z_i)}{K(j,Z_i)}\cdot 1838. \qquad (2)$$

For the $6p\,^2P_{1/2}$ state $j=1/2$, $l=1$, $Z_i=Z-4=53$, $\lambda(l,Z_i)=1.06$, $\Delta\nu=3096$ cm^{-1}, $K(j,Z_i)=1.35$, and $a_{6p}(1/2)=0.059$ cm^{-1}. The substitution of these values in Eq. (2) gives $g(I)=0.82$. For the $6p\,^2P_{3/2}$ state only three of the above factors have different values, namely: $j=3/2$, $K(j,Z_i)=1.06$, and $a_{6p}(3/2)=0.010$ cm^{-1}. These data substituted in Eq. (2) give $g(I)=0.88$.

The $g(I)$ values 0.78 and 0.82 calculated from the splittings of $^2S_{1/2}$ and $^2P_{1/2}$, respectively, are in good agreement. The former is the more reliable since the experimental error in the $^2S_{1/2}$ separation is considerably smaller than that in the $^2P_{1/2}$ separation. According to our judgment the former merits four times as much weight as the latter. This weighting gives $g(I)=0.79$.

The $g(I)$ derived from the $^2P_{3/2}$ is not sufficiently accurate to merit consideration in estimating the most probable value of $g(I)$. It, however, agrees with the latter well within the limits imposed by the experimental error in $a_{6p}(3/2)$. Thus the hyperfine splittings of the three terms $6s\,^2S_{1/2}$, $6p\,^2P_{1/2,\,3/2}$, give a consistent value of 2.8 nuclear magnetons for the magnetic moment of the lanthanum nucleus.

The $g(I)$ of La has also been computed by Anderson[3] from the hyperfine structures of $5d^26s\,^4F$ of La I. His value, 0.72, is in fair agreement with ours, but as his treatment of the three-electron configuration involves a number of approximations in addition to those made in the one-electron problem our value appears to be the more reliable.

It is interesting to compare the $g(I)$ factor of $_{57}La^{139}$ with those of other M odd Z odd nuclei that have the same spin. $_{55}Cs^{133}$ is one of these. As Cs I and La III are members of the same isoelectronic sequence the $g(I)$ values derived from the splittings of their $6s\,^2S_{1/2}$ states can be compared with some assurance. According to Jackson[11] the splitting of the $6s\,^2S_{1/2}$ state of Cs I is 0.305 cm^{-1}. The $g(I)$ obtained from this separation by a computation similar to that used for $6s\,^2S$ of La III is 0.74. This is in good agreement with the values derived from other terms of Cs I.[11, 12, 13] Thus the $g(I)$ factors of Cs and La are nearly equal. Whether or not the small difference is significant is difficult to decide since the formulae used in the calculation of $g(I)$ are only approximate.

$_{51}Sb^{123}$ also is of the M odd Z odd type with $I=7/2$[14] and $g(I)=0.87$. This $g(I)$ value,[6] computed from the interaction constant of a $5s$ electron in a two-electron configuration of Sb IV, is not as accurate as those of Cs and La. Although a comparison cannot be made with great certainty, it appears that the $g(I)$ of $_{51}Sb^{123}$ is not very different from those of La and Cs; and for the present limit of accuracy the possibility of these three nuclei having the same magnetic moment certainly is not precluded.

[9] S. Goudsmit, Phys. Rev. **43**, 636 (1933).
[10] E. Fermi and E. Segrè, Zeits. f. Physik **82**, 729 (1933).
[11] D. A. Jackson, Proc. Roy. Soc. **A147**, 500 (1934). See also V. W. Cohen, Phys. Rev. **46**, 713 (1934).
[12] N. P. Heydenburg, Phys. Rev. **46**, 802 (1934).
[13] L. P. Granath and R. K. Stranathan, Phys. Rev. **46**, 317 (1934).
[14] According to S. Tolansky (Proc. Roy. Soc. **A146**, 182 (1934)) I (Sb^{123}) $=5/2$. His value is based mainly on the structures of three unclassified lines of Sb II. I (Sb^{123}) $=5/2$, however, is definitely incompatible with the completely resolved structure of the classified line 3735A ($5s6s\,^3S_1-5s6p\,^3P_0$) of Sb IV[4].

Two other M odd Z odd nuclei $_{27}Co^{59}$ [15] and $_{21}Sc^{45}$ [16] have $I=7/2$ and $g(I)$-factors 0.77 and 1.0, respectively. These $g(I)$ values which the respective writers give only as estimates are of the same order of magnitude as those of $_{55}Cs^{133}$, $_{57}La^{139}$ and $_{51}Sb^{123}$.

The apparent regularity in mechanical and magnetic moments pointed out above suggests that the nuclei Cs^{133}, La^{139}, Sb^{123} and possibly Co^{59} and Sc^{45} have some structural feature in common.

In conclusion the authors wish to thank Professor E. F. Burton, Director of the McLennan Laboratory, for his interest in this investigation and for the facilities placed at our disposal.

[15] K. R. More, Phys. Rev. **46**, 470 (1934). See also H. Kopfermann and E. Rasmussen, Naturwiss. **22**, 219 (1934).
[16] H. Kopfermann and E. Rasmussen, Zeits. f. Physik **92**, 82 (1934). See also H. Schüler and Th. Schmidt, Naturwiss. **22**, 758 (1934).

APRIL 1, 1935 PHYSICAL REVIEW VOLUME 47

Symmetry Properties and the Identity of Similar Particles

E. E. WITMER AND J. P. VINTI,* *Randal Morgan Laboratory of Physics, University of Pennsylvania*

(Received February 18, 1935)

It is demonstrated that in a system of N similar particles, the permissible wave functions are either symmetrical or antisymmetrical with respect to interchanges of the particles, if the following principles are assumed to be valid: (1) The interchange of two like particles produces no change in any measurable property of the system. In particular, if ψ is to be a permissible wave function, $\psi\bar{\psi}$ must be unaltered by such an interchange. (2) All the wave functions obtained from a given permissible wave function by permuting the similar particles are also permissible wave functions for the same eigenvalue.

IT has often been remarked that the principle of antisymmetry of the wave function for electrons appears in quantum mechanics as something simply superimposed on the theory to take into account the Pauli exclusion principle. Also in the treatment of photons a corresponding principle of symmetry must be superimposed to obtain the Bose-Einstein statistics, which one must assume photons to obey in order to obtain the Planck radiation law. These and other facts have led to the empirical principle that for any given type of particle only symmetrical states occur or else only antisymmetrical states. It is the purpose of this paper[1] to show that this empirical principle follows logically from other more fundamental principles, *viz.*:

(1) *The interchange of two like particles in a dynamical system will produce no change in any measurable property of the system.*

(2) *All the mathematical quantities obtained from a given permissible mathematical quantity appearing in the theory, by permuting the similar particles, are also permissible.* We have in mind especially the quantity ψ.

These two principles together we shall call the principle of the identity of similar particles. They appear to be necessary from the physical point of view; in other words they are physical axioms. It has often been assumed that wave functions neither symmetrical nor antisymmetrical would distinguish between like particles but explicit proofs are lacking. We shall show that the symmetry or the antisymmetry follows from the principles stated above.

Let there be N particles of the type considered, besides other particles. The coordinates $(x_i, y_i, z_i, \sigma_i)$ including spin σ_i, if present, of the ith particle we shall indicate by x_i. The wave function of the system may be indicated as follows:

$$\psi=\psi(x_1, x_2, \cdots x_N; b). \qquad (1)$$

* Now at the Massachusetts Institute of Technology.
[1] E. E. Witmer and J. P. Vinti, Phys. Rev. **43**, 780 (1933).

Here the b symbolizes the coordinates of all the other particles; we shall henceforth omit it. Let us now permute the particles by permuting the positions of their corresponding coordinates in the wave function. The permutation operator we shall call P, where P stands for

$$x_i' = x_j; \quad i, j = 1, 2 \cdots N, \tag{2}$$

so that

$$P\psi(x_1, x_2, \cdots x_N) = \psi[P(x_1, x_2, \cdots x_N)]$$
$$= \psi(x_1', x_2', \cdots x_N') = \psi_P(x_1, x_2, \cdots x_N). \tag{3}$$

Here x_i' stands for the coordinates of the ith particle after the permutation.

$\psi_P(x_1, x_2, \cdots x_N)$ is now a new function of the coordinates $(x_1, x_2, \cdots x_N)$. The permutation which simply interchanges the particles α and β, we shall denote by $P_{\alpha\beta}$.

Now $|\psi(x_1, x_2, \cdots x_N)|^2$ is in concept a measurable physical quantity, since it is a probability density. Hence the first principle above requires

$$|\psi(x_1, x_2, \cdots x_N)|^2 = |\psi(x_2, x_1, \cdots x_N)|^2$$
$$= |\psi(x_1', x_2', \cdots x_N)|^2.$$

Here we have interchanged merely the particles 1 and 2, so that

$$\psi(x_1', x_2', \cdots x_N) = P_{12}\psi(x_1, x_2, \cdots x_N).$$

Now all permutations can be expressed as a product of transpositions, i.e., interchanges of two particles. Therefore we shall restate the principle of the identity of like particles as applied to the probability density in the following manner. If $\psi_1, \psi_2, \psi_3, \cdots$ represent the *totality* of permissible eigenfunctions of states of the system of N particles, then $P_{\alpha\beta}(\psi_k\bar{\psi}_k)$ must equal $\psi_k\bar{\psi}_k$, where ψ_k is *any* of the permissible eigenfunctions. This principle will be used in the sequel to carry out proofs by the method of *reductio ad absurdum*.

We need a preliminary theorem. If

$$P_{\alpha\beta}\psi = \pm\psi \tag{4}$$

the sign must be positive for all interchanges or else negative for all interchanges.

Let us suppose that in Eq. (4) some of the interchanges give rise to plus signs and others to minus signs. Let us divide interchanges into two classes, the first class (A) containing those associated with plus signs and the second class (B) those associated with minus signs. Now there is some particle α in class A which also occurs in class B. To prove this, pick any particle n at random from class A. If it does not occur in class B, then all the interchanges $(n, 1)$, $(n, 2) \cdots (n, n-1)$, $(n, n+1)$, $\cdots$ (n, N) are in class A. But then every one of the particles 1, 2, $\cdots$ N occurs in interchanges of class A, so that if class B has any members, there must be at least one particle α common to both classes. Accordingly, let $P_{\alpha\beta}$ give a plus sign in Eq. (4) and $P_{\alpha\gamma}$ a minus sign.

Now
$$P_{\beta\gamma}\psi = P_{\alpha\beta}P_{\alpha\gamma}P_{\alpha\beta}\psi, \tag{5}$$

or
$$P_{\beta\gamma}\psi = P_{\alpha\gamma}P_{\alpha\beta}P_{\alpha\gamma}\psi. \tag{6}$$

Thus by Eq. (5) $P_{\beta\gamma}\psi = -\psi$, but by Eq. (6) $P_{\beta\gamma}\psi = +\psi$. We are thus led to a contradiction, so that either class A or class B must be empty. The signs must therefore all be alike.

An alternative,[2] more direct proof, is as follows. We may write $P_{\alpha\beta}\psi = C_{\alpha\beta}\psi$, where $C_{\alpha\beta} = \pm 1$.

Eq. (5) gives $C_{\beta\gamma} = C_{\alpha\beta}C_{\alpha\gamma}C_{\alpha\beta} = C_{\alpha\gamma}C_{\alpha\beta}^2 = C_{\alpha\gamma}$.

From $C_{\beta\gamma} = C_{\alpha\gamma}$ it follows by letting α, β, γ take on all values from 1 to N that the C's are all equal, so that the signs must all be plus or else all minus.

Thus if we can show that $P_{\alpha\beta}\psi = \pm\psi$, the wave function must be either symmetrical or antisymmetrical. Suppose we let

$$\psi = \rho e^{i\eta} \quad (\rho, \eta \text{ real}). \tag{7}$$

If P is any permutation, $P\psi = P\rho e^{iP\eta}$

and $\rho^2 = \psi\bar{\psi} = P(\psi\bar{\psi}) = (P\psi)(P\bar{\psi}) = (P\rho)^2$.

Thus $P\rho = \pm\rho = \rho e^{im\pi}$, $m = 1$ or 2,

so that
$$P\psi = \rho e^{i[P\eta + m\pi]} = e^{i\alpha}\psi, \tag{8}$$

[2] This proof was called to our attention by Dr. G. H. Shortley (private communication).

where $\epsilon = P\eta - \eta + m\pi$, a real function of the coordinates. Thus $P\psi = e^{i\epsilon(x_i)}\psi$ is a necessary and sufficient condition that $P(\psi\bar{\psi}) = \psi\bar{\psi}$.

Now let P be $P_{\alpha\beta}$, a simple transposition. Then $\eta = \eta_{s,\alpha\beta} + \eta_{a,\alpha\beta}$, where $\eta_{s,\alpha\beta} = \frac{1}{2}(\eta + P_{\alpha\beta}\eta)$ and $\eta_{a,\alpha\beta} = \frac{1}{2}(\eta - P_{\alpha\beta}\eta)$, so that $P_{\alpha\beta}\eta_{s,\alpha\beta} = \eta_{s,\alpha\beta}$, and $P_{\alpha\beta}\eta_{a,\alpha\beta} = -\eta_{a,\alpha\beta}$. Then, easily, $\epsilon = -2\eta_{a,\alpha\beta} + m\pi$. Thus if $P_{\alpha\beta}\eta$ differs from η only by a constant, ϵ is a constant. Application of $P_{\alpha\beta}$ to the equation,

$$P_{\alpha\beta}\psi = e^{i\epsilon}\psi$$

then shows at once that $e^{i\epsilon} = \pm 1$, and we should have proved our theorem. However, there is no reason for assuming $\eta_{a,\alpha\beta}$ to be a constant, so that we are forced to attack the problem in another way.

Wigner, Hund and Heisenberg[3] showed that the eigenfunctions of a set of N similar particles fall into a number of non-combining sets with different symmetry properties. One of these sets S is symmetrical with respect to interchanges, another A is antisymmetrical. When $N \geqq 3$ there are also sets C neither symmetrical nor antisymmetrical. The sets C have equivalence degeneracy which cannot be removed by any perturbation symmetrical in the like particles. Now if ψ is a permissible eigenfunction, then $P_{\alpha\beta}\psi$ must also be an eigenfunction corresponding to the same value of energy (since $P_{\alpha\beta}H = H$, where H is the energy operator). From the linearity of the wave equation any linear combination $c_1\psi + c_2P_{\alpha\beta}\psi$ must also be an eigenfunction corresponding to the same energy as ψ. In case $P_{\alpha\beta}\psi$ is simply a constant times ψ, this linear combination reduces essentially to ψ. Otherwise $c_1\psi + c_2P_{\alpha\beta}\psi$ is an independent eigenfunction, and we have degeneracy. This degeneracy is the above-mentioned equivalence degeneracy non-removable by any perturbation symmetrical in the like particles. The function $c_1\psi + c_2P_{\alpha\beta}\psi$ must thus be considered equally as permissible as ψ.

For in the case of removable degeneracy one can always apply some perturbation which will pick out certain of the eigenfunctions as preferred; which set is singled out by this procedure depends, of course, on the type of perturbation (e.g., an electric field applied to the hydrogen atom selects as preferred eigenfunctions different ones than those selected by a magnetic field applied to a hydrogen atom). In the case of non-removable degeneracy on the other hand there is no perturbation symmetrical in the like particles which will select any of the eigenfunctions as preferred. We must therefore treat them all impartially and consider $c_1\psi + c_2P_{\alpha\beta}\psi$ as permissible as ψ.

One might, of course, simply lay down the postulate that if ψ is a permissible eigenfunction, then the eigenfunction $P_{\alpha\beta}\psi$ is also permissible, and hence, from the linearity of the wave equation, any linear combination $c_1\psi + c_2P_{\alpha\beta}\psi$. To permit ψ and reject $P_{\alpha\beta}\psi$ would be to treat the similar particles α and β differently, so that this postulate (No. 2 above) is physically acceptable even without the degeneracy argument.

We have then as permissible eigenfunctions

$$\psi_{s,\alpha\beta} = \psi + P_{\alpha\beta}\psi, \quad \text{and} \quad \psi_{a,\alpha\beta} = \psi - P_{\alpha\beta}\psi,$$

$\psi_{s,\alpha\beta}$ being symmetrical with respect to $P_{\alpha\beta}$ and $\psi_{a,\alpha\beta}$ antisymmetrical. If δ is an arbitrary constant, the eigenfunctions

$$\Phi_{1,2} \equiv \psi_{s,\alpha\beta} \pm e^{i\delta}\psi_{a,\alpha\beta}$$

must likewise be permissible. In general, however,

$$P_{\alpha\beta}(\Phi_1\bar{\Phi}_1) \neq \Phi_1\bar{\Phi}_1. \tag{9}$$

This is demonstrated in the following manner.

$$P_{\alpha\beta}\Phi_1 = \Phi_2, \quad P_{\alpha\beta}\Phi_2 = \Phi_1 \tag{10}$$

and $$P_{\alpha\beta}(\Phi_1\bar{\Phi}_1) = (P_{\alpha\beta}\Phi_1)(P_{\alpha\beta}\bar{\Phi}_1) = \Phi_2\bar{\Phi}_2,$$

so that

$$P_{\alpha\beta}(\Phi_1\bar{\Phi}_1) - \Phi_1\bar{\Phi}_1 = \Phi_2\bar{\Phi}_2 - \Phi_1\bar{\Phi}_1$$

$$= -2(e^{-i\delta}\psi_{s,\alpha\beta}\bar{\psi}_{a,\alpha\beta} + e^{i\delta}\bar{\psi}_{s,\alpha\beta}\psi_{a,\alpha\beta}), \tag{11}$$

$$= -4\rho_s\rho_a \cos(\gamma_s - \gamma_a - \delta), \tag{12}$$

where $\psi_{s,\alpha\beta} = \rho_s e^{i\gamma_s}$ and $\psi_{a,\alpha\beta} = \rho_a e^{i\gamma_a}$, the ρ's and γ's being real. Now $\cos(\gamma_s - \gamma_a - \delta)$ does not in general vanish, so that (9) follows.

We have thus shown that if the result of $P_{\alpha\beta}$ operating on a permissible eigenfunction ψ is not a constant times ψ, that there must be *other* permissible eigenfunctions for which the proba-

[3] E. Wigner, Zeits. f. Physik **40**, 492 (1927); **40**, 883 (1927); **43**, 624 (1927); F. Hund, Zeits. f. Physik **43**, 778 (1927); W. Heisenberg, Zeits. f. Physik **41**, 239 (1927).

bility density is not symmetric. This result violates our hypothesis that the probability density must be symmetric for any permissible eigenfunction. We must therefore have

$$P_{\alpha\beta}\psi = c\psi, \tag{13}$$

where c is a constant. Application of $P_{\alpha\beta}$ to this equation shows that $c=\pm 1$; the preliminary theorem then shows that the signs are the same for all interchanges.

We have therefore demonstrated that the wave functions must be either symmetrical or antisymmetrical if the two principles stated above are assumed to be valid.

This idea can be generalized. Using Dirac's notation, the ψ we have been using is

$$(q_1' \cdots q_{3N}' | H') \equiv (q' | H'),$$

where H is the energy. Let

$$(p_1' \cdots p_{3N}' | H') \equiv (p' | H').$$

Then[4]

$$(p'|H') = h^{-3N/2} \int_{-\infty}^{\infty} e^{-(2\pi i/h)(p_1' q_1' + p_2' q_2' + \cdots)} dq' (q'|H').$$

If we apply the permutation $P_{\alpha\beta}$ to this equation, we see that $(p'|H')$ will be symmetrical or antisymmetrical according as $(q'|H')$ is symmetrical or antisymmetrical. It is assumed that the application of $P_{\alpha\beta}$ to

$$e^{-(2\pi i/h)(p_1' q_1' + p_2' q_2' + \cdots p_{3N}' q_{3N}')}$$

is to be made in such a way that p_α and p_β are interchanged at the same time that q_α and q_β are interchanged. Thus the transformation function is symmetrical with respect to an interchange of particles and leads to the result that $(p'|H')$ is antisymmetrical for electrons and protons.

This can be generalized still further. We can require on the basis of the principles stated at the beginning of this article that the probability associated with two sets of observables ξ and η shall be invariant with respect to interchanges of like particles. In Dirac's symbolism $|(\xi'|\eta')|^2$ shall be invariant with respect to interchanges of similar particles. This will lead to the result that $(\xi'|\eta')$ must be either symmetrical or antisymmetrical, provided that the idea of permuting particles applies to the quantity in question.

One of us (J. P. V.) wishes to acknowledge interesting discussions with Professor P. M. Morse and Dr. G. H. Shortley in regard to some of the points in this paper.

[4] P. A. M. Dirac, *Principles of Quantum Mechanics*, p. 106.

APRIL 1, 1935 PHYSICAL REVIEW VOLUME 47

Ion Distribution During the Initial Stages of Spark Discharge in Nonuniform Fields

CHARLES D. BRADLEY AND L. B. SNODDY, *University of Virginia*

(Received February 8, 1935)

A method is given whereby a direct study of ion distribution during the initial stages of spark discharges may be made by means of a Wilson cloud chamber and a potential impulse of less than 10^{-7} sec. duration. Photographs are shown for ion distribution between a point and plane with the point both negative and positive. The mechanisms responsible for the initiation in these cases has not been discovered. It was found that a maximum field of 10^5 to 10^6 volts/cm was a necessary condition for ionization. With the point negative this could cause sufficient auto-electronic emission to start the discharge. With the point positive it is shown that it is improbable that free electrons in the gas are necessary for initiation of ionization.

THE methods ordinarily used in the investigation of the initial stages of spark discharge give little direct information concerning the ion distribution in the gap space before sufficient luminosity for visual or photographic observations has developed. A knowledge of this ion distribution is essential for an understanding of the process involved in the starting of a spark discharge. This paper is the report of an attempt which has been made to determine it in a direct manner.

The method with preliminary results was

reported some time ago.[1, 2] It has been considerably improved and extended since that time. To determine the ion distribution a very short potential impulse is applied to the spark gap electrodes which are placed in a Wilson cloud chamber. The impulse can be applied at any time during the expansion of the chamber. Provided the voltage wave is sufficiently short it is possible in this way to arrive at a picture showing the progressive stages in the ionization of the gap space.

Two accounts of spark discharge investigations have appeared recently which were carried on more or less simultaneously with this one and by similar methods. The first is that of U. Nakaya and F. Yamasaki[3] and the second that of H. Kroemer.[4] Both make use of a Wilson cloud chamber but differ in the method used for the generation of the voltage impulse. Nakaya and Yamasaki employ a potential pulse cut off by a second spark gap used as a short circuiting switch. They suggested that their circuit is oscillatory in character, so it is impossible to draw any conclusions from the photographs shown. Kroemer discharges a condenser through a resistance and applies the voltage drop across this resistance to the gap electrodes. It is difficult to obtain information concerning the initial processes in this latter way since the voltage impulse is quite long.

Peek[5] has shown that visual corona, with most of the characteristics of 60-cycle corona, appears on short impulses which reach their maximum value in 3×10^{-7} sec. Consequently it is necessary to use potential waves shorter than this to obtain definite information concerning the starting processes. In only three of Kroemer's photographs was the duration of the impulse short enough ($1.7-2\times10^{-6}$ sec.) to be comparable with the time of starting of the initial mechanism.

[1] L. B. Snoddy and C. D. Bradley, Phys. Rev. **45**, 432 (1934).
[2] L. B. Snoddy and C. D. Bradley, Phys. Rev. **45**, 751 (1934).
[3] U. Nakaya and F. Yamasaki, Nature **134**, 496 (1934). This letter calls attention to an earlier report of their work in "Kwagaku," Tokyo, 4, Jan. 1, 1934. Unfortunately, we have not seen this article as the University of Virginia Library has up to this time been unable to obtain a copy in this country.
[4] H. Kroemer, Archiv. f. Elektrotechnik **28**, 703 (1934).
[5] F. W. Peek, Jr., Trans. A. I. E. E. **34**, 1857 (1915).

Apparatus and Circuit Characteristics

The two types of circuits and cloud chambers used in this investigation are shown schematically in Figs. 1a and 1b. In both types the impulse is obtained by discharging a condenser (C_1, C_2) through a spark gap (G_1, G_3) into a short two-wire transmission line.

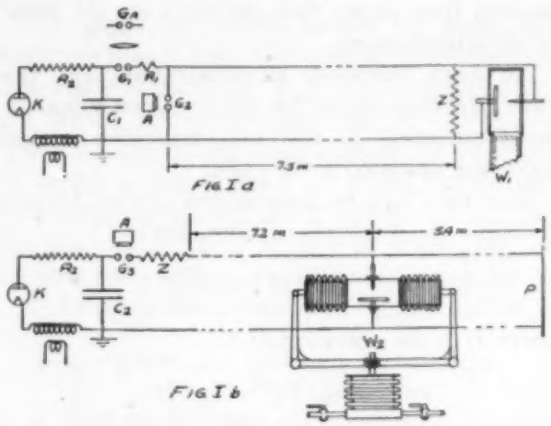

FIG. 1 (a). Impulse circuit with cloud chamber at end of line. Impulse produced by short circuiting the input. (b). Uniform impulse circuit with the potential removed by means of reflection from the shorted end of the line.

In the first type (Fig. 1a) the short potential wave is obtained by placing the cloud chamber at the end of the line and shunting the input end by a second gap G_2 set to be about 30 percent overvolted upon the breakdown of G_1. This gap was constantly irradiated by a quartz Hg arc, A, to reduce its time lag. The total duration of the wave is then composed of the time required to build up a potential across G_2, the time lag of G_2, and the time taken by G_2 to discharge. Since the time lag of G_2 is probably variable, the length of this impulse could change by an amount equal to the maximum value of this lag. This was rather roughly determined as 3×10^{-8} sec.

In the second type (Fig. 1b) the cloud chamber is placed at some point along the line and the end of the line short-circuited by a large metal plate, P. The duration of the impulse is then determined by the distance between the chamber and the end of the line. In both circuits resistances, Z, equal in value to the surge impedance of the lines are introduced at the proper

points to prevent reflections and thus insure that a single impulse is obtained.

The circuits used for obtaining synchronization with the cloud chamber expansion are not shown. For this purpose the voltages of C_1 and C_2 were held at about 1 or 2 percent below the breakdown values of G_1 and G_3, respectively. At this voltage accidental breakdowns do not often occur. In the first case the discharge of G_1 was produced by irradiation with ultraviolet light from an auxiliary spark gap, Ga, and, in the second case, the voltage of C_2 was rapidly increased until the breakdown of G_3 occurred, by short-circuiting a part of the resistance in the primary of the charging transformer. These auxiliary circuits were operated by mechanical switches on the pistons of the cloud chambers.

From the curves of Street and Beams[6] on potential fall in spark gap discharges it is seen that the voltage applied to the lines by the breakdown of G_1 or G_3 can be represented approximately by $e=E(1-\epsilon^{-\delta t})$ where E is the maximum potential, t the time after breakdown starts, and δ is taken as $\frac{1}{2}\times 10^8$ sec.$^{-1}$. With this assumption the voltage impulses for the two circuits are shown in Fig. 2. For part of the

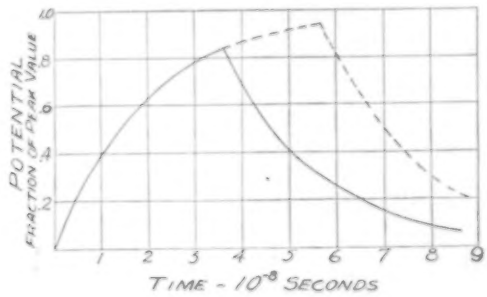

FIG. 2. Computed impulse. Broken curve gives maximum duration of impulse to be expected from circuit in Fig. 1a. Continuous curve gives uniform impulse from circuit in Fig. 1b.

work the gap G_3 was not irradiated by ultraviolet light and was consequently considerably overvolted before discharge took place. This probably resulted in the application of a much steeper wave front than that shown in Fig. 2. Oscillograms of voltage waves in circuits practically identical with this are given by Buss and Masch[7] and by Rosenlocher.[8] The curve of Fig. 2 agrees reasonably well in form with the experimental result. The capacity of the electrode system in the cloud chamber and the inductances and capacities of the input system were found by computation not to alter the wave form appreciably. The current through the cloud chamber was also proven to be insufficient to cause distortion. No oscillations in the lines could be detected. The broken line curve gives the maximum duration of potential impulse to be expected by using the type of circuit shown in Fig. 1a. The continuous curve gives a close approximation to the impulse as applied to the cloud chamber by the circuit shown in Fig. 1b.

The cloud chamber, W_2, is nicely adapted to a study of spark discharges. The expansion occurs in opposite directions at both ends of the cloud chamber. A plane at the electrodes is then undisturbed by motion of the gas in expansion. The operation of this chamber is effected by means of air pressure in the operating bellows. This gives a very flexible and easily adjusted control.

The electrodes in the cloud chamber W_1, which is of the common piston type, consist of a steel needle and a brass plate. They were spaced at 1.1 cm. The point electrode in the chamber W_2 was of tungsten; the plate of brass 3.8 cm in diameter. The spacing of these electrodes is 1.0 cm.

RESULTS

In Fig. 3 are shown typical photographs of the ion distribution occurring during the application of the impulse characterized by the continuous curve in Fig. 2. The point is the negative electrode. The two upper photographs were taken without irradiating the gap G_3. As mentioned above, this gap was probably much overvolted before its breakdown occurred. The wave applied to the electrodes by the breakdown of this gap is probably much steeper than that shown in Fig. 2. The minimum value of the potential, however, must be at least 7.2 kv as determined from this curve assuming the peak potential to be $\frac{1}{2}$ of the static breakdown value of the gap G_3.

[6] J. C. Street and J. W. Beams, Phys. Rev. **38**, 416 (1931).
[7] K. Buss and K. Masch, Archiv. f. Elektrotechnik **25**, 744 (1931).
[8] P. Rosenlocher, Archiv. f. Elektrotechnik **26**, 19 (1932).

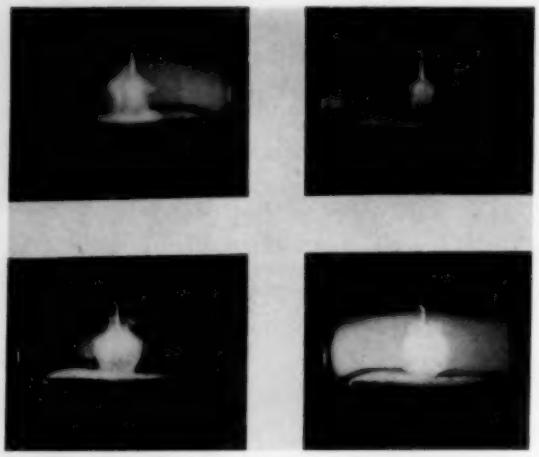

FIG. 3. Ion distribution with negative point. Upper two at a minimum potential of 7.2 kv. Lower two at a peak potential of 15.9 kv. Electrode spacing 1.0 cm.

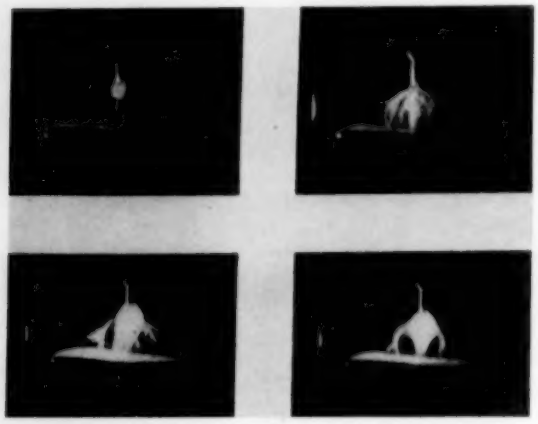

FIG. 4. Ion distribution with positive point. Upper two minimum potential of 7.2 kv. Lower two at a peak potential of 13.0 kv. Electrode spacing 1.0 cm.

The two lower pictures are typical of photographs taken with the gap G_3 irradiated, and set to apply an impulse with a maximum potential of 15.9 kv. With the point negative, the static breakdown potential was determined at 12.8 kv under conditions such as exist in the chamber when the impulse is applied. The two upper pictures in Fig. 3 were therefore taken at a peak voltage below the static breakdown value while, for the lower two, the electrodes are overvolted. The expansion ratio of the chamber is 1.32; a sufficient amount to cause condensation on both positive and negative ions, but not to produce condensation in the chamber unless ions are present. In all cases the chamber is expanded from a pressure of 1 atmos. The diffuse background of condensation, quite apparent in the lower right photograph, is not uncommon when the point is negative.

In Fig. 4 are shown typical photographs obtained with the point electrode positive. The upper pictures were taken under conditions described for the upper photographs in Fig. 3, i.e., a minimum potential of 7.2 kv. The lower photographs were taken with a potential of 13.0 kv. The static breakdown potential for these electrodes, with the point positive, and under conditions existing at the end of the expansion, was determined at 9.3 kv.

Using the set-up shown in Fig. 1a, visual studies were made with a steel point and brass plane. It was found that, with the needle positive, streamers of ionization were obtained with the gap G_1 set at 1.7 mm and the gap G_2 at 1.2 mm. The spacing of the point and plane was 1.1 cm. The steel needle was removed and a polished brass sphere, 3 mm in diameter, was placed in the chamber at the same spacing. Several expansions, with the same potential pulse, produced no ionization in the chamber. No trace of ionization appeared until the potential impulse was increased to a value determined by setting G_1 to 7.2 mm and G_2 to 6.5 mm.

DISCUSSION

When the point is negative, the possibility of field emission from the point as a source of electrons sufficient to start the ionization seems to offer a plausible explanation. In order to estimate the field intensity at the point, photomicrographs of the tungsten and steel needles were made and the field computed using a relation given by Eyring, Mackeown and Millikan.[9] The maximum field intensity as computed with 7.2 kv applied to the electrodes is 6×10^5 volts/cm. Such a field has been observed by many experimenters to give appreciable field currents from points.

A study of the upper right photograph in Fig. 3, in which the point is negative, reveals

[9] Eyring, Mackeown and Millikan, Phys. Rev. **31**, 900 (1928).

that ionization extends out from the point toward the plane a distance of 7 mm. The computed value of X/p at this distance is only 7.8 volts/cm/mm, a value far too low to produce ionization by electron impact. The sharpness of the positive streamers leads us to believe that ionization shows up only close to the region where it is produced. If this is ionization by impact, we must assume that already in this early stage of the discharge the field has been so altered in this region by space charge that ionization by impact is possible.

The diffuse background, which is prominent in some of the photographs (Fig. 3) is never observed without accompanying ionization at the point. It cannot be due to light reflected from the background of the chamber. Nor can it be excess supersaturation, since the expansion ratio of the chamber was accurately controlled. It may be photoionization produced by ultraviolet radiation from the region near the point.

A plausible explanation of the mechanism responsible for the initiation of ionization at the positive point within such short time intervals has not been discovered. The initiation by free electrons in the gas producing ionization by impact as they move into the region of high field near the point seems unlikely in view of the results obtained when the needle was replaced by the 3 mm sphere. By this replacement the field was made more uniform between the electrodes and consequently it was necessary to increase the potential of the applied impulse to produce ionization. This starting potential was found to be quite critical. If it is assumed that an electron moving from a region where X/p =40 volts/cm/mm to a region of higher values will produce ionization by impact, it is difficult to understand the necessity for such an increase in impulse potential before ionization is observed in the case of the sphere. Under conditions where the initiation of ionization occurs, the region where X/p is greater than 40 volts/cm/mm extends out from the sphere surface 2.8 mm, while for the point this distance is 0.35 mm. Unless it is necessary for the electron to move into a region where X/p has a critical and abnormally high value, it seems that such a mechanism for initiating the ionization photographed in Fig. 4 is very improbable. The maximum field under conditions producing ionization, is 4×10^5 volts/cm for the point and 1.5×10^5 volts/cm for the sphere.

It is probable that these starting processes are connected with surface conditions at the electrode. It is known that visual corona is obtained at lower potentials than normal with wet conductors.[10] We have observed that a slight increase in temperature of the positive point increases the potential at which ionization is obtained. However, this increase in temperature was not observed to produce any obvious change in the character of the ion distribution.

It is a pleasure to acknowledge the authors' indebtedness to Professor J. W. Beams who suggested this line of attack on the problem of initiation of spark discharges, and to Professor L. G. Hoxton who made valuable suggestions concerning the design of the cloud chamber.

[10] Peek, *Dielectric Phenomena in High Voltage Engineering*, McGraw-Hill, 1929, p. 76.

An Objective Study of the Allison Magneto-Optic Method of Analysis

MYRON A. JEPPESEN AND RAYMOND M. BELL, *Department of Physics, Pennsylvania State College*

(Received January 15, 1935)

Objective methods have been used to investigate the reliability of the Allison magneto-optic method of analysis. Readings have been taken by a large number of unbiased observers to reduce the personal factor. Probability theory has been introduced to determine how much of the data can be explained as random. Minima in fair agreement with Allison's results have been obtained with the usual set-up, but just as good agreement has been obtained with wrong solutions in the cells, or none at all. This indicates that the minima are not a function of the chemical solutions used.

THE Allison magneto-optic method of chemical analysis[1] has been the subject of considerable discussion. The present study was begun in an attempt to find a satisfactory explanation for the effect. At the time it was started little doubt was entertained as to the existence of an effect, and preliminary results appeared to be favorable. Since the observations consist in the detection of small changes in the intensity of a faint light from a flickering spark gap, the need for objective readings was recognized.

In order to apply objective methods the observer and the scale used for taking readings were placed in different rooms. A second person recorded the readings, and a third person controlled the movement of the trolley. At the same time, the observer was not informed as to the position of the trolley at the beginning or during a set of observations. As soon as the apparatus was in proper adjustment minima were observed, and the readings which occurred most frequently check fairly well with those published by Allison. At no time, however, was it possible to make a setting with absolute certainty. Since continued observations did not increase the certainty of the settings, it seemed advantageous to use large numbers of observers unfamiliar with the apparatus to obtain more objective data. Because of their unfamiliarity, the psychological element was greatly reduced. As each observer looked for only a short period, the troublesome effect of eye fatigue was eliminated.

The data presented in the accompanying curves are the result of some 4000 readings taken over a period of about one year on apparatus similar to that used by Allison. The number of minima observed are plotted against the scale readings at which they occur. Inspection of the curves shows that there are peaks. The question arises as to whether such peaks can be accounted for on the basis of probability. If it is assumed that each setting is equally probable, then from the theory of probability it is practically certain that all peaks which are random will fall within the range, $pn \pm 3(npq)^{\frac{1}{2}}$. In this expression, n is the total number of readings, p the probability that a particular setting will be made, and q the probability that it will not be made. The peaks in each curve which are higher than is predicted on this basis are marked by a square.

Curve *A* (Fig. 1) is the result of readings taken by the writers with chloride solutions in the cells. These data are not entirely objective because the general region in which the settings were made was known to the observers. According to Allison's data this curve should have twelve peaks. Of the eleven which occur, eight check with those published. One of these is higher than would be expected on the basis of probability, and it checks with Allison. Curve *B* (Fig. 2) represents readings taken by 150 observers with no previous experience. The minima were described to each observer before he took any readings. To avoid confusing them with spark flickers a brief preliminary observation was made without moving the trolley. The observer did not know where the minima should occur, nor how many there should be. Another individual controlled the trolley, while still another recorded the settings. The latter did not know what the correct readings should be.

[1] Allison and Murphy, J. Am. Chem. Soc. **52**, 3796 (1930).

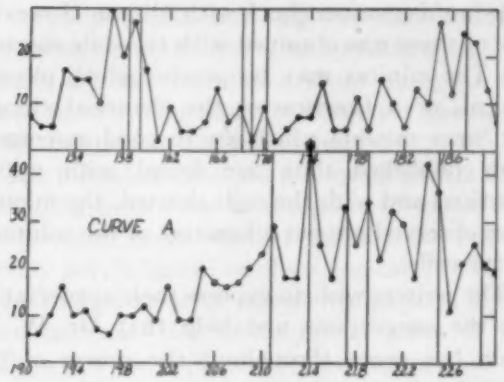

FIG. 1. Curve *A*: 1074 readings taken by the writers using solutions of HCl, $MgCl_2$, NaCl, $ZnCl_2$ and KCl. In all the curves the vertical lines represent values obtained by Allison. Points rising above probability are marked with squares.

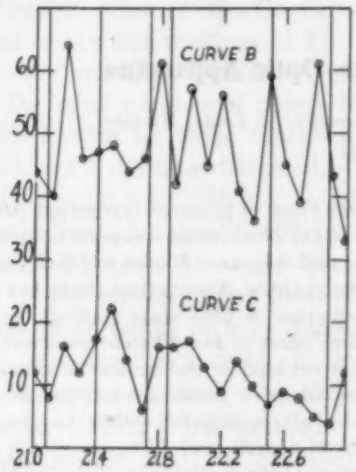

FIG. 2. Curve *B*: 996 readings taken by 150 observers with solutions of $ZnCl_2$ and KCl. Curve *C*: 247 readings taken by three observers with the same solutions.

The zero of the scale was shifted several times to avoid repetition of certain contact minima. This curve should show six peaks. Three of the six which occur are not in agreement with Allison's findings.

To determine whether experience was a factor three students took the readings in curve *C* (Fig. 2) over a period of three months. Their results are not in as good agreement as those in curve *B*. They were unfamiliar with the problem and did not know what the correct readings were. In curve *D* (Fig. 3) are given the results of readings taken by the writers with the coils surrounding the solutions shorted. This modification was known to the observers. The results are similar to those obtained with proper connections. The single peak which rises above probability is also found in curve *A*. Curve *E* (Fig. 3) represents readings taken by 23 students under the conditions described for curve *B*. These readings were taken with the solutions removed from both coils, unknown to the observers. Care was taken to make the intensity the same as under normal conditions. It was thought advisable to discontinue observations before the students discovered the change. For this reason a smaller number of readings was taken than in curve *B*. The results obtained with no solutions check better with Allison's data for chlorides than those obtained by any other of the objective tests.

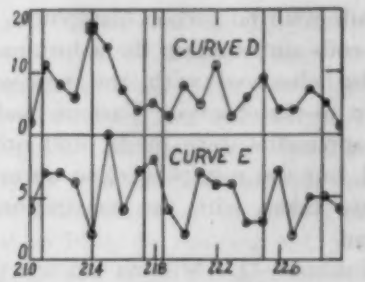

FIG. 3. Curve *D*: 140 readings taken by the writers with the coils shorted. Curve *E*: 110 readings taken by 23 observers with no solutions in the cells.

As a crucial test of this method of analysis it is highly desirable to make changes in the set-up unknown to the observer. Tests with wrong solutions in the cells with the writers as observers gave the following results: (with the region known) 21.10, 21.08, 21.05, 21.38, 21.40, 21.35, 21.40, 21.75, 21.80, 21.70, 21.70, 21.95, 22.20, 22.20, 22.20, 22.45, 22.50, 22.50, 22.85, 22.85. The readings obtained by Allison for the chlorides which the observers thought were in the cells are as follows: 21.08, 21.40, 21.73, 21.85, 22.50, 22.87. The reading which Allison did not report, 22.20, also appears in some of the curves. In one instance, the above modifications were made by visitors from another institution. In no case did the observers know of, or even suspect the changes. Obviously, to be of value, such tests could not be repeated with the same observers, which made it difficult to obtain many readings.

Minima were observed in other non-objective

tests made with no carbon bisulphide, and with smaller coils surrounding the solutions. Minima were also observed with the trolley at rest unknown to the observer. Various modifications in the apparatus were made, and others were planned, but the results were so uncertain that only data taken with the conventional set-up were used.

Conclusions: (1) Minima occur. (2) Some minima check with Allison's data. (3) Most of the minima obtained can be explained by probability on the basis of random settings. It should be pointed out that the two not explainable in this manner check with Allison. However, one of these was obtained with the coils shorted. (4) The minima may be psychological, physiological, or a function of the electrical circuit. (5) Since minima which are in good agreement with published data are found with wrong solutions and with the coils shorted, the minima here observed are not a function of the solutions in the cells.

The writers wish to express their appreciation for the suggestions and help that Dr. W. R. Ham has given throughout the course of the investigation.

APRIL 1, 1935 PHYSICAL REVIEW VOLUME 47

Observations on the Allison Magneto-Optic Apparatus

T. R. BALL, *Chemical Laboratory of Washington University, St. Louis, Missouri*

(Received January 2, 1935)

The Allison magneto-optic apparatus has been subjected to critical tests by the checking of minima reported from other laboratories, by the working of unknowns and by the distribution of scale readings over a given range. About 300 of Allison's minima have been checked. Two sets of three unknowns, prepared in such a way that there was one chance in six of a fortuitous correct solution, have been successfully analyzed. One set in which three salts were chosen out of a list of seven was correctly analyzed after the three had been mixed. The chances were 34 to 1 against a lucky selection of the correct combination. A second set of three out of seven, similarly run, resulted in the identification of only one constituent. The overall average shows 10 out of 12 correctly reported. All unknowns were given to the observer at concentrations of 1 part in 10^7 of water and they were diluted to 1 part in 10^{10} before subjecting to analysis. A statistical study has been made of the distribution of 1698 scale readings, made over a period of three years by five different observers. The readings were plotted against the number of times they were observed and definite peaks are evident in the curve. 84.2 percent of all readings fall within the limits of experimental error of a peak, and 30.1 percent fall on a peak. This is contrary to the results of Slack and of MacPherson, who found only chance distribution.

THE magneto-optic method of analysis has been the subject of a very heated controversy since its discovery by Dr. Fred Allison several years ago. Recently a paper by Francis G. Slack[1] has shown data purporting to prove that the distribution of observed minima, when hydrochloric acid is placed in the observation cell, is similar to that obtained when numbers are drawn at random from a box. In plotting these data the method of Ball and Cooper[2] and of Ball and Crane[3] was followed in which the scale readings for minima are plotted against the number of times they are observed. It is true that Slack's data show nothing more than a random distribution of readings.

An abstract of a paper by H. G. MacPherson[4] read before the Los Angeles meeting of the American Physical Society, Dec. 21 and 22, 1934, in Los Angeles, shows the same results, both by optical and photographic means. The magneto-optic apparatus is admittedly a difficult instrument to use and unless great care is used

[1] Slack, J. Frank. Inst. **218**, 445 (1934).
[2] Ball and Cooper, J. Am. Chem. Soc. **55**, 3207 (1933).
[3] Ball and Crane, J. Am. Chem. Soc. **55**, 4860 (1933).
[4] MacPherson, Phys. Rev. **47**, 254A (1935). Complete paper, Phys. Rev. **47**, 310 (1935).

in its construction and long hours are spent in mastering the technique of its operation, negative results are sure to follow. About one year was spent in this laboratory to construct the apparatus and perfect the technique.

The following data are presented with a view of adding something to the positive side of the controversy as to whether minima are real or merely psychological or physiological.

In the progress of our investigations it has been necessary for us to repeat some of Dr. Allison's work, either because we wished to confirm the data, or with a view of satisfying ourselves that our apparatus was properly calibrated to read directly in Allison units. In all, 162 of these minima have been checked on our apparatus by Mr. S. S. Cooper and 224 by Mr. R. E. Wingard. Most of Mr. Cooper's data are duplicated in the 224 readings of Mr. Wingard, but there are enough which are not duplicates to bring the total number of points checked to about 300. Except for some confusion between cobalt and nickel minima, discussed by Ball and Cooper in the article referred to above, our results have been practically 100 percent confirmatory of Allison's. It might be mentioned that our trolley system differs from Allison's in that it has three banks of wire instead of two. This was necessary because of the small room in which our apparatus had to be placed.

In February, 1933, solutions of three different substituted benzoic acids, at concentrations of one part in 10^9 were taken to Auburn by the author, and three different observers who knew nothing regarding the position of the minima which had been found in our laboratory by Mr. Cooper, checked the results to within 0.01 to 0.02 Allison units. In making these tests the trolley was set about a foot off the position of the minima and the observer was told which way to move the trolley. No other information was given. In all, six minima were checked by each of three observers. These acids had not been studied at Auburn.

The only published report of the identification of unknowns by the magneto-optic method is by McGhee and Lawrenz.[5] They state that "in December, 1930, one of us (McGhee) handed out by number to Professor Allison twelve (to him) "unknowns" which were tested by him and checked by two assistants 100 percent correctly in three hours." As a further check upon the objectivity of the method and its reliability, four sets of unknowns were run in this laboratory in the fall of 1934. In the first set, the author received from Mr. S. S. Cooper and Mr. R. E. Wingard a list of three salts whose minima had been checked on our apparatus. Solutions of these were made up in separate flasks at concentrations of one part in 10^7. These flasks were numbered and left in the laboratory in the late afternoon after the two who were to make the identification had left. During the evening, these solutions, after dilution to one part in 10^{10}, were run separately by each observer and the name of the compound in each flask determined from the observed minima The report was made by telephone to the author's home on all three salts at once and the results were entirely correct.

In order to guard against the accusation made by Slack that in working unknowns at Auburn, a hint was given, unconsciously, by a second party, the one who made up the unknowns purposely absented himself from the laboratory while the tests were being made and had no contact with the observers after the list of salts was submitted. This applies to subsequent tests as well.

A second set of three salts or acids was run in exactly the same manner as the above and each solution was again correctly identified. There are six ways in which three solutions may be arranged so that the observers had only one chance in six of making a lucky guess on each set.

At a later date, a list of seven salts and acids was submitted by Messrs. Cooper and Wingard. Three of these were chosen at random by the author and solutions were made up containing one part in 10^7 in three flasks which bore no identification mark. The observers mixed the three and diluted the resulting solution so that each constituent was present in one part in 10^{10} of water. The search was then made over the scale regions in which the minima of each of the seven salts are known to be found, the observers knowing that three compounds would be present. In this test, one observer recorded the readings

[5] McGhee and Lawrenz, J. Am. Chem. Soc. **54**, 405 (1932).

of the other without informing him as to the settings he was making. They worked alternately at the instrument and when each had satisfied himself that he had read three groups of minima, their results were compared. The field of all seven salts was covered carefully but only three sets of minima appeared. Both observers had read the same minima and their results were reported by telephone. Again the report was correct. There are thirty-five combinations of three out of seven, making the odds 34 to 1 against a chance selection of the correct combination.

A second set of three salts out of seven was prepared and the tests carried out exactly as described above. This time, however, the results were not entirely satisfactory; one out of the three was correctly reported. There were some mitigating circumstances in connection with these tests which may partially account for the failure. However, we prefer to let it stand as it is without offering any explanation. Even with this failure, ten out of a possible twelve have been correctly identified giving an overall average of 83.3 percent. Previous tests by Ball, Crane and Cooper had shown about the same overall average on tests similarly carried out about two years ago. When it is considered that there was under observation 30 ml of a solution containing only one part of salt in 10^{10} of water, or 3×10^{-9} grams, it is doubtful if any other known method would be as successful in identifying the compounds present. In most published articles involving the recording of numerous data, those which are obviously wrong never find their way into print. It would be interesting to know what percentage of readings have to be discarded.

We have heard indirectly that the above method of preparing unknowns from a limited list has been adversely criticized on the ground that the observers knew what compounds were

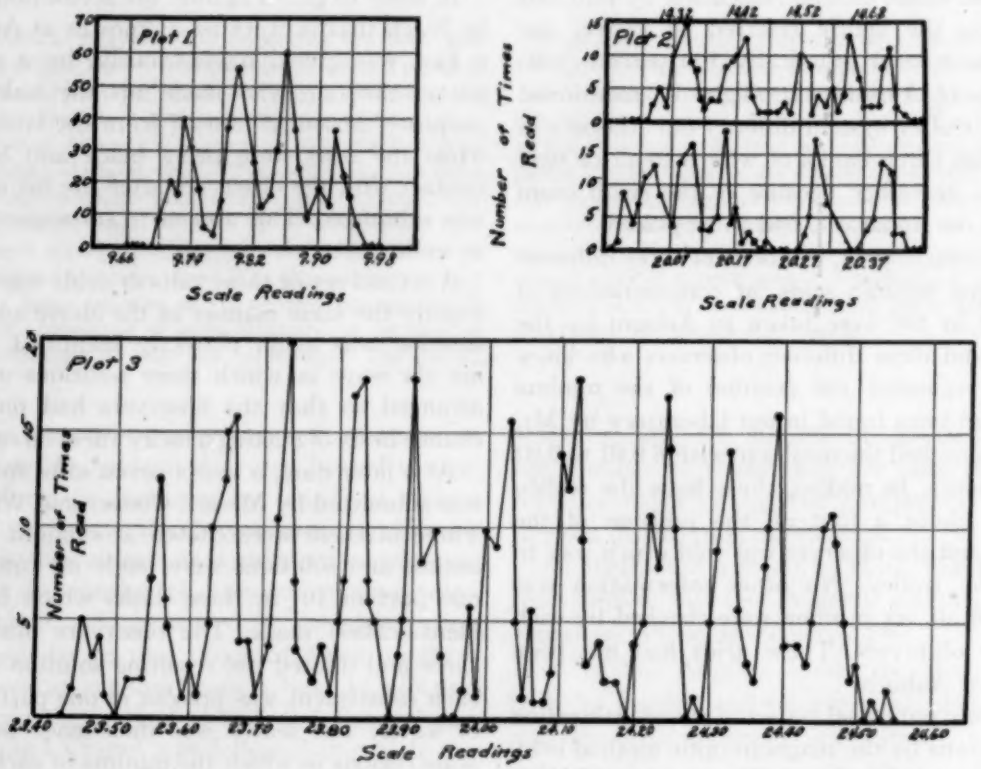

FIG. 1. Plot No. 1. Scale readings plotted against frequency of observation. Pentavalent chromium sulfate; Plot No. 2. Frequency distribution of readings for cobalt and nickel mixed sulfates (upper graph) and chlorides (lower graph); Plot No. 3. Frequency distribution of observations on oxidation products of stannous chloride.

present. This would scarcely need an answer if everyone were familiar with the method of operation. The full range in which minima might be found, if there were no limitation, would extend over 9.9 meters of trolley scale and the settings would have to be made within a space of 2 or 3 millimeters. Obviously this would be a very time consuming task.

Slack and MacPherson, whose work has already been cited, have found the distribution of observed minima merely one of chance. The accompanying plots of some of the data obtained in this laboratory show quite a different result (Fig. 1). Plot No. 1 shows a curve in which scale readings are plotted against the number of times they were observed. These readings were taken by Mr. Keith D. Crane in 1932 and have been interpreted as being due to pentavalent chromium sulfate. This curve has been published elsewhere, and since we are interested here in the distribution of minima only, we shall omit any chemical interpretation. In all, 615 readings are involved and 31 percent fall on a peak of the curve and 93.4 percent fall within 0.02 scale division of a peak. This is 3 mm. In getting the data, no reading was ever discarded. This applies to subsequent graphs as well.

The upper and lower graphs of Plot 2 show the distribution of readings for cobalt and nickel (mixed) sulfates and chlorides, respectively. These data were obtained by Ball and Cooper in 1933, with a few readings by Crane. There are 454 recorded settings and 81 percent fall within 0.02 scale division of a peak.

Plot No. 3 is made from the unpublished data obtained by Mr. Walter Wulfkuehler in this laboratory in 1934 in a study of the oxidation products of stannous chloride. The minima are interpreted as being due to the chloride of trivalent tin. There are 629 readings, 77.5 percent of which fall within 0.02 unit of a peak. In making the computation the small peak at the extreme left is disregarded, as all of the readings in that region were obtained on the first solution studied and they did not appear from the many other solutions involved in later readings. They may, therefore, be assumed to be due to something other than a tin salt.

An overall analysis of the data of these four plots shows that 1698 readings have been recorded from the work of four different observers, and that 84.2 percent fall within 0.02 scale division of some peak and 30.1 percent fall on a peak. It must be remembered that the trolley is moving at the time the observation is made and the physiological time lag in stopping the motion frequently causes the exact position of the minima to be over-shot. By approaching the position from both sides a very uniform distribution is obtained on either side of the peak.

There can be no doubt but that some of the readings recorded above are spurious and are due to deceptive spark flickers. We believe, however, that these are reduced to a minimum as it has always been our custom to re-explore the immediate region in which an indication of a minimum has been obtained and to disregard it unless it can be seen to recur. Thus, the 1698 minima which are recorded really represent from two to three times that many observations. There could be no preferential selection of readings by this method because each initial indication of a minimum is treated exactly like every other. Contrary to the conclusions of Slack and of MacPherson, the above graphs certainly show distributions that are not merely those of chance. The identification of unknowns also indicates that the positions of the minima are a function of the solution placed in the cell and are not merely the result of retinal fatigue as has been suggested by several critics. While we realize that our results have not been perfect, there is certainly incontrovertible evidence of the reproducibility and reliability of the magneto-optic method.

Some Studies Concerning Rotating Axes and Polyatomic Molecules

CARL ECKART, *University of Chicago and Institute for Advanced Study*

(Received February 18, 1935)

The theory of small vibrations when the potential energy is invariant under the rotation-displacement group is developed. The results are compared with the Brester-Wigner theory of the normal coordinates, and it is shown that the use of these coordinates implies the use of a particular (normal) system of rotating axes whose construction is given. It is shown that when the motion of a normal molecule is referred to these axes, those terms of the Hamiltonian which are linear in the angular momenta will be especially small and of the same order of magnitude as the quadratic terms (Casimir's condition). When the amplitude of one or more of the normal vibrations becomes large, this is no longer true of the normal axes; this will always be the case when one of the normal frequencies is small compared to the others, as has been noted by other writers. The normal axes are not the principal axes of inertia of the instantaneous configuration of the system, and certain conclusions recently published by the author are wrong for that reason.

1. INTRODUCTION

IN the theory of polyatomic molecules, free use is made of the possibility of referring the positions of the individual atoms to rotating axes. It has become conventional to suppose that these axes satisfy two conditions, but, so far as I am aware, no investigation has shown that these two conditions are compatible, nor has any construction been given for finding the axes which satisfy them. The present paper will give a construction for finding these axes for normal molecules; it is doubtful if such axes exist for anomalous molecules.

The first of the two conditions was formulated by Casimir[1] and depends on the fact that the Hamiltonian will always be a quadratic function of the components of the total angular momentum along the moving axes. This function will always have terms of the zeroth, first and second degrees in these components. If the molecule is quasi-rigid, and the quantum conditions are taken into account, the division into terms of zeroth, first and second orders for the purpose of a perturbation calculation will ordinarily coincide with the division into degrees just mentioned. Casimir showed that it was plausible to suppose that a particular coordinate system could be found such that the terms of the first degree were exceptionally small and of the same order of magnitude as the quadratic terms.

The second condition on the coordinate axes has entered the theory in a somewhat casual manner. It is automatically imposed by the ordinary use of those normal coordinates introduced by Wigner[2] and Brester,[3] and can be avoided only by extraordinary care. The normal coordinates may be defined as linear functions of the cartesian coordinates in a particular set of rotating axes. Conversely, the coordinates in this set of axes are linear functions of the normal coordinates, the coefficients of which have been tabulated by Brester. If another set of rotating axes is used, the cartesian coordinates will not in general be linear functions of the normal coordinates, or if this should accidentally be the case, the coefficients will not be those tabulated by Brester. Another set of considerations enters to obscure this rather simple relation: the normal coordinates are supposed to have infinitesimal values in those cases where they are actually used. Then Taylor's theorem is invoked to make it plausible to suppose that the functions mentioned will be linear in every case. This does not alter the fact that their coefficients will have Brester's values only in rare cases. Furthermore, it is a troublesome fact that the functions (direction cosines) involved in the transformation from one set of cartesian axes to another will have branch points; it is therefore not clear that the use of Taylor's theorem is justified. To summarize: it may be said that the use of the normal coordinates practically implies the use of one definite set of rotating axes. The question

[1] H. B. G. Casimir, *The Rotation of a Rigid Body in Quantum Mechanics*, Chap. V. Dissertation, Leyden (1931).

[2] E. Wigner, *Göttinger Nachrichten*, p. 133 (1930).

[3] C. J. Brester, *Kristallsymmetrie und Restrahlen*. Dissertation, Utrecht (1923).

arises: is Casimir's condition fulfilled by this set? This will be shown to be the case provided only that none of the normal frequencies is unusually small, or what amounts to the same thing, that none of the normal vibrations has an unusually large amplitude.

A survey of the literature discloses no previous investigation of this problem, but seems to indicate that different authors have held divergent opinions as to the probable outcome of such an investigation. Many of these opinions are not clearly expressed but must be deduced from the analytic procedure adopted. In a recent paper, I have studied the use of the principal axes of inertia as the rotating axes.[4] I was led to this by the erroneous belief that it was this system that is associated to the normal coordinates, and that Casimir's condition would be fulfilled provided only that the molecule is quasi-rigid. After publication, it was noticed that this belief was wrong, and that therefore the usual methods of calculation need modification when used with this system of axes. Professors Casimir and Van Vleck have both considered these modifications and shown that one of my conclusions was wrong. The latter has recently published an account[5] of his calculations which contains an excellent explanation of the matter. Apparently no one noticed that the axes are not those associated to the normal coordinates, but a comment from Professor W. V. Houston led directly to a recognition of this fact.

2. The General Transformation to Rotating Axes

When the motion of a system of particles is referred to a moving set of cartesian axes, the latter may be defined in several ways: (1) As an explicit function of the time only; (2) as an explicit function of the instantaneous positions of the particles only; (3) in more general ways. The first method of definition is treated fully in the standard texts on dynamics, but is quite irrelevant to the molecular problem. In this section it is proposed to give an account of the second.

Let the mass of the ath atom ($a=1, 2\cdots N$) be m_a and its coordinate vector (from a fixed origin) be $\mathbf{x}_a$. If the unit vectors along fixed axes are $\mathbf{e}_i$ ($i=x, y, z$) then

$$\mathbf{x}_a=\sum_i \mathbf{e}_i x_{ia}. \tag{1}$$

Suppose that a moving system of axes has been defined in some way which need not be specified further at the moment than to say that its origin is at the point $\mathbf{X}=\sum_i \mathbf{e}_i X_i$ and that unit vectors along its axes are $\boldsymbol{\varepsilon}_j$. It is convenient to suppose at the outset that the origin $\mathbf{X}$ is at the center of mass of the molecule and that both fixed and moving systems are right-handed. Then the Eq. (1) may also be written

$$\mathbf{x}_a-\mathbf{X}=\sum_j \boldsymbol{\varepsilon}_j y_{ja}$$

or

$$x_{ia}-X_i=\sum_j c_{ij} y_{ja}, \tag{2}$$

where

$$c_{ij}=\mathbf{e}_i\cdot\boldsymbol{\varepsilon}_j$$

are the direction cosines of the moving axes and the y_{ja} are the components of the vectors $\mathbf{x}_a-\mathbf{X}$ along the moving axes.

The specification of the instantaneous position of the moving axes requires six numbers, which may be taken to be the three X_i and the Eulerian angles of $\boldsymbol{\varepsilon}_j$. There being $3N$ of the quantities x_{ia}, it follows that at most $3N-6$ of the y_{ja} are independent and that they may be expressed as functions of $3N-6$ generalized coordinates q_λ. The y_{ja} will thus satisfy six equations identically in the q_λ; three of these will be

$$\sum_a m_a y_{ja}=0, \tag{3}$$

and the others will be left in the undetermined form

$$Y_i(y_{ja})=0. \tag{4}$$

These last equations constitute the definition of the moving system.

The vectors $\boldsymbol{\varepsilon}_j$ are functions of the Eulerian angles only, and through these, of the time. As they vary, they remain of unit length and mutually perpendicular; from this it follows that

$$d\boldsymbol{\varepsilon}_j/dt=\Omega\times\boldsymbol{\varepsilon}_j, \tag{5}$$

where Ω is the angular velocity of the moving axes. It is a linear function of the time-derivatives of the Eulerian angles but depends on the angles themselves in a somewhat complicated way,

[4] C. Eckart, Phys. Rev. **46**, 383 (1934).
[5] J. H. Van Vleck, Phys. Rev. **47**, 487 (1935).

described in all standard texts. From Eq. (5) it follows that

$$d(\mathbf{x}_a-\mathbf{X})/dt=\sum_j(\Omega\times\epsilon_j y_{ja}+\epsilon_j\dot{y}_{ja}),$$

and hence that the angular momentum about the center of mass is

$$\mathbf{M}=\sum_a\sum_i\sum_j m_a(\epsilon_i y_{ia})\times(\Omega\times\epsilon_j y_{ja}+\epsilon_j\dot{y}_{ja}). \quad (6)$$

It is important to note at the outset that when $\Omega=0$, $\mathbf{M}$ is not zero but equal to

$$\Lambda=\sum_a m_a\{\epsilon_x(y_{ya}\dot{y}_{za}-y_{za}\dot{y}_{ya})+\cdots\}. \quad (7)$$

Λ can be defined by the same formula when $\Omega\neq0$ and is then the angular momentum of the atoms relative to the moving axes. It is necessary to distinguish this from the components of the total angular momentum in the moving system, which are M_j and defined by $\mathbf{M}=\sum_j\epsilon_j M_j$. Similar equations define the components of Λ and Ω in the moving system; in terms of these, Eq. (6) may be written

$$M_i=\sum_j A_{ij}\Omega_j+\Lambda_i, \quad (8)$$

where

$$A_{xx}=\sum_a m_a(y_{ya}^2+y_{za}^2),$$

$$A_{xy}=-\sum_a m_a y_{za}y_{ya}, \quad \text{etc.}$$

are the components of the moment of inertia tensor in the moving system. Eq. (7) may also be written

$$\Lambda_i=\sum_\lambda\dot{q}_\lambda B_{\lambda i}, \quad (9)$$

where

$$B_{\lambda x}=\sum_a m_a[y_{ya}(\partial y_{za}/\partial q_\lambda)-y_{za}(\partial y_{ya}/\partial q_\lambda)], \quad \text{etc.} \quad (10)$$

The kinetic energy, T (after ignoring the energy of the center of mass) is given by

$$2T=\sum_a m_a[d(\mathbf{x}_a-\mathbf{X})/dt]^2$$
$$=\sum_i\sum_j A_{ij}\Omega_i\Omega_j+2\sum_i\sum_\lambda\dot{q}_\lambda B_{\lambda i}\Omega_i+\sum_\lambda\sum_\mu C_{\lambda\mu}\dot{q}_\lambda\dot{q}_\mu,$$

where $C_{\lambda\mu}=\sum_i\sum_\mu m_a(\partial y_{ia}/\partial q_\lambda)(\partial y_{ia}/\partial q_\mu)$.

From this it follows that the momentum conjugate to q_λ is

$$p_\lambda=\sum_\mu C_{\lambda\mu}\dot{q}_\mu+\sum_i B_{\lambda i}\Omega_i. \quad (11)$$

It is to be noted that $p_\lambda\neq0$ when $\dot{q}_\lambda=0$; the general analogy between the Coriolis forces and a magnetic field becomes apparent in these equations. To find the Hamiltonian kinetic energy it is necessary to solve Eqs. (8), (9) and (11) for Ω_i and $\dot{q}_\mu$ in terms of M_i and p_λ. The solution will be given only for the case $C_{\lambda\mu}=\delta_{\lambda\mu}$, which is sufficiently general to illustrate the important points:

$$\Omega_i=\sum_j\alpha_{ij}M_j-\sum_\lambda p_\lambda\beta_{\lambda i},$$

$$\dot{q}_\lambda=\sum_\mu\gamma_{\lambda\mu}p_\mu-\sum_i\beta_{\lambda i}M_i,$$

where

$$A_{ij}-\sum_\lambda B_{\lambda i}B_{\lambda j}=(\alpha^{-1})_{ij},$$

$$\beta_{\lambda i}=\sum_j B_{\lambda j}\alpha_{ji},$$

$$\gamma_{\lambda\mu}=\delta_{\lambda\mu}+\sum_j B_{\lambda j}\beta_{\mu j}.$$

From this the Hamiltonian kinetic energy is obtained as

$$2T=\sum_i\sum_j\alpha_{ij}M_iM_j-2\sum_\lambda\sum_i p_\lambda\beta_{\lambda i}M_i+\sum_\lambda\sum_\mu\gamma_{\lambda\mu}p_\lambda p_\mu. \quad (12)$$

It will at once occur to the reader that a sure way of satisfying Casimir's condition is to require $\beta_{\lambda i}=0$ for all q_λ, which amounts to requiring $B_{\lambda i}=0$. These are $3N-6$ differential equations for the, as yet undefined, y_{ja}. However, it is probable that these equations possess more than six integrals independent of q_λ, and it has been seen that only this number of identities in the y_{ja} is permissible. The probability of this event becomes apparent on noting that the condition is equivalent to $\Lambda_i=0$, and the possibility of securing this for all q_λ and $\dot{q}_\lambda$ by a definition depending only on the positions of the particles is not reasonable. It is, however, always possible to require that $B_{\lambda i}=0$ for one definite set of values of q_λ. This no longer restricts the definition of the y_{ja} to an impossible extent. It is then reasonable to suppose that those terms of the kinetic energy which are linear in M_i will be especially small for those values of q_λ near the chosen set. If this is also the region in which the motion of the system takes place, a first step in the direction of fulfilling Casimir's condition will have been taken. This matter will be considered in greater detail at the end of the next section.

3. The Theory of Small Vibrations when the Potential Energy is Invariant under the Rotation-Displacement Group

The usual theory of small vibrations considers only two cases:[6] (1) All coordinates vary only by infinitesimal amounts; (2) those coordinates which vary by finite amounts are ignorable. Neither case is realized by the polyatomic molecule; the Eulerian angles vary by finite amounts and are not ignorable, since the kinetic energy depends on the components of the total angular momentum in the moving system, which are not integrals of the motion. The potential energy is independent of these angles, however, so the most general case is not yet at hand. It is none the less necessary to build the theory from first principles, and little reliance may be placed on analogies with the results proven in the standard texts.

The invariance of the potential energy U under the rotation-displacement group results in

$$U(x_{ia}') = U(x_{ia})$$

whenever $$x_{ia}' = \sum_j R_{ij} x_{ja} + \xi_i,$$

where R_{ij} is an arbitrary rotation matrix and ξ_i the components of an arbitrary vector. According to the general postulate of the theory of small vibrations, U is supposed to have a minimum for some configuration $x_{ia} = z_{ia}$; because of the invariance, it will have this same minimum value for a six-dimensional continuum of other configurations, and any one of these might be chosen for the following considerations. It is well to make the choice somewhat carefully, and to require z_{ia} to be a configuration whose center of mass is at the origin, and whose principal axes are parallel to the fixed coordinate axes.

Since U is supposed not to have a singularity at z_{ia} it may be expanded in the form

$$U(z_{ia} + \delta z_{ia}) = U(z_{ia}) + A \sum_\lambda (\omega_\lambda \delta q_\lambda)^2, \quad (13)$$

where $$\delta q_\lambda = \sum_i \sum_a q_{\lambda ia} \delta z_{ia} \quad (14)$$

are linearly independent functions. The quantities A and ω_λ are positive constants not equal to zero, but whose values are as yet quite arbitrary. The coefficients $q_{\lambda ia}$ are also arbitrary to a certain extent: to see this, note that Eq. (13) remains quite unchanged if the quantities $(\omega_\lambda \delta q_\lambda)$ are subjected to an orthogonal substitution. This may be utilized later to normalize the definition of the δq_λ. The $q_{\lambda ia}$ are not entirely without restriction, however; the most important arises from the invariance of U: the most general infinitesimal rotation-displacement is given by

$$\delta z_{xa} = \delta \xi_x + \delta \Omega_y z_{za} - \delta \Omega_z z_{ya}, \quad \text{etc.}, \quad (15)$$

where $\delta\xi$ and $\delta\Omega$ are six arbitrary infinitesimals. If these values of δz are substituted into Eq. (14) the δq must vanish, since otherwise $U(z+\delta z) \neq U(z)$. This results in the equations

$$\sum_a q_{\lambda ia} = 0, \quad \sum_a (z_{ia} q_{\lambda ja} - z_{ja} q_{\lambda ia}) = 0. \quad (16)$$

These will be linearly independent unless all N of the points z_a lie in a straight line, i.e., unless the equilibrium configuration of the molecule is linear. This case will be excluded from further consideration. It follows that there are at most $3N-6$ of the δq_λ; it will also be supposed that this maximum is reached. There will thus be many solutions of Eq. (14), all of the form

$$\delta z_{ia} = \sum_\lambda \delta q_\lambda z_{\lambda ia}.$$

The difference between any two of these will have the form of the right side of Eq. (15), $\delta\xi$ and $\delta\Omega$ now representing linear functions of the δq, determined by the two solutions in question. It is thus seen that the $z_{\lambda ia}$ are arbitrary to a greater extent than the $q_{\lambda ia}$.

To remove this additional arbitrariness, it is necessary to impose six linear equations on the $z_{\lambda ia}$ for every value of λ. These may be taken to be

$$\sum_a m_a z_{\lambda ia} = 0, \quad (17)$$

$$\sum_j \sum_a Y_{ija} z_{\lambda ja} = 0, \quad (18)$$

where the Y_{ija} are $9N$ numbers restricted only by the requirement that a certain determinant shall not vanish. This determinant has the matrix

$$Z_{iz} = \sum_a (Y_{iya} z_{xa} - Y_{ixa} z_{ya}), \quad \text{etc.}$$

These equations are all invariant under a change of normalization, and this may now be carried out so that

$$\sum_i \sum_a m_a z_{\lambda ia} z_{\mu ia} = A \delta_{\lambda\mu}, \quad (19)$$

[6] See, e.g., E. T. Whittaker, *Analytical Mechanics*, Chap. VII; 3rd ed., Cambridge (1927).

provided that the ω_λ are given certain values determined by the form of the potential energy function and called the normal frequencies. The constant A in Eq. (19) must have the same value as in Eq. (13), but is otherwise arbitrary. If it is given the dimensions of a moment of inertia, the δq will be dimensionless and $z_{\lambda ia}$ will have the dimensions of a length.

It will now be shown that it is always possible to define a system of rotating axes such that

$$y_{ja} = z_{ja} + \sum_\lambda q_\lambda z_{\lambda ja}. \tag{20}$$

For Eq. (3) is fulfilled because of the choice of the z_{ia} and Eq. (17). The definition of the axes is obtained by eliminating the q from Eq. (20) and is

$$\sum_i \sum_a Y_{ija}(y_{ja} - z_{ja}) = 0. \tag{21}$$

The quantities determining the kinetic energy are readily computed and have the form

$$\begin{aligned} A_{ij} &= A_i \delta_{ij} + \sum_\lambda q_\lambda A_{\lambda ij} + \sum_\lambda \sum_\mu q_\lambda q_\mu A_{\lambda\mu ij}, \\ B_{\lambda i} &= B_{\lambda i}^{(0)} + \sum_\mu q_\mu B_{\lambda\mu i}, \\ C_{\lambda\mu} &= A \delta_{\lambda\mu}. \end{aligned} \tag{22}$$

The coefficients of these equations are functions of z_{ia} and $z_{\lambda ia}$ only; all of the A's are symmetric in i and j, while $B_{\lambda\mu i} = -B_{\mu\lambda i}$.

It is now possible to consider the relation between the coordinate systems just defined (they will be called linear systems, since their defining equations are linear) and more general systems, defined by Eqs. (4). It is supposed that these latter are satisfied by $y_{ja} = z_{ja}$; then for small values of $y_{ja} - z_{ja}$ they are approximately the same as Eqs. (21) with

$$Y_{ija} = \text{const.} \times (\partial Y_i / \partial y_{ja})_{y=z}. \tag{23}$$

In general there is thus a linear system which differs from a given system only by quantities of the second order in $(y_{ja} - z_{ja})$. This approximate set of axes is uniquely determined by the original definition, and other linear systems differ from it by quantities of the first order. Occasionally, however, no such approximate linear system exists: this is true whenever the Z-determinant vanishes.

These matters may be illustrated by the principal axes, for which

$$Y_x(y_{ja}) = \sum_a m_a y_{ya} y_{za}, \quad \text{etc.},$$

and the approximate set is defined by

$$\sum_a m_a (y_{ia} z_{ja} + y_{ja} z_{ia}) = 0, \quad i \neq j. \tag{24}$$

In this case, the Eqs. (22) are somewhat simplified because Eqs. (24) are equivalent to $A_{\lambda ij} = 0$. The Z-determinant is $(A_x - A_y)(A_y - A_z) \times (A_z - A_x)$, so that no approximate set exists when two or more of the principal moments of inertia are equal at equilibrium.

It is also possible to carry the considerations of the end of the preceding section to a conclusion: let it be required to find a linear set of axes for which $B_{\lambda i} = 0$ when $q_\lambda = 0$. This can be done by choosing the Y_{ija} so that Eq. (18) reduces to $B_{\lambda i}^{(0)} = 0$, which is explicitly

$$\sum_a m_a (z_{ia} z_{\lambda ja} - z_{ja} z_{\lambda ia}) = 0. \tag{25}$$

This requires that

$$Y_{zza} = 0, \quad Y_{zya} = -Y_{yza} = m_a z_{xa}, \quad \text{etc.}$$

The Z-determinant is now simply $A_x A_y A_z$, and cannot vanish since the linear molecules have been excluded. Eq. (21) becomes

$$\sum_a m_a (z_{ia} y_{ja} - z_{ja} y_{ia}) = 0,$$

or, because of Eq. (2)

$$\sum_k (F_{ki} c_{kj} - F_{kj} c_{ki}) = 0, \tag{26}$$

where $$F_{ki} = \sum_a m_a (x_{ka} - X_k) z_{ia}.$$

These results can be given a geometric interpretation: defining the three vectors $\mathbf{F}_i = \sum_k \mathbf{e}_k F_{ki}$, Eq. (26) becomes

$$\mathbf{F}_i \cdot \mathbf{e}_j = \mathbf{F}_j \cdot \mathbf{e}_i. \tag{27}$$

The vectors $\mathbf{F}_i$ can be determined before the rotating axes are known; Eq. (27) states that these are defined so that the projection of $\mathbf{F}_x$ on the y axis is equal to the projection of $\mathbf{F}_y$ on the x axis, etc. The analytical procedure for finding them is not much more complicated than that for finding the principal axes: Eq. (27) is equivalent to

$$\mathbf{F}_i = \sum_j f_{ij} \mathbf{e}_j, \quad f_{ij} = f_{ji}$$

and the symmetric matrix f_{ij} can be determined from

$$\mathbf{F}_i \cdot \mathbf{F}_j = \sum_k f_{ik} f_{kj}.$$

It is thus the square root of the Gram matrix of the vectors **F**. Its elements will always be real, since the characteristic values of the Gram matrix can never be negative. If none of these are zero, the **F** will not be coplanar, and the solution of Eq. (27) will be simply

$$\varepsilon_i = \sum_j f_{ij}[\mathbf{F}_j],$$

where the $[\mathbf{F}_j]$ are the vectors reciprocal to the $\mathbf{F}_i$. For the important special case of molecules having a plane configuration, one of the vectors **F** will vanish identically. It can be shown that in this case two of the vectors ε are in the plane of the non-vanishing **F** and the third perpendicular to it.

This system of axes will be called the normal system, and its associated q_λ the normal coordinates; this does not conflict with established custom, since it will be shown in Section 5 that these are the coordinates studied by Brester and Wigner.

4. Casimir's Condition

It will now be shown that the normal axes satisfy Casimir's condition except in the case of molecules which are not really to be considered as rigid. In doing so, free use will be made of a proposition which is strictly true only in classical mechanics, and whose extension to quantum mechanics involves assumptions which have not been adequately studied. This is the proposition that, when the energy of the system is small only those values of $y_{j\alpha}$ need be considered which differ from $z_{j\alpha}$ by small amounts. If the arbitrary constant A be chosen to have a value of the order of magnitude of the A_i, this is equivalent to considering only values of q_λ which are much less than unity.

The Eqs. (8) and (11) may be written, in the case of the normal axes,

$$M_i = A_i\Omega_i + \sum_j\sum_\lambda q_\lambda A_{\lambda ij}\Omega_j + \sum_j\sum_\lambda\sum_\mu q_\lambda q_\mu A_{\lambda\mu ij}\Omega_j + \sum_\lambda\sum_\mu \dot{q}_\lambda q_\mu B_{\lambda\mu i},$$

$$p_\lambda = A\dot{q}_\lambda + \sum_\mu\sum_i q_\mu B_{\lambda\mu i}\Omega_i.$$

The A's and B's are all independent of the q_λ and the Eulerian angles and all have the order of magnitude of A. The solution of these equations may be written

$$\dot{q}_\lambda = (p_\lambda - \sum_i\sum_\mu q_\mu B_{\lambda\mu i}\Omega_i)/A,$$

$$\Omega_i = (M_i - \Lambda_i')/A + \sum_j(\sum_\lambda q_\lambda a_{\lambda ij} + \cdots)(M_j - \Lambda_j'),$$

$$\Lambda_j' = \sum\sum_{\lambda>\mu}(p_\lambda q_\mu - p_\mu q_\lambda)B_{\lambda\mu i}/A.$$

Here Λ_i' must not be confused with the previous Λ_i, from which it differs by terms of the order of pq^2; the dots in the second equation indicate quantities of the order of magnitude q^2/A or smaller, and the constants $a_{\lambda ij}$ have the magnitude $1/A$ and can easily be calculated explicitly. The expression for the kinetic energy is

$$2T = \sum_\lambda p_\lambda^2/A + \sum_i(M_i - \Lambda_i')^2/A_i + \sum_\lambda\sum_i\sum_j q_\lambda a_{\lambda ij}(M_i - \Lambda_i')(M_j - \Lambda_j') + \cdots. \tag{28}$$

It is now necessary to investigate the order of magnitude of the terms entering into this expression. It may be supposed that

$$q_\lambda \sim (\hbar/A\omega_\lambda)^{\frac{1}{2}}, \quad p_\lambda \sim (\hbar A\omega_\lambda)^{\frac{1}{2}}.$$

Furthermore, $M_i \sim \hbar$ and it is easily seen that

$$p_\lambda q_\mu \sim \hbar(\omega_\lambda/\omega_\mu)^{\frac{1}{2}}. \tag{29}$$

If all the normal frequencies are of the same order of magnitude, it follows that $\Lambda_i' \sim \hbar$. The quantity $\epsilon \sim (\hbar/A\omega_\lambda)^{\frac{1}{2}}$ may be taken as the perturbation parameter, and the three sums of Eq. (28) are of the order $\hbar\omega$, $\epsilon^2\hbar\omega$ and $\epsilon^3\hbar\omega$, respectively. Casimir's condition is thus fulfilled.

It may happen that one of the normal frequencies is much smaller than the others, in which case Eq. (29) indicates that some of the terms in Λ_i' will have an undesirably large value. This situation has come to be known as the "phenomenon of slip." In this case also, the amplitude of variation of the corresponding normal coordinate will no longer be small, and the molecule can no longer be called quasi-rigid. It may thus be said that the normal system satisfies Casimir's condition for all quasi-rigid molecules, this being really a definition of quasi-rigidity. It is doubtful whether it will ever be necessary to consider any other linear system of axes in connection with the molecular problem, for when the normal axes are not suited for its discussion, it is not clear that any other linear system will be better adapted to the purpose.

5. The Symmetry of the Normal Coordinates

The discussion of the normal coordinates given by Brester and Wigner[2, 3] differs from that given here in certain formal respects, and it must be shown that the two lead to identical definitions. In the quadratic form of Eq. (13), the ω_λ have here been supposed not to be zero, and as a consequence, there are only $3N-6$ of the δq's. Brester and Wigner, on the other hand, require the form to depend on $3N$ δq's, and consequently must admit the value zero as possible for ω_λ. This is always permissible, but there is then an arbitrariness in the six additional δq's which corresponds exactly to the arbitrariness in the $z_{\lambda i\alpha}$ described in Section 3. This additional arbitrariness is not considered further by them, but is removed by the device of requiring the additional $q_{\lambda i\alpha}$ to satisfy the same Eq. (16) which are satisfied by the others. There being now $3N$ of the Eq. (14), the $z_{\lambda i\alpha}$ are completely determined except for normalization; this may be carried out so that Eq. (19) are valid for all $3N$ values of λ. The number of these equations is thus increased from $(3N-6)(3N-5)/2$ to $3N(3N+1)/2$; the new equations, insofar as they do not merely determine constant factors, prove to be precisely the Eqs. (17) and (25). The former has here been made common to all linear systems, the latter expresses the characteristic property of the normal system. It is interesting to note that the six additional δq's obtained in this way are essentially the $\delta\xi$'s and $\delta\Omega$'s of Eq. (15).

The elegant device of the null-frequencies thus leads directly to the normal system, without the necessity of considering the other linear systems. Its only disadvantage is that it does not make it clearly evident that a rotating system of axes has been defined, and that the symmetry of the q_λ depends as much on the choice of the axes as on the symmetry of the equilibrium configuration. This can be most clearly seen from the present point of view: the relation between the q's and the cartesian coordinates (either $x_{i\alpha}$ or $y_{j\alpha}$) will depend on the $Y_{ij\alpha}$ as well as on the $z_{i\alpha}$. If the former are chosen in a very unsymmetric manner, no amount of symmetry of the latter will avail to make the q's symmetric functions of the cartesian coordinates. It is thus not permissible to define a system of rotating axes in an unsymmetric manner, then approximate them by a linear system, and suppose the resulting q_λ to be the normal coordinates.

This has frequently been done in the literature, and it is not always easy to determine whether a serious error has resulted or not. Fortunately there are certain quantities which are invariant under a change of the $Y_{ij\alpha}$: the normal frequencies are such quantities. Hence conclusions concerning the degeneracy of these, obtained from a consideration of the normal system, will be equally valid in any linear system. There must also be some way to show that the determination of their activity in emission and in the Raman effect is invariant. If it should ever prove to be really necessary to use the general linear systems, it will be useful to precede it by the development of the theory of these invariants. For the present it appears sufficient to use only the normal system.

Confining the attention to this, certain possibilities for the further application of symmetry considerations become apparent. Since Λ_i' must have the character of a vector product (it must behave like M_i), it follows that its components and also the $B_{\lambda\alpha i}$ and $B_{\lambda i}$ must have certain determinate symmetry properties. These may be discussed in the same way as the properties of the dipole and quadrupole moments, and it is often possible to show that they must vanish. In other cases, they are related by linear equations, and in still others, the matrix elements of Λ_i' which enter into the secular equation may be shown to vanish. A very interesting elementary treatment of these matters has been given by Teller.[7]

Professor Wigner has kindly read the manuscript of this paper.

[7] E. Teller, Hand- und Jahrbuch d. chemischen Physik **9**, 125 (1934).

The Thomas-Fermi Method for Metals

J. C. SLATER AND H. M. KRUTTER, *Massachusetts Institute of Technology*

(Received February 9, 1935)

The Thomas-Fermi method is applied to metals, by replacing each atom by a sphere, assuming the potential to be spherically symmetrical within it, and solving the Thomas-Fermi equation subject to the boundary condition that the electronic charge within the sphere shall balance the nuclear charge, rendering it electrically neutral. Calculations are presented giving potential field, charge density, and kinetic, potential, and total energy of the metal, as function of lattice spacing. The virial theorem is verified for the energy. The total energy shows no minimum, the pressure being always positive. Calculations are also made using the Dirac method of correcting for exchange, for three atoms, Li, Na and Cu. The exchange lowers the energy, but still not quite enough to produce a minimum of energy and an equilibrium at zero pressure. The result should be useful as a first approximation in self-consistent field approximations for the structure of metals, and could be adapted to give approximate treatment for matter under very high pressure, as in stars.

THE application of the Thomas-Fermi equation to metals has been mentioned in an earlier paper,[1] in which some of the results to be described in the present paper were sketched. The method rests on the same fact which makes possible the Wigner-Seitz calculation:[2] the potential acting on an electron in the neighborhood of one of the nuclei of the metal is very nearly spherically symmetrical, the nucleus being the center, so that the same method of solving differential equations, as for example the Thomas-Fermi method or the Schrödinger equation, which is applicable in an isolated atom, can be used in the metal, simply by using different boundary conditions. More precisely, we surround each nucleus in the metal by a cell, its boundaries being the planes bisecting perpendicularly the lines joining the nucleus to its nearest or next nearest neighbors. Each such cell contains just enough electrons to neutralize the nuclear charge, so that, being of a high order of symmetry, its electric field at external points is very small, falling off very rapidly with the distance, and can be neglected. Within a cell, then, the potential arises only from the charges within that cell. Since these charges are distributed almost spherically, their resultant field is almost spherical, so that it is a self-consistent hypothesis to assume that, to a first approximation, the potential, and consequently the resultant charge distribution, are both exactly spherically symmetrical. To this approximation, we can replace the polyhedral cell by a spherical one of the same volume. Our method, then, is to solve the Thomas-Fermi equation within this spherical cell, subject to the two boundary conditions that the potential approach Ze/r at the nucleus, and that the total electronic charge contained within the sphere (of radius R, which varies as the crystal is compressed or expanded) is equal to $-Ze$.

The Thomas-Fermi[3] method as applied to isolated atoms is well known, but some of its applications to other problems have resulted in misunderstandings. For that reason it will pay to sketch briefly its application to the present case. This has been done to some extent in the paper quoted above.* There is also a treatment of the whole Thomas-Fermi problem, though without taking up the present application to metals, given by Brillouin.[3] Because of the existence of these discussions, to which the reader is particularly referred, the present treatment will be brief.

First we consider the original Thomas-Fermi method, which neglects effects of exchange. We

[1] J. C. Slater, Rev. Mod. Phys. **6**, 209 (1934).

[2] E. Wigner and F. Seitz, Phys. Rev. **43**, 804 (1933); **46**, 509 (1934).

[3] L. H. Thomas, Proc. Camb. Phil. Soc. **23**, 542 (1927); E. Fermi, Zeits. f. Physik **48**, 73 (1928); E. A. Milne, Proc. Camb. Phil. Soc. **23**, 794 (1927); J. Frenkel, Zeits. f. Physik **51**, 232 (1928); P. A. M. Dirac, Proc. Camb. Phil. Soc. **26**, 376 (1930); E. B. Baker, Phys. Rev. **36**, 630 (1930); E. Guth and R. Peierls, Phys. Rev. **37**, 217 (1931); V. Bush and S. H. Caldwell, Phys. Rev. **38**, 1898 (1931); W. Lenz, Zeits. f. Physik **77**, 713 (1932); H. Jensen, Zeits. f. Physik **77**, 722 (1932); H. Jensen, Zeits. f. Physik **93**, 232 (1934); L. Brillouin, *L'Atome de Thomas-Fermi, Actualités scientifiques et industrielles*, Hermann, Paris, No. 160, 1934. The last named reference has a more complete bibliography than is given here.

* Reference 1, p. 223.

replace the energy of interaction between electrons by an average potential depending only on position, so that the total potential energy of an electron, including the interactions with the nuclei as well as with other electrons, is a function of position, $-eV$. If the energy of an electron in such a field is $-eE$, its momentum p is given by the equation $p^2/2m-eV=-eE$, so that p is real, and the motion can occur classically, only in those regions where $-e(E-V)$ is positive. We now apply the Fermi statistics to the electrons, but otherwise treat them classically. For the absolute zero of temperature, these statistics take the form of a statement that the number of electrons per unit volume in a six-dimensional phase space is $2/h^3$ ($1/h^3$ for electrons of each spin) at all points corresponding to an energy less than an arbitrary value $-eE_0$, zero at points corresponding to energy greater than $-eE_0$. At a given point of coordinate space, those points of momentum space within a sphere of radius P, where $P=(-2me(E_0-V))^{1/2}$, are occupied by electrons, those outside the sphere unoccupied. We can then get the charge density of electrons in ordinary space by integrating the density in phase space over this sphere, and multiplying by the charge on the electron, $-e$. Since the density in phase space is constant, the result is $-2e/h^3$ times the volume of the sphere, or

$$\rho_e=-8\pi eP^3/3h^3=(-8\pi e/3h^3)(-2me(E_0-V))^{3/2}.$$

From this equation we see that once V is determined, different values of E_0 correspond to different density of charge; in any particular case, E_0 is to be so chosen that the integral of ρ_e over all space adds to the known amount of electronic charge present in the problem. We now make the requirement of self-consistency: we demand that the potential V be the electrostatic potential of the nuclei and of the electrons themselves. By Poisson's equation, $\nabla^2V=-4\pi\rho$, where ρ is the sum of ρ_e given above in terms of V, and the charge density of nuclei. Assuming spherical symmetry, the resulting equation is:

$$\frac{1}{r^2}\frac{\partial}{\partial r}\left(r^2\frac{\partial V}{\partial r}\right)=\frac{32}{3}\pi^2\frac{e}{h^3}P^3$$

$$=\frac{32\pi^2}{3}\frac{e}{h^3}(2me(V-E_0))^{3/2}.$$

We now let $r=\mu x$, where $\mu=a_0(9\pi^2/128Z)^{1/3}$, $a_0=h^2/4\pi^2me^2$, or numerically, μ, our new unit of length, is equal to $0.88634a_0/Z^{1/3}$ where a_0 is the radius of the first Bohr orbit for hydrogen. We also let $V-E_0=\gamma\phi/x$, where $e\gamma$, our new unit of energy, equals Ze^2/μ, or $(2^{10}/3^2\pi^2)^{1/3}Z^{4/3}Rhc$ $=2.2590Z^{4/3}Rhc$, where $Rhc=2\pi^2me^4/h^2$, the Rydberg energy. The quantity $Ze\phi=(V-E_0)r$ is of the nature of an effective nuclear charge, or the charge which must be divided by the distance from the nucleus to give the potential, so that as r goes to zero, $Ze\phi$, the effective nuclear charge, approaches Ze, and ϕ approaches unity. In terms of these definitions, the equation takes the form $\phi''=\phi^{3/2}/x^{1/2}$, the Thomas-Fermi equation. We have seen that the boundary condition at the nucleus is that $\phi(0)=1$. At the boundary of the spherical cell, since the total charge contained within the cell must be zero, the electric field must vanish, or $\partial V/\partial r=0$, which in terms of our new variables becomes $\phi'=\phi/x$. The interpretation of this condition is simply that the tangent to the curve of ϕ against x, at the distance $x=X$ corresponding to $r=R$, should pass through the origin, making a simple condition to apply graphically.

As shown in Fig. 1, the curve for ϕ starting from $x=0$ with a particular slope, $-B_0$ $=-1.58808$, approaches the axis asymptotically. The tangent to this curve through the origin is then the x axis itself, which is tangent at infinite distance, so that for this solution there are just enough electrons in infinite space to neutralize the nucleus. In other words, this solution is the one for the isolated atom, the familiar solution of the Thomas-Fermi equation usually discussed. The solutions we desire are those with initial slopes smaller numerically than $-B_0$, and corresponding to spheres of finite radii. The solutions of slope greater than B_0 numerically will cut the axis of abscissas. They correspond to positive ions, as is discussed by Brillouin,[3] and do not concern us here.

Solutions have been carried out for a number of slopes smaller numerically than $-B_0$. A series expansion was used about $x=0$, and the function was then extended by numerical integration out to the radius X. These solutions are presented in Fig. 1, which is drawn accurately to scale. The authors will be glad to send detailed

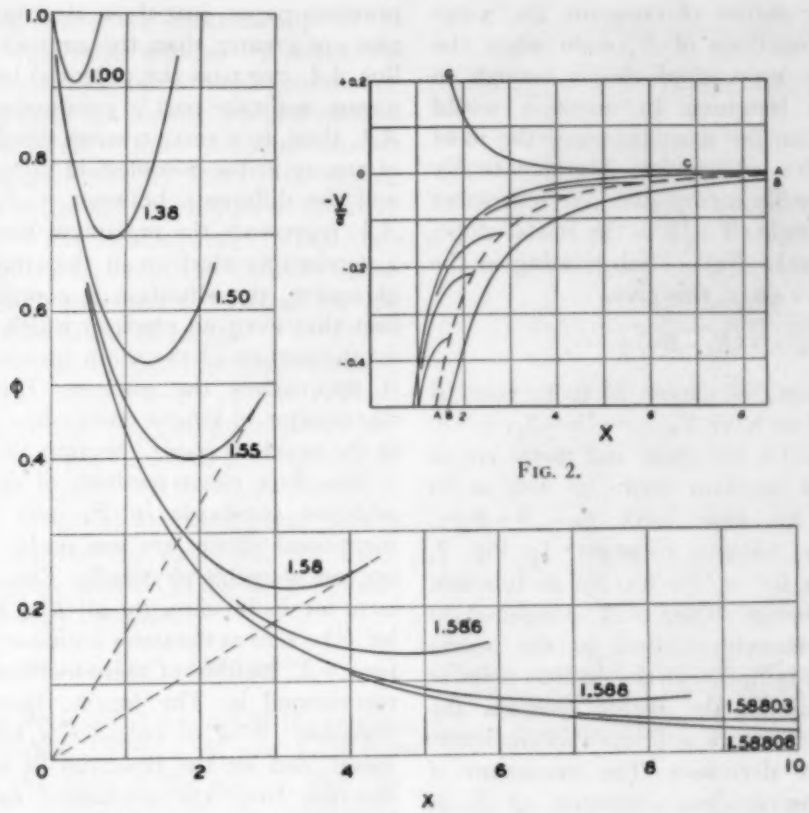

FIG. 1.

FIG. 1. Thomas-Fermi function ϕ, as function of x, for different initial slopes. The following table gives X, the minimum radius, or point of tangency of the curve and the straight line through the origin, as function of initial slope:

B	1.00	1.38	1.50	1.55	1.58	1.586	1.588	1.58803	1.58806	1.58808
X	1.19	1.69	2.20	2.80	4.23	5.85	8.59	11.3	16.	∞

FIG. 2. Potential $-V/\gamma$ as function of distance x from nucleus, Thomas-Fermi method. The curves terminating in the dotted line AA are potentials for different lattice spacings, the values of x at the intersections being the lattice spacings X, showing that the potential $-V/\gamma$ is lowered as X decreases. The dotted line AA represents the maximum height of the potential barrier between atoms, BB represents the average potential through the cell, and CC the maximum total energy $-E_0/\gamma$ of an electron in the Fermi distribution, all as functions of X.

numerical tables to any one who may have occasion to use them, but it seems unnecessary to publish them in full.

From these solutions, we can find at once the quantity $V-E_0$, as function of x, for a number of values of X, or of the lattice spacing, and for any metal. No unique method is provided for defining the potential V and the energy E_0 separately, for as usual there is an arbitrary additive constant in the potential, and a compensating one in E_0. This is a problem which appears in more accurate treatments, as well as in the Thomas-Fermi method. At least four different methods of choosing the arbitrary constant have some advantages; we shall discuss them briefly. First, we may choose our constants so that the potential V in the immediate neighborhood of the nucleus has a value independent of X. This is the method adopted in the earlier paper.* When one carries out a wave-mechanical calculation, finding wave functions in the potential field V, this results in having the x-ray energy levels, which depend only on the part of V near the nucleus, independent of X, whereas

* Reference 1, p. 212, Fig. 1.

with any other choice of constant the x-ray levels will be functions of X, even when the atoms have not approached closely enough so that the wave functions in question would overlap. It is thus for most purposes the most reasonable choice physically. Mathematically the method is easily formulated. We remember that near the origin, if $-B$ is the initial slope, we can write $\phi=1-Bx\cdots$. Substituting in the equation $V-E_0=\gamma\phi/x$, this gives

$$V=\gamma/x+(E_0-B\gamma)+\cdots.$$

For the free atom, we choose E_0 to be zero, B equal to B_0, and we have $V_{\text{atom}}=\gamma/x-B_0\gamma+\cdots$. If the potentials for the atom and metal are to agree as to the constant terms as well as to those in $1/r$, we must have $E_0=(B-B_0)\gamma$, determining the additive constant. In Fig. 2, we show curves for $-V/\gamma$ for Na as function of x, for a number of values of X, computed on this basis. It is evident that as the atoms approach, the potential near the nucleus remains unchanged, while in the region between the atoms it decreases more and more as the internuclear distance decreases. The maximum of the potential barrier, as a function of X, is shown by the dotted line AA. This is to be compared with the line AA in the Fig. 9 of the previous paper, though in that case, following Wigner and Seitz in using Prokofieff's field, the change in curvature of the potential with changing X was not considered. Also we have computed, by numerical integration, the average value of V over the sphere, for each value of X and have plotted this in the line BB, Fig. 2, to be compared with line BB, Fig. 9.[1] These potential functions as determined by the Thomas-Fermi method should be useful in the first steps of a calculation of the wave functions of electrons in metals by the method of self-consistent fields, as the corresponding functions are for isolated atoms. In Fig. 2, we also give a curve CC, representing the maximum energy $-E_0/\gamma$ of the Fermi distribution as a function of X. In contrast to the more exact wave-mechanical case, we find that this energy continuously increases as the metal is squeezed, whereas a minimum is shown by more exact methods, closely connected with the minimum of total energy of the metal. As mentioned in the previous paper, just those electrons whose energies are greater than the amount given by the line AA, can pass the potential barrier between atoms, and take part in conduction. The energy AA, then, in a certain sense stands for the zero of energy in the Sommerfeld picture of a metal, and the difference between $-eE_0$, or CC, and AA, represents the maximum kinetic energy of a conducting electron in that model. Actually, of course, the situation is complicated by the fact that even an electron which moves slowly on the surface of the atom speeds up greatly as it approaches the nucleus. This problem of distribution of kinetic energy has been discussed in the previous paper,[1] Section 10.

The three other methods of determining the additive constants in E_0 and V, which we mentioned above, are less useful, because they are less plausible physically. The second method is to let E_0 be zero, for all R's. The third is to let V be zero at the outer boundary of the sphere, for $x=X$. Neither of these methods has much to recommend it. The fourth, however, is more plausible: it is to consider a finite sample of metal, and let the potential be zero at infinite distance from the uncharged sample. This is more complicated, for it involves a discussion of the potential barrier and electrical double layer at the surface of the metal. With this definition of potential, the potential energy within the atom, the x-ray levels, and $-eE_0$, the top of the Fermi distribution, will all move up or down together as the jump of potential at the boundary changes, for any such reason as the addition of a surface layer of foreign atoms. For purposes of thermionic and photoelectric emission, this last definition of potential is the most useful. But since it involves a discussion of the surface effects, a problem outside the range of the present paper (though, as has been shown by Frenkel and Brillouin,[3] a treatment on the basis of Thomas-Fermi theory is possible), it is a less practical method when dealing with the interior of the metal, and we shall not follow it further at the moment.

From the values of $V-E_0$ as function of x, we can compute the charge density, and find how it changes as X is changed. The point of particular interest is the way in which the density at the edge of the sphere, midway

between atoms, increases continuously as X decreases, so that the number of electrons capable of carrying current is much greater for tightly packed than for loosely packed metals. This conclusion seems to have no counterpart in the actual metals, where, as Mott[4] has shown, the alkalies have the largest number of effective free electrons. The discrepancy arises undoubtedly from the fact that the Thomas-Fermi method cannot be expected to account for the periodic properties of the elements.

Knowing the potential, and the charge density, we can find the total energy of the crystal, kinetic and potential. The potential energy per atom is $\frac{1}{2}\int \rho_e V dv + \frac{1}{2}ZeV_0$, where ρ_e is the charge density due to electrons, V is the whole potential, and V_0 is the potential at the nucleus, whose charge is Ze, due to the electrons. By using partial integrations similar to those of Milne,[3] the potential energy becomes

$$\text{P.E.} = (6/7)Ze\gamma[\phi_0' - \tfrac{3}{5}X^{1/2}\phi_X^{5/2}],$$

where ϕ_0' is the slope of the ϕ curve at the origin, which we have denoted by $-B$, and ϕ_X is the value of ϕ at the edge of the sphere. For the kinetic energy, we note that the maximum kinetic energy at any point is $e(V-E_0)$, and that according to the Fermi statistics the mean kinetic energy is 3/5 of this. Weighting the mean kinetic energy at each point by the charge density of electrons at that point and integrating over the volume, we obtain the total kinetic energy, which is

$$\text{K.E.} = -(3/7)Ze\gamma[\phi_0' - (4/5)X^{1/2}\phi_X^{5/2}].$$

The potential, kinetic and total energy are plotted in Fig. 3, as functions of X. At infinite separation, where ϕ_X is zero, the potential energy becomes $-(6/7)B_0Ze\gamma$, the kinetic energy is $(3/7)B_0Ze\gamma$, evidently verifying the result of the virial theorem that the potential energy should be minus twice the kinetic energy. These limiting values of potential, kinetic and total energy are subtracted from the curves of Fig. 3, so that they really represent changes in energy on compression. We see that the total energy increases continuously with decreasing X, with no minimum, so that this model cannot explain the cohesion of metals. The increase of kinetic energy with decreasing X, because of the adiabatic compression of the Fermi gas, is partly but not wholly compensated by the decrease of potential energy, arising because the electrons on the average are closer to the nucleus in the compressed state.

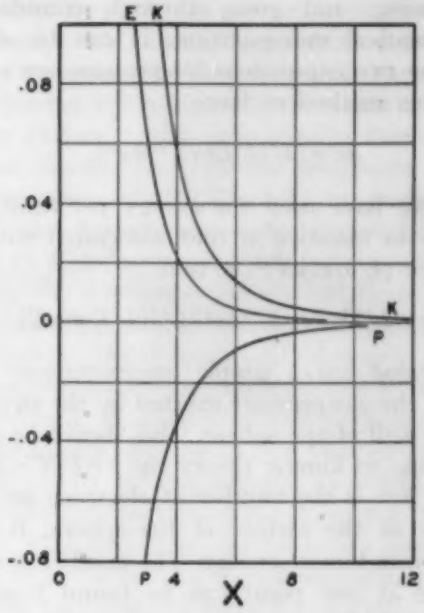

FIG. 3. Kinetic, potential and total energies as function of lattice spacings X, Thomas-Fermi method. The quantities plotted, K, P and E, are in units of $(3/7)Ze\gamma$, and represent differences between the corresponding energies at spacing X and the values of the isolated atom.

In the general case, for arbitrary X, the kinetic and potential energies are related through the virial theorem,[5] which for a solid in which all forces are derived from the Coulomb law, takes the form $\text{K.E.} + 1/2\text{P.E.} = 3/2pv$, where p is the pressure, v the volume. For the Thomas-Fermi method, Fock has shown in general that this theorem must apply, and we can easily check it in the present case. Thus we substitute in the expression above the values of kinetic and potential energies already derived, and compute pv in that way. Next we find the total energy as a function of X, differentiate to get dE/dX and from that find dE/dv, which must be equal $-p$.

[4] N. F. Mott, Proc. Phys. Soc. **46**, 680 (1934); N. H. Frank, Phys. Rev. **47**, 282 (1935).

[5] V. Fock, Physik. Zeits. Sowjetunion **1**, 747 (1932); J. C. Slater, J. Chem. Phys. **1**, 687 (1933); H. Hellmann, Zeits. f. Physik **85**, 180 (1933).

Comparing, and going through considerable mathematical manipulation, it can be shown that the two expressions for pressure are equal. By either method we have

$$pv=(2/15)Ze\gamma X^{1/2}\phi_X^{5/2}.$$

Since we have used the energy per atom, the volume in question is that associated with an atom, or $(4/3)\pi(\mu X)^3$, so that

$$p=\{(2/15)Ze\gamma X^{1/2}\phi_X^{5/2}\}/\{(4/3)\pi(\mu X)^3\}.$$

This value has a simple interpretation: it is simply the gas pressure exerted by the electrons on the wall of the sphere. This should be given according to kinetic theory by $p=\frac{2}{3}(N/v)$K.E., where N/v is the number of electrons per unit volume at the surface of the sphere, K.E. is their mean kinetic energy. The number per unit volume at any point can be found from the density which enters into the formulation of the Thomas-Fermi method, and in our present notation it is

$$N/v=\{\tfrac{1}{3}Z(x\phi)^{3/2}\}/\{(4/3)\pi(\mu x)^3\}.$$

The mean kinetic energy of the electrons at any point is $\frac{3}{2}e\gamma\phi/x$. Substituting $x=X$, and putting these values into the formula for p, we immediately verify the statement as to the interpretation of the pressure. Since the pressure is that of a perfect Fermi gas, it is obvious that no cohesive forces are found in this model. Such forces could come only from electrostatic attraction of one atom for its neighbors, and that is impossible with the uncharged spherical atom which we have considered.

A considerable improvement over the Thomas-Fermi method can be attained by introducing the effect of exchange, as Dirac has done, and as Brillouin[5] describes. The principle of the method can best be described in terms of the Fock[6] equation. These equations can be written

$$(-(h^2/8\pi^2m)\nabla^2-e(V_i(x)-E_i))u_i(x)=0,$$

where $u_i(x)$ is the wave function corresponding to the ith state of an electron, so that the whole wave function is made of a determinant of functions $u_i(x_k)$, and $-eE_i$ is the corresponding one electron energy. Here the potential V_i is different for each stationary state, and is given by

$$V_i(x)=\int[\rho_i(x,x')dv'/|r-r'|],$$

where $\rho_i(x,x')$ is the effective charge density at x' of all electrons but the one we are considering, when that one is at x, and is in the ith stationary state. Analytically, $\rho_i(x,x')$ = charge density of nuclei

$$-e\sum_k\frac{u_k^*(x')u_k(x')u_i^*(x)u_i(x)-u_k^*(x')u_i(x')u_i^*(x)u_k(x)}{u_i^*(x)u_i(x)}.$$

The latter term, involving the summation, is the charge density of other electrons, and consists of two parts. The first, which can be rewritten $-e\sum_k u_k^*(x')u_k(x')$, is simply the density of all electrons including the one we are considering. It is this density which, added to the density of nuclei, we identified with the density ρ in the Thomas-Fermi method, so that that method corresponds to neglecting the last term above, which can be rewritten $e\sum_k u_k^*(x')u_i(x')u_k(x)/u_i(x)$. Remembering the orthogonality of the u's in the Fock method, this term, the so-called exchange term, can be immediately shown to represent a charge of total amount e, so that the density $\rho_i(x,x')$ is that of the nuclei and $N-1$ electrons, if there are N electrons in the problem. The correction which we have neglected in the Thomas-Fermi method, in other words, arises from the fact that an electron exerts no forces on itself, only on other electrons.

If now we assume a perfect gas of free electrons, obeying Fermi statistics in a field free space, it has been shown[7] that we can compute the charge density $\rho_i(x,x')$, and consequently the potential $V_i(x)$ acting on an electron of any arbitrary momentum (corresponding to the

[6] V. Fock, Zeits. f. Physik **61**, 126 (1930). For a new discussion of these equations see L. Brillouin, *Les Champs "self-consistents" de Hartree et de Fock*, Actualités scientifiques et industrielles, Hermann, Paris, No. 159 (1934).

[7] See P. A. M. Dirac, Proc. Camb. Phil. Soc. **26**, 376 (1930), and particularly Brillouin, *L'Atome de Thomas-Fermi*, quoted above.

quantum number i). The charge of one electron which must be removed from ρ to get ρ_i proves to be localized about the point x with spherical symmetry. The linear dimension of the sphere from which the charge e is removed is a function of the density of the electron gas, if it is compressed, changing proportionally to the linear dimension of the sample of gas. The correction to the potential on account of this removed charge can be shown to be $4eP/h\ F(p/P)$, where P is the maximum momentum of the electrons in the gas, p the momentum of the electron in question, and

$$F(\eta)=\tfrac{1}{2}+[(1-\eta^2)/4\eta]\log[(1+\eta)/|1-\eta|],$$

where $\eta=p/P$. Now the Thomas-Fermi method consists essentially of assuming that the electrons at any point within the system can be treated as a small part of an infinite perfect gas of free electrons of the same maximum kinetic energy. Hence it is a reasonable extension of this method to assume that the correction above, which is strictly correct only for a field-free gas where P is independent of position, can be applied in general by making P the appropriate function of position. This is the essence of the method which can be called the Thomas-Fermi-Dirac method.

Now let us apply the correction we have just discussed to the Thomas-Fermi method. In phase space, we assume as before that the number of electrons per unit volume is $2/h^3$ within a certain energy surface $-eE_0$, zero outside this energy surface. At any point of the coordinate space, the electrons will fill a sphere in momentum space, the momentum of the fastest electron being P. This fastest electron, corresponding to $\eta=1$ in the expression above, will be in a potential field equal to the potential of all charges, corrected by the exchange term for $\eta=1$. If we call the uncorrected potential V_0, and if we note that $F(1)=\frac{1}{2}$, then the potential V_P appropriate for this fastest electron is $V_P=V_0+2eP/h$. The kinetic energy of this electron is $-e(E_0-V_P)=-e(E_0-V_0-2eP/h)$, and of course equals $P^2/2m$. Equating these, we have the quadratic $P^2/2m-2e^2P/h+e(E_0-V_0)=0$, whose solution is $P=2e^2m/h\pm(4e^4m^2/h^2+2em(V_0-E_0))^{1/2}$, where the positive sign for the square root must be chosen to agree with the Thomas-Fermi case. The charge density is again $-8\pi eP^3/3h^3$, to be expressed in terms of the revised formula for P. As before, we apply Poisson's equation, stating that the Laplacian of the potential V_0 of all charge should equal -4π times the density of charge, so that

$$\frac{1}{r^2}\frac{\partial}{\partial r}\left(r^2\frac{\partial V_0}{\partial r}\right)=\frac{32\pi^2e}{3h^3}\left\{\frac{2e^2m}{h}+\left[\frac{4e^4m^2}{h^2}+2em(V_0-E_0)\right]^{1/2}\right\}^3.$$

As changes of variables, we introduce $r=\mu x$ as before, and let $V_0-E_0+2me^4/h^2=\gamma\psi/x$, where γ is as before. We also introduce $d=(3/32\pi^2)^{1/3}Z^{-2/3}=0.211783Z^{-2/3}$. In terms of these, the equation becomes $\psi''=x(d+\psi^{1/2}/x^{1/2})^3$, which differs from the Thomas-Fermi equation by the term d. On closer examination, the boundary conditions prove to be, as before, $\psi(0)=1$, and $\psi x'=\psi x/X$, the latter defining the radius μX of the sphere which contains Z electrons.

Integration of the equation above has been carried out as for the Thomas-Fermi problem, expanding in series for small values of x, and integrating numerically from there out. Calculations have been made for three different values of d, corresponding to Li, $Z=3$, Na, $Z=11$, and Cu, $Z=29$, as well as for $d=0$, the Thomas-Fermi case. In each of these three cases, a number of initial slopes were chosen, and curves computed for each of them. For each value of d, there is a particular value of the initial slope, $-B_0$, for which the ψ curve is tangent to the x axis. For the Thomas-Fermi case, this tangency is for infinite x, but for the general case it comes at a finite value of x. Brillouin has tried to connect these solutions with the neutral atoms, assuming that the charge density was given by the relations we have used out to the point of tangency, at which point the nuclear charge is just neutralized by the electrons, and assuming the charge density and field to be zero from there out. This does not seem a particularly

satisfactory suggestion, for it involves a discontinuity of charge density at the sphere. The charge density is proportional to ψ''/x, and as we see this attains its minimum value, d^3, when ψ is zero, and can never fall to zero. We prefer to consider, as Dirac did in his original paper on the subject, that the Thomas-Fermi-Dirac method is not applicable to neutral atoms without modification. We should interpret the solution of initial slope $-B_0$, which becomes tangent to the axis at distance X_0, simply as the solution of the metallic problem in which the radius of the cell equals X_0. For any radius larger than X_0, the method does not provide a solution. It is fortunate, however, that X_0 is much larger than the interatomic distance, except for the lightest atoms, so that this limitation is not of practical importance. Unfortunately for large radii the numerical integration is very sensitive to small errors, as well as to small changes in the initial slope, so that even approximately accurate values of X_0 have not been obtained, except for the case of Li. Here X_0 is in the neighborhood of 6, only slightly larger than the normal value of x in the metal. For heavier atoms, X_0 is much larger than 6, but its value cannot be accurately stated. The values of B_0 as function of d, however, can be found within narrow limits, and the curve is plotted in Fig. 4. It is practically a straight line, and should be useful for starting integrations for other atoms. For values of B less numerically than B_0, the boundary condition $\psi x' = \psi x/X$ can be satisfied for a value of X smaller than X_0, so that these values correspond to states of the metal more compressed than the limiting case X_0. In Fig. 5 these curves of ψ against x are given, for Cu, for a number of values of B, again accurately to scale.

From ψ, we can calculate the charge density, and by the equation already given find $V_0 - E_0$ and $V_P - E_0$. A convenient choice of E_0 is made as follows. Since we cannot solve the problem of the isolated atom, we choose the case of maximum radius, $X = X_0$, as a standard, and demand that V_0 in the neighborhood of the nucleus have the same value for any X that it has for $X = X_0$. For $X = X_0$, at the edge of the sphere, we have

$$\psi = (x/\gamma)(V_0 - E_0 + 2me^4/\hbar^2) = 0.$$

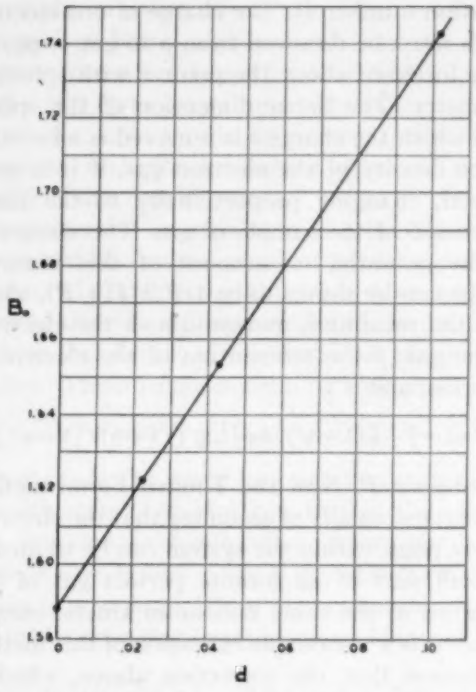

FIG. 4. Initial slopes B_0, in Thomas-Fermi-Dirac method; for solutions where ψ curves are tangent to x axis, as function of d; parameter depending on atomic number. The four points plotted are as follows:

atom	Z	d	B_0
Thomas-Fermi		0	1.58808
Cu	29	0.022437	1.6225
Na	11	0.042818	1.6536
Li	3	0.101815	1.7427

Let us determine E_0 by assuming that in this case $V_0 = 0$ at the edge of the sphere, giving $E_0 = 2me^4/\hbar^2 = \gamma d^2$. Now near the nucleus for $X = X_0$, we have $\psi = 1 - B_0 x + \cdots$, where B_0 is given in Fig. 4. Thus we have $V_0 = \gamma/x - B_0\gamma \cdots$. Next, for an arbitrary X, we have $V_0 - E_0 + 2e^4m/\hbar^2 = \gamma/x - B\gamma \cdots$. To make this agree with the limiting case, we must have $E_0 = 2me^4/\hbar^2 + (B - B_0)\gamma$. Making this choice of E_0, the potential is definitely determined, and in Fig. 6 we plot curves of V_0, V_P and E_0, as functions of X, similar to the Thomas-Fermi curves of Fig. 2. Qualitatively the curves resemble those of Fig. 2, and it is seen that V_0 closely resembles the V of Fig. 2. The potential energy $-eV_P$ of an electron, however, is decidedly lower on account of exchange than with the original Thomas-Fermi method, and as a result the exchange leads to a tighter binding.

To find the total energy, and the potential and kinetic energies, with the Thomas-Fermi-

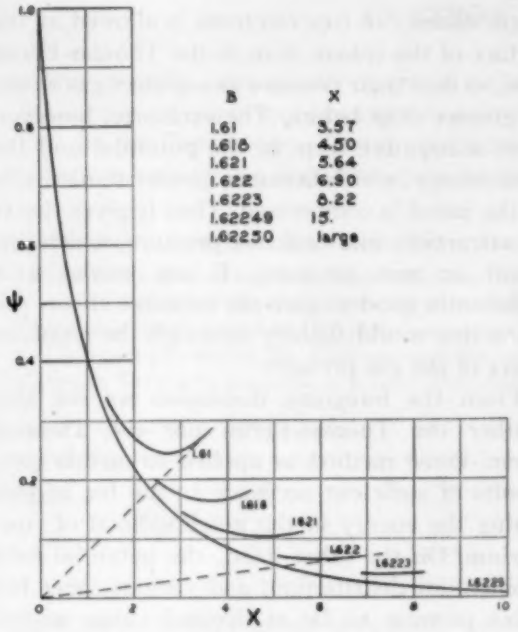

FIG. 5. Thomas-Fermi-Dirac function ψ as function of x, for Cu, $Z=29$. Table of X as function of B.

Dirac method, we proceed much as in the Thomas-Fermi method. The problem is complicated, however, by the fact that the electron of momentum p moves in a potential $V_p=V_0+4eP/h\ F(p/P)$, which is a function of p. At a point of space where V_0 has a particular value, the density of electronic charge connected with electrons with momentum between p and $p+dp$ is equal to $-(8\pi ep^2/h^3)dp$ if p is less than P, zero if p is greater than P, where P is the root of the quadratic written above. For the potential energy of interaction between electrons, instead of the simple expression $\frac{1}{2}\int \rho_v V dv$ of the Thomas-Fermi method, we must multiply the charge density for each value of p by the corresponding value of V_p, and integrate over p, as well as over v. In this way we obtain

$$\tfrac{1}{2}\int \rho_v V_0 dv+\tfrac{1}{2}\int\int(-8\pi ep^2/h^3)(4eP/h)F(p/P)dpdv,$$

where the integration with respect to p is from 0 to P. Carrying out the integration over p, the result is

$$\tfrac{1}{2}\int \rho_v V_0 dv-4\pi e^2/h^4\int P^4 dv.$$

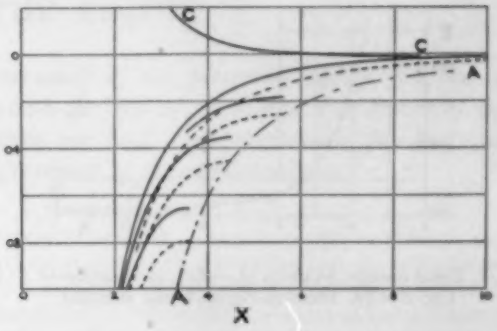

FIG. 6. Uncorrected potential $-V_0/\gamma$ (full lines), and potential acting on an electron $-V_P/\gamma$ (dotted lines), for Thomas-Fermi-Dirac method, for several lattice spacings. Line AA represents the maximum potential barrier of the potential acting on an electron. CC represents the maximum total energy of an electron, $-E_0/\gamma$.

The total potential energy is the sum of these terms, and $\frac{1}{2}ZeV_{00}$, where V_{00} is the value of the potential due to the electrons, at the nucleus. In contrast to the Thomas-Fermi method, no method has been found for carrying out all the integrations explicitly in terms of the values of known quantities at $x=0$ and $x=X$. Instead, most of the integration must be performed numerically.

The kinetic energy of an electron of momentum p is $p^2/2m$, as with the Thomas-Fermi case, and the mean kinetic energy at a given point of space is $\frac{3}{5}P^2/2m$. To get the total kinetic energy, we multiply this by the number of electrons per unit volume, and integrate over all space. As with the potential energy, the integrals have not all been evaluated, and some had to be computed by numerical integration, so that it is not worth while to give the details of the integration. In Fig. 7 we give the total energy as function of X for Cu. In comparison with the Thomas-Fermi method, the effect of including exchange is to lower the total energy decidedly. It is still not lowered enough, however, to give a minimum, but the energy is practically constant within the error of the calculation in the neighborhood of the observed distance of separation.[8] It is to be noted, however, that Wigner and Seitz[2] have found that a considerable part of the cohesive energy of sodium comes from the

[8] In the earlier paper (reference 1, p. 234) it was stated that approximate calculations appeared to give a minimum in the curve. This is not verified in more accurate computations.

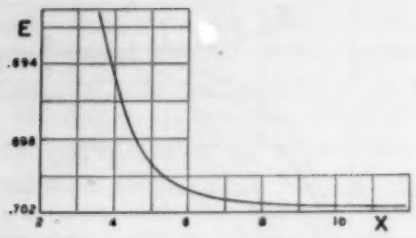

FIG. 7. Total energy, in units of $-Ze\gamma$, as function of X, for Cu, $Z=29$, Thomas-Fermi-Dirac method.

correlation energy between electrons of opposite spin, a feature which the Fock and Thomas-Fermi-Dirac methods neglect, so that we could not expect to get nearly as low an energy as is observed.

The virial theorem, as far as the writers are aware, has not been discussed in general for the Thomas-Fermi-Dirac model, and since we have not obtained analytical forms for the kinetic and potential energies, it has not been possible to verify it analytically in the present case. However, we have computed pv both from the virial method and from the slope of the total energy curve, and the two values agree within the error of the numerical calculation, so that we infer that the theorem holds in the present case. The pressure is quite different in physical interpretation from what it was in the Thomas-Fermi method. There, as we have pointed out, it is the perfect gas pressure of the electrons striking the boundary of the sphere. Here, a larger density of free electrons is allowed at the surface of the sphere than in the Thomas-Fermi case, so that their pressure as a perfect gas would be greater than before. The exchange, however, gives a negative term in the potential and the total energy, which becomes greater numerically as the metal is compressed. Thus it gives rise to an attraction, and negative pressure, which just result in zero pressure. If our model were sufficiently good to give the cohesive effect, this attraction would slightly outweigh the repulsive effect of the gas pressure.

From the foregoing discussion we see that neither the Thomas-Fermi nor the Thomas-Fermi-Dirac method as applied to metals gives results of sufficient accuracy to use for investigating the energy in the neighborhood of equilibrium. On the other hand, the potential field, momentum distribution, and various other features promise to be of decided value as first approximations in more accurate treatments of the metals. One further field in which the method might be advantageous is in investigating the limiting behavior of matter under high pressure, as it is found particularly in astrophysics. Stellar material, either at low temperature and very high density as in the dense stars, or at high temperature and more normal density, as in hot stars, could be approximated as in the present paper, and a much better approximation to the equation of the state could be found than has been so far obtained.

LETTERS TO THE EDITOR

Prompt publication of brief reports of important discoveries in physics may be secured by addressing them to this department. Closing dates for this department are, for the first issue of the month, the twentieth of the preceding month; for the second issue, the fifth of the month. The Board of Editors does not hold itself responsible for the opinions expressed by the correspondents.

The Symmetric C – D Bond Vibration in Heavy Acetylene

In the study of the Raman spectrum of C_2D_2 carried out in this laboratory we have reported[1] the acetylene bond frequency in heavy acetylene. By prolonged exposure we have succeeded in finding the other symmetrical valency frequency. The results are given in Table I. The calculated

TABLE I.

Vibration	C_2H_2 obs.	C_2D_2 calc.	C_2D_2 obs.
$\rightarrow\rightarrow\leftarrow\leftarrow$	1975	1757	1762
$\rightarrow\leftarrow\rightarrow\leftarrow$	3374	2678	2700

values were obtained from the two-constant formula of Mecke.[2] The force constants used were:

$$K_{C-H} = K_{C-D} = 5.868 \times 10^5$$
$$K_{C-C} = 15.49 \times 10^5.$$

Since our first note[1] on the subject appeared Sutherland[3] and Morino[4] have made similar calculations on the basis of our experimental results.

GEORGE GLOCKLER
CHARLES E. MORRELL

School of Chemistry,
University of Minnesota,
March 6, 1935.

[1] Glockler and Davis, Phys. Rev. **46**, 535 (1934).
[2] R. Mecke, Zeits. f. Physik **64**, 173 (1930).
[3] G. B. B. M. Sutherland, Nature **134**, 775 (1934).
[4] Y. Morino, Sci. Pap. Inst. Phys. Chem. Res. **25**, 232 (1934).

High Energy Formulae

In a recent paper in the *Physical Review*, Oppenheimer[1] discusses the validity of the theoretical formulae for the production of x-radiation, and the production of ionization, by high energy electrons, energy $\xi mc^2 \gg mc^2$. He refers to previous discussions of the radiative formula by Weizsaeker[2] and by the writer.[3] These authors pointed out that in a system S', in which the radiating electron is initially at rest, a resolution of the perturbing field of the nucleus into Fourier components shows that the quantum mechanics involved in the derivation of the radiative formula may be reduced to the quantum mechanics of the scattering, by a stationary electron, of radiation of frequency of the order of mc^2/h and less, however big ξ may be. The new point which Oppenheimer claims to make is that though the scattering of such frequencies is undoubtedly correctly given by quantum mechanics there is, on theoretical grounds, still a possibility that the radiative formula is not correct. Such a possibility was however clearly recognized in the earlier discussion of the problem by the writer, and for essentially the same reasons as those put forward by Oppenheimer, *viz.*, the possible inapplicability of the Lorentz expression, $F = (E + [H \cdot v])e$, for the force on an electron when the external field is so contracted by the Lorentz effect that its scale of variation d is of the order of, or less than, the electron radius $\sigma = e^2/mc^2$. In fact Oppenheimer's statement that under these conditions the force on an electron cannot be taken as the sum of the forces exerted by the separate Fourier components of the field, is practically equivalent to the statement in the writer's note that it is "the Fourier spectrum of the force on an electron that should be considered in the Fourier analysis method and not the Fourier spectrum of the field at a point."[4]

The extent to which the radiative effect and the ionization are contributed to by collision with $d < \sigma$, impact parameter $p < \xi\sigma$, is considered at length in Oppenheimer's paper, and was also discussed in the writer's previous note. In both discussions it is found that, while leaving out such collisions appreciably reduces the radiative effect for electrons with energy of the order of 3.10^8 volts (thus affording a possible explanation of Anderson's experimental results),[5, 6] it little affects the primary ionization even for electrons of 10^9–10^{10} volts energy. If therefore the high energy particles of cosmic radiation are electrons the difficulty of accounting for their observed ionization, previously emphasized by the writer, still remains.

In view of the observed failure of the quantum-mechanical radiative formula for high energy electrons, it is of interest to consider the *scattering* of such electrons, since this also concerns collisions with an atomic nucleus. In fact for the scattering by a lead plate about $\frac{1}{4}$ cm thick (as in Anderson's experiment)[5] the relative contributions of different parts of the nuclear field to the scattering is very much the same as for the radiative effect. In both cases the effective part of the nuclear field extends from about $\hbar/mc^2$ to the shielding radius $137Z^{-1/3}\hbar/mc$. This is so because the scattering is multiple. As regards the magnitude of the scattering we find, using Mott's relativistic formula, that the average projection on a plane of the resultant deflection produced by a plate containing n atoms per cm^3, atomic number Z, is

$$\theta = (2n^{1/2}Ze^2/\xi mc^2)(\log 2\pi n Z^{1/3}(\hbar/mc)^2)^{1/2}.$$

This formula accounts satisfactorily for the observed deflection of 10^8–3.10^8 volt electrons by lead,[5] and does

not appear to give too big an effect. This contrasts with the radiative effect where the observations[5] indicate that for 10^8–3.10^8 volt electrons the theoretical value is too big by at least a factor of 2. The data are, however, not sufficient to enable us to say definitely that the scattering formula holds where the radiative formula fails, though such a conclusion would seem to be corroborated by the observations of Anderson and Neddermeyer[6] on the production of secondary electrons by high energy cosmic particles (assuming the latter to be electrons). Such a result would mean that when an electron is subjected to the field of a moving nucleus the effective intensity of the components of the perturbing force with frequencies of the order of mc^2/h is less than that required by existing theory, while the intensity of the components which determine the scattering, *viz.*, those with infinitely small frequencies, is correctly given. Since the frequency mc^2/h has no special significance in classical theory this would be difficult to interpret on a classical basis.

E. J. Williams

Physics Laboratory,
Manchester,
February 16, 1935.

[1] Oppenheimer, Phys. Rev. **47**, 44 (1935).
[2] Weizsaecker, Zeits. f. Physik **88**, 612 (1934).
[3] Williams, Phys. Rev. **45**, 729 (1934).
[4] This statement was meant merely as an indicator of the nature of the possible failure of the Fourier analysis treatment, and not necessarily as a practicable procedure. There is a difficulty that while in classical theory we can under these conditions give a definite meaning to the force as acceleration divided by ordinary electron mass, this is not possible in quantum theory because of the different reaction of the electron in different collisions.
[5] Anderson, Phys. Rev. **44**, 406 (1933).
[6] Anderson and Neddermeyer, International Conf. on Phys., London, 1934.
[7] In the case of scattering the general expression for the lower limit is $\hbar/mc\theta'$, where θ' is such that an electron traversing the plate suffers on the average one collision in which it is deflected through more than θ'.

Induced Ultraviolet Fluorescence and Its Release by Visible Light

In the course of investigations on the detection of induced radioactivity and of extremely weak ultraviolet radiation we have recently observed that the ultraviolet fluorescence of certain substances following their exposure to and their removal from roentgen or gamma-irradiation persists for unexpectedly long periods of time. This ultraviolet fluorescence, furthermore, is conspicuously increased if the irradiated compounds be exposed to visible light. This is in agreement with an observation made by W. Kudrjawzewa.[1]

Of twenty-five compounds we have thus far examined sodium chloride, potassium chloride, rocksalt and fluorite crystals exhibit these effects most clearly. Impurities inhibit, but previously repeated recrystallization facilitates the subsequent induction of ultraviolet fluorescence. Heating the crystals impairs their fluorescence which, indeed, is completely stopped by dissolving the compounds in distilled water.

A photoelectric Geiger-Müller-counter tube equipped with a cadmium electrode and a quartz window has been used for measuring the ultraviolet fluorescence. This counter is very sensitive to ultraviolet radiation and hardly responds to visible light. The ultraviolet light has also been registered by means of the darkening produced on Eastman hypersensitive panchromatic dry plates.

The fluorescent effects described have been elicited in the following way: Samples of crystals were exposed to radon (100 millicuries, 1½ mm brass filter, close distance) or to roentgen rays (200 kv, cardboard filter, 40 cm focal distance, 25 *r*/min.) for periods of time ranging from a few seconds to ten hours. A few particles thus irradiated cause discharges in the Geiger counter; in general, the number of counts is proportional to the intensity and to the duration of the primary irradiation; but, in each case, it is found that illumination by visible light at once results in a tremendous increase of the counts. Thus, samples primarily irradiated for only a few seconds may require the stimulus of visible light before their acquired property of ultraviolet fluorescence becomes demonstrable with the counter. On the other hand, samples irradiated for several hours produce counter discharges in the dark even though they be removed from the counter window by as much as one meter. In this case, illumination by visible light so greatly increases the number of counts that satisfactory observations can only be made by placing the irradiated substance several meters from the window.

The counter discharges are completely stopped when a thin glass plate, 0.2 mm thick, is interposed between the material and the counter window. Spectrographic examination by means of a Leiss quartz monochromator in the case of sodium chloride, shows that the emitted radiation has one maximum in the neighborhood of 2450A. This agrees with Kudrjawzewa's[1] findings and is also of interest because J. O. Perrine[2] demonstrated that sodium chloride fluoresces in this same region as long as the substance is directly exposed to roentgen rays.

The ultraviolet fluorescence subsequent to primary gamma or roentgen irradiation, undergoes decay, very likely of the exponential type. The half-life of induced ultraviolet fluorescence ranges from a few minutes to many days depending upon the intensity and duration of exposure to the primary source of irradiation. The half-life, furthermore, is shortened if the substance is illuminated by visible light, which, if sufficiently intense, completely stops the emission of ultraviolet light, although the latter may again be detected after the substance has been allowed to rest in the dark.

The response to visible light is, moreover, characterized by lag, which increases as decay progresses. There is almost no measurable lag following either the onset or the cessation of visible illumination during the early life of induced ultraviolet fluorescence. But, lag in both respects becomes more prominent as time, measured from the moment at which the substance is removed from exposure to the primary radiation, continues to elapse.

Otto Glasser
I. E. Beasley

Cleveland Clinic Foundation,
Cleveland, Ohio,
March 12, 1935.

[1] W. Kudrjawzewa, Zeits. f. Physik **90**, 489 (1934).
[2] J. O. Perrine, Phys. Rev. **22**, 48 (1923).

Resonance Interaction Between Deuterons and Alpha-Particles

In a recent paper before the American Physical Society[1] we have presented some of the results of experiments on the scattering of alpha-particles by deuterium which show that the non-Coulombian field between the particles is confined to smaller distances of separation than it is in the case of scattering by hydrogen. A continuation of these experiments in which we investigated the precise nature of the anomalous scattering for low energies (at which the deviation from Coulomb scattering first becomes effective) shows an important difference from the scattering by protons. We suggest that this difference is due to a resonance interaction similar to those already established in disintegration experiments on heavier elements.

The experiments to be described consist in bombarding a thin layer of $Ca(OD)_2$ by alpha-particles whose range (and hence energy) can be varied by varying the pressure of gas (oxygen) between a polonium source and the target. The recoil deuterons emitted in directions close to that of the impinging alpha-particles are counted by means of a proportional Geiger counter. The results of bombarding an annular target covered first with a thin layer of $Ca(OD)_2$ and later with vaseline (containing ordinary hydrogen) under identical geometrical conditions are shown in Fig. 1

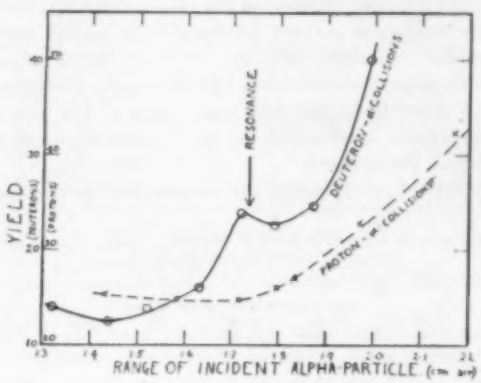

FIG. 1.

which is typical of numerous similar runs. For short alpha-particle ranges both curves show a falling yield, which is expected according to the classical theory, and both show a considerable increase for greater ranges, corresponding to anomalous scattering. The curve for protons rises smoothly in the way found by Chadwick and Bieler,[2] while that for deuterons rises more sharply, drops slightly and rises rapidly as the range of the alpha-particle increases.

According to Mott's theoretical treatment[3] the existence of an energy level in the composite nucleus (such as gives peaks in disintegration yield curves for elements like Be, N, Mg, Al) should cause a rise and fall in the yield of scattered alpha-particles. For light nuclei the effect is marked, depending on the quantity $(137/2Z)(v/c)$ (where v is the velocity of the alpha-particle) while for nuclei such as aluminum it would require extremely careful counting to be detected.

If we suppose that the incident alpha-particle in these experiments has an energy equal to that of a level in the $_3Li^6$ nucleus then an anomalous rise and fall would be expected, as we find it. The fact that the fall does not occur as markedly as the rise is due to the circumstance that anomalous scattering is taking place independently, so that a rise is superposed on the decreasing resonance yield. A similar superposition is apparent in the disintegration of beryllium by alpha-particles.[4]

In the case of hydrogen a resonance effect of the type here described is unlikely because it would imply the existence of a combination like $_3Li^5$ whose ratio of charge to mass is too great for stability.

The energy of the alpha-particles at resonance is 4.9×10^{-6} erg or 3.1 MEV. The present example appears to be the first instance of a resonance effect observed in alpha-particle scattering.

Our thanks are due to Dr. L. R. Hafstad for preparing the Po-source, and to Drs. Burnam and West for providing the radon tubes.

E. POLLARD*
H. MARGENAU

Yale University,
March 14, 1935.

[1] New York meeting, Feb. 23, 1935.
[2] J. Chadwick and E. S. Bieler, Phil. Mag. 42, 923 (1921).
[3] N. F. Mott, Proc. Roy. Soc. A133, 228 (1931).
[4] G. Bernadini, Zeits. f. Physik 85, 555 (1933).
* Sterling Fellow.

The Abundance Ratio of the Isotopes of Lithium

The marked divergence existing between the mass spectrograph and the optical values for the abundance ratio of the isotopes of lithium has made it seem advisable to recheck the ratio with the new mass spectrograph and improved technique now in use. A previous value of $Li^7/Li^6 = 12.14 \pm 0.4$ was obtained,[1] while 8.1 ± 0.4 observed by Ornstein, Vreeswijk and Wolfsohn[2] from the intensity of the resonance line $\lambda = 6708$A is perhaps the best of the optical values.

The new mass spectrograph was of the 180° focusing type with a 4 cm radius. It was operated at a pressure of about 3×10^{-6} mm as recorded by an ionization manometer. The filament slit was 0.22×3.0 mm and the collector slit 0.77×5 mm. The resolved current was read with an FP-54 balanced circuit hook-up.

The lithium source was coated on a platinum disk 2 mm in diameter spot-welded to a tungsten filament. The disk was placed in the center of the opening of a nickel washer 1.5 cm in diameter with a 3.5 mm opening; both were maintained at a constant potential of 1080 volts positive to the filament slit.

A typical resolution curve is shown in Fig. 1. The peaks were flat topped and the resolution was complete, the peaks being separated by nearly five times their base width.

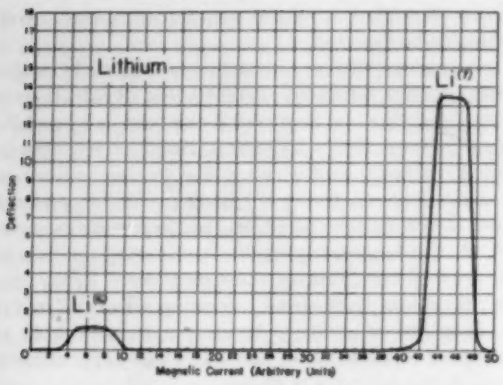

FIG. 1.

The results obtained with two different samples of lithium aluminum silicate tested under widely different conditions as to temperature, thickness of coating, and periods of heating are shown in Table I.

TABLE I. *Abundance ratios Li^7/Li^6.*

No.	No. of check	Average ratio	Average deviation
A	19	11.65	0.09
B	3	11.52	0.06
C	6	11.62	0.06
D	6	11.59	0.07
E	26	11.55	0.05
F	4	11.60	0.02
	Average	11.60 ± 0.06	

Experiment *E* represents a series of checks made with one filament in which the coating was heated to near whiteness for three consecutive periods of 1 hour each. No appreciable change in the ratio was observed. After the results in experiment *F* had been obtained the filament was heated to near the fusion temperature of the silicate for 2 hours; the average of 10 check runs was then 12.20 ± 0.1, while an additional heating period of 1 hour raised the ratio to 12.47 ± 0.1.

Results obtained with the platinum disk from which the lithium aluminum silicate had been carefully scraped and washed after the experiments described in Table I had been made are shown in Table II. The platinum thus contaminated with lithium is an excellent low temperature emitter of positive ions.

Runs *A* and *B* were taken at temperatures just above redness. *C* was made after filament *A* had been heated to bright redness for 1/2 hour. *D* was taken after *B* had been heated a similar period and *E* after an additional 1½ hour of heating; during this process the Li^+ emission showed definite signs of fatigue.

TABLE II. *Abundance ratios Li^7/Li^6 from cleaned Pt disk contaminated with lithium.*

No.	No. of checks	Average ratio	Average deviation
A	5	11.63	0.09
B	5	11.55	0.02
C	13	12.74	0.11
D	13	12.90	0.10
E	6	13.88	0.09

The results described yield a consistent value of $Li^7/Li^6 = 11.60 \pm 0.06$, which is materially higher than that obtained by optical means.

Insofar as can be told the abundance ratio remains constant for crystalline emitters until heated to near the fusion temperature where an isotope effect of free evaporation is detectable, the lighter isotope then being emitted more readily than the heavy. The effect of free diffusion appears more evident in the impregnated platinum, an appreciable separation of the isotopes being obtained on prolonged heating.

A. KEITH BREWER

Bureau of Chemistry and Soils,
U. S. Department of Agriculture,
Washington, D. C.
March 16, 1935.

[1] Brewer and Kueck, Phys. Rev. **46**, 894 (1934).
[2] Ornstein, Vreeswijk and Wolfsohn, Physica **1**, 53 (1934).

Shower Groups in the Cosmic Radiation

In a recent letter[1] on transition effects, reference was made to observations on showers. These were recorded as sharp jumps superimposed on the photographic trace of the steady ionization current produced in a small, spherical ionization chamber (230 cc volume, 30 atmospheres pressure argon). On the time axis each jump corresponded to 2.6 seconds, which was the period of the recording galvanometer, and could be easily distinguished from statistical fluctuations.

In Table I are recorded the number and rates of occur-

TABLE I. *Rates of occurrence of shower groups.* Total numbers of showers for each group (*N*) and corresponding rates (*N*/min.).

	Size of showers in number of rays: 10–14		15–19		20–29		30–39		>40		Total >20	
Thickness of lead above chamber (cm)	*N*	*N*/min.	*N*	*N*/min.	*N*	*N*/min.	*N*	*N*/min.	*N*	*N*/min.	*N*	*N*/min.
Cambridge; barometer 76, magnetic latitude 53 N												
0	172	0.051	55	0.019	33	0.011	9	0.004	5	0.002	47	0.017
0.64	82	.071	24	.022	11	.010	5	.005	1	.001	17	.016
1.27	147	.116	39	.031	33	.026	6	.005	4	.003	43	.034
3.18	56	.065	18	.021	12	.014	5	.006	1	.001	18	.021
6.66	104	.050	30	.014	27	.013	6	.003	2	.001	35	.017
9.2	22	.030	16	.022	7	.01	2	.003	2	.001	16	.014
14.3	18	.033	10	.018	2	.004	2	.004	2	.004	6	.012
Huancayo; barometer 51.3; magnetic latitude 1 S												
0					30	0.039	11	0.014	10	0.013	51	0.066
0.64					44	.082	14	.026	7	.013	65	.121
1.27					79	.115	22	.032	16	.023	117	.170
3.18					32	.075	13	.030	12	.028	57	.133
6.66					22	.059	7	.019	11	.029	40	.107
9.2					38	.057	13	.02	11	.017	62	.094
14.3					15	.039	4	.01	7	.018	26	.067
Cerro de Pasco; barometer 45; magnetic latitude 1 S												
0					44	0.081	9	0.016	13	0.024	66	0.121
0.64					64	.280	29	.126	22	.092	115	.498
1.27					74	.247	21	.070	23	.077	118	.394
3.18					30	.105	18	.063	39	.090	87	.258
6.66					27	.089	7	.023	15	.027	49	.139
9.2					17	.045	8	.014	12	.020	37	.079
14.3					22	.049	11	.02	12	.021	45	.090

rence of the showers for various thicknesses of lead above the chamber at the stations indicated. The observed jumps were arbitrarily classified according to size into various groups. By using the value of 100 ion pairs per cm path for air under standard conditions as the specific ionization produced by a single ray,[2] together with the average diameter of the sphere, these groups could be expressed in terms of the number of rays passing through the chamber. No jumps representing less than 10 rays are included in the Cambridge data, and none less than 20 for the South American stations.

The results are plotted in Fig. 1 for the group of 20–30 rays. The curves all have a maximum at about 1 cm lead, though there are indications that the maximum shifts to

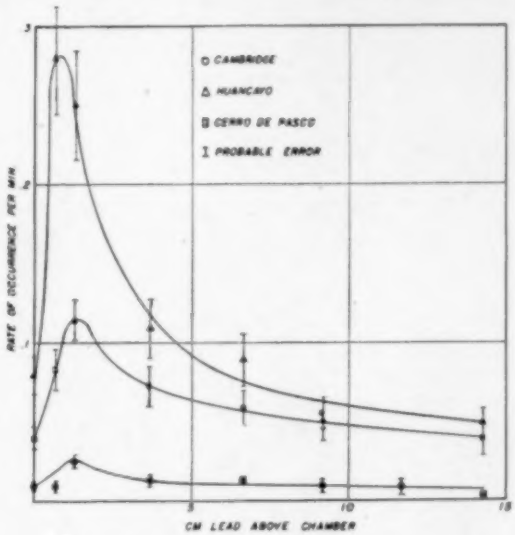

FIG. 1. Shower curves for group of 20–30 rays.

smaller thicknesses of lead for the higher elevations. This maximum becomes increasingly pronounced with increasing elevation. The curves for the other groups, while not given, are of the same general form, and show the same variation in shape with altitude. For the group of 20–30 rays for 1.27 cm lead, on which there are the most data, the ratios of the rates of occurrence (corrected for side shielding by subtracting the value for zero lead above) are: Huancayo to Cambridge, 5.0 : 1; Cerro de Pasco to Cambridge, 11.0 : 1. Johnson,[3,4] from counter observations, gives for the same thickness of lead, the ratio 7.8 : 1 between Cerro de Pasco and Swarthmore, which is to be compared with the Cerro de Pasco to Cambridge ratio. It has been suggested[5] that the transition effect may be explained in terms of a shower-producing radiation, having a much higher equilibrium intensity in air than lead. Our data indicate this to be the case, both from the form of the curves in Fig. 1, which are of the general shape of transition curves, and from the fact that the transition difference increases with altitude in approximately the same ratio as the showers, namely: Huancayo to Cambridge, 3.9 : 1; Cerro de Pasco to Cambridge, 7.5 : 1.[1]

Taken in conjunction with our ionization data,[1] the showers consisting of more than 10 rays contribute approximately 2 percent to the general ionization for 1.27 cm lead at Cambridge. As seen from Table I, the rate of occurrence increases rapidly with decreasing shower size. Measurements made on a few traces indicate that this increase continues for the groups of still smaller sized showers than given in the table. (For 1.27 cm lead at Cambridge, the rate for the group of 6–9 rays is 0.40 per min.) Taking into account the increasing abundance of the smaller showers, one concludes that the shower phenomenon contributes appreciably to the general radiation. Since the showers increase more rapidly with altitude than the general radiation, this contribution is of increasing importance at higher elevation.

This research was supported in part by grants from the Carnegie Institution of Washington and the Harvard Milton Fund.

J. C. STREET AND R. T. YOUNG
Jefferson Physical Laboratory,
Harvard University,
March 14, 1935.

[1] J. C. Street and R. T. Young, Phys. Rev. **46**, 823 (1934).
[2] J. C. Street and R. H. Woodward, Phys. Rev. **46**, 1029 (1934).
[3] T. H. Johnson, Phys. Rev. **45**, 569 (1934).
[4] T. H. Johnson, Phys. Rev. **47**, 318 (1935).
[5] C. W. Gilbert, Proc. Roy. Soc. **A144**, 559 (1934).

Collisions of High Energy Protons in Hydrogen

Since September, 1934, some 250,000 proton (750 kv) tracks in hydrogen have been photographed and about 160 collisions observed. The protons were obtained by the apparatus of Lawrence and Livingston,[1] the apparatus being capable of producing a 1.3 MEV proton beam at a current of 10^{-9} amp. A Wilson cloud chamber and stereoscopic camera were used to make a study of intimate collisions of protons with hydrogen ions. The data, though still very meager, are sufficiently at variance with the concept of a "point-charge" proton to make a brief report of interest to theoretical physicists.

The salient features of the results are as follows:

1. All collisions technically accurately photographed show conservation of energy and momentum. Certainly no energy in excess of 20 kv is radiated in any form even for collisions of 750 kv.

2. The total number of scattered protons as a function of the energy of the incident proton does not fall off as the inverse square of the energy.

3. The angular distribution of scattered protons does not follow Mott's[2] formula, but is much too large at large angle deflection.

Table I shows the expected and the observed number of collisions in a given angular range and energy range. It must be again emphasized that such few numbers of collisions are represented as to make statistical fluctuations quite serious. Of course where identical nuclei are concerned no angle of scattering greater than 45° should appear if one always chooses the angle of deflection of the longer tine.

TABLE I. *Number of 600–750 kv collisions.*

Angle	15°–20°	20°–25°	25°–30°	30°–35°	35°–40°	40°–45°
Theoretical	8.7	3.8	2.1	1.1	0.74	0.55
Observed	10.5	5.5	0.5	1.5	3.5	5.0

If we accept these results at face value, they indicate a serious departure from Coulomb's law for two protons at distances of 5×10^{-13} cm. These deviations are much larger than those to be expected from the theory of the positron, and are not to be expected at all on the basis of classical electron theory,[3] according to which a proton should act like a point charge down to 10^{-16} cm. The present results can be accounted for by assuming a Gamow potential[4] with radius small compared to the de Broglie wavelength of the proton, but more certain and much more detailed data are needed to justify any theoretical interpretation.

The work is being continued with improved technique using a Wilson cloud chamber and in addition a new electrical counting method is being developed to avoid the inevitable paucity of data obtainable from the cloud chamber. It is hoped in the near future to submit these further results in detail to the *Physical Review*.

The author wishes to express his appreciation to Professor E. O. Lawrence and Professor J. R. Oppenheimer for constant encouragement during the progress of this research. He is also indebted to the General Electric Company for the award of a Charles A. Coffin Foundation Fellowship during the past two years.

MILTON G. WHITE

Department of Physics,
University of California,
March 18, 1935.

[1] Lawrence and Livingston, Phys. Rev. **40**, 19 (1932).
[2] Mott, Proc. Roy. Soc. **A126**, 259 (1929).
[3] Mohr and Massey, Proc. Roy. Soc. **A148**, 206 (1935).
[4] Taylor, Proc. Roy. Soc. **A136**, 605 (1932).

THE AMERICAN INSTITUTE OF PHYSICS

INCORPORATED

GOVERNING BOARD

For The American Physical Society:

KARL T. COMPTON, *Chairman*
Massachusetts Institute of Technology

GEORGE B. PEGRAM, *Secretary*
Columbia University

JOHN T. TATE
University of Minnesota

For The Optical Society of America:

E. C. CRITTENDEN
Bureau of Standards

PAUL D. FOOTE
The Gulf Companies

F. K. RICHTMYER
Cornell University

For The Acoustical Society of America:

HARVEY FLETCHER
Bell Telephone Laboratories

VERN O. KNUDSEN
University of California at Los Angeles

WALLACE WATERFALL
The Celotex Company

For The Society of Rheology:

E. C. BINGHAM
Lafayette College

A. STUART HUNTER
du Pont Rayon Company

S. E. SHEPPARD
Eastman Kodak Company

For The American Association of Physics Teachers:

HOBART L. DODGE
University of Oklahoma

PAUL E. KLOPSTEG
Central Scientific Company

FREDERIC PALMER
Haverford College

ADMINISTRATIVE STAFF

HENRY A. BARTON, *Director* JOHN T. TATE, *Adviser on Publications*

MARGARET M. MITCHELL, *Editorial Secretary*

Office: 11 East 38th Street, New York, New York

JOURNALS

THE PHYSICAL REVIEW

REVIEWS OF MODERN PHYSICS

PHYSICS

JOHN T. TATE, *Editor*
J. W. BUCHTA, *Assistant Editor*
E. C. BINGHAM, *Rheology Editor*

THE JOURNAL OF THE OPTICAL SOCIETY OF AMERICA

THE REVIEW OF SCIENTIFIC INSTRUMENTS
WITH PHYSICS NEWS AND VIEWS
F. K. RICHTMYER, *Editor*

JOURNAL OF THE ACOUSTICAL SOCIETY OF AMERICA
F. R. WATSON, *Editor*

THE JOURNAL OF CHEMICAL PHYSICS
HAROLD C. UREY, *Editor*

THE AMERICAN PHYSICS TEACHER
DUANE ROLLER, *Editor*

The American Institute of Physics is a membership corporation of which five societies are the founding members. These five societies are the principal national societies devoted to pure and applied physics in America. Their names, and those of their representatives who form the Governing Board of the Institute, are given above. The principal work of the Institute is the publication of journals sponsored by the societies or by itself. The names and the editors of the journals are also listed above.

The broad purpose of the Institute is to represent, in all matters of wide or common interest, the five thousand or more members and subscribers associated with the Founder Societies and the journals. It aims to advance the science and profession of physics, and to promote cooperation between pure research, the applied sciences and the industries. To achieve these aims, it is greatly in need of an endowment and is empowered by law to administer grants and funds of any kind.

CONTENTS

...Rev. 47 (1935) ... APRIL 1

...ry and Tertiary Particles Produced by Cosmic Rays ... J. H. SAWYER, JR. 515

...figurations of Cobalt ... H. H. MARVIN 521

...Effect in the Arc Spectrum of Cobalt ... FRANK L. ROTH AND PAUL F. BARTUNEK 526

...n of Element 91-Protactinium ... W. C. PIERCE AND A. V. GROSSE 532

...ey of the Velocity of Light ... ROY J. KENNEDY 533

...ine Structures in La III. Nuclear Magnetic Moment of Lanthanum ... M. F. CRAWFORD AND NORMAN S. GRACE 536

...ry Properties and the Identity of Similar Particles ... E. E. WEMER AND J. P. VINTI 538

...Ionization During the Initial Stages of Spark Discharge in Nonuniform ...lds ... CHARLES D. BRADLEY AND L. B. SNODDY 541

...ve Study of the Allison Magneto-Optic Method of Analysis ... MYRON A. JEFFERSON AND RAYMOND M. BELL 546

...ations on the Allison Magneto-Optic Apparatus ... T. R. BALL 548

...Studies Concerning Rotating Axes and Polyatomic Molecules ... CARL ECKART 552

...-Fermi Method for Metals ... J. C. SLATER AND H. M. KRUTTER 559

...the Editor:

...ymmetric C–D Bond Vibration in Heavy Acetylene ... GEORGE GLOCKLER AND CHARLES E. MORRELL 569

...High Energy Formulae ... E. J. WILLIAMS 569

...ced Ultraviolet Fluorescence and Its Release by Visible Light ... OTTO GLASSER AND J. E. BRADLEY 570

...Resonance Interaction Between Deuterons and Alpha-Particles ... E. POLLARD AND H. MARGENAU 571

...Isotopic Ratio of the Isotopes of Lithium ... A. KEITH BREWER 571

...Meson Groups in the Cosmic Radiation ... J. C. STEARNS AND R. T. YOUNG 572

...Collisions of High Energy Protons in Hydrogen ... RICHARD G. WILSON 573

LANCASTER PRESS, INC., LANCASTER, PA.